Год науки и технологии

XXVII Симпозиум «Биоинформатика и компьютерное конструирование лекарств»

От малых и больших данных - к молекулярным мишеням и лекарствам

"ДИЗАЙН СПЕЦИФИЧЕСКИХ АНТИТЕЛ НА ОСНОВЕ QM/MM ПОДХОДА"

академик А.Г.Габибов

6 апреля 2021

MESSAGE

•ERA OF BIG DATA

- **HOW TO PRODUCE EXPANDED REPERTOIARES WITH NOVEL PREDISIGNED FUNCTIONALITIES**
- **HOW PROCEED SCREENING OF EXISTING HUGE FUNCTIONAL REPERTOIARES WITH DEMANDED PROPERTIES**

BioCat Lab

MESSAGE

Combinatorial Chemistry and Biology a hallmark of XXI century

Chemical Libraries

- ✓Mimotope Strategy
- ✓Parallel Synthesis of Combinatorial libraries
- ✓One-Bead, One-Peptide Solid-Support Technology
- ✓Positional Scanning, and Robotics Library Technology

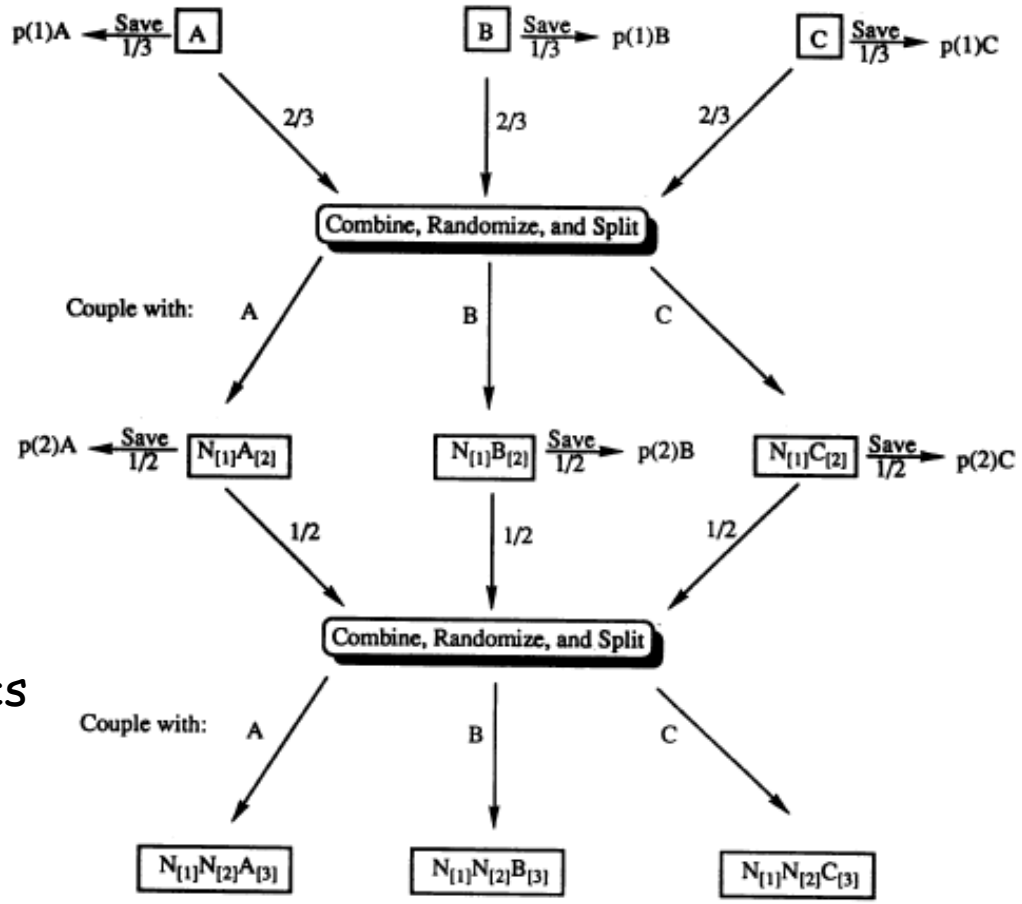

"Biological libraries"

Tagged Methodologies:

- ✓Phage Technology
- ✓Peptides on Plasmids
- ✓Peptide coded Libraries
- ✓Electrophoric Polyhalobenzene Coded Libraries
- ✓Encoded Combinatorial Libraries

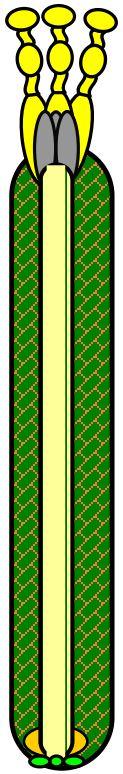

Filamentous phage

Based on a physical link between a protein and its encoded gene – the best known system is phage display.

The product of gene 8 (g8p) – is a small protein that forms the cylinder of the capsid; its number of copies (2700 for the wild-type phage). The other coat proteins (g3p, g6p, g7p and g9p) close the extremities of the cylinder. The product of gene 3 – present in three to five copies – is responsible for phage infectivity.
Proteins of interest are usually fused by their C-terminal to g3p or to g8p.

Phenotype-information-phenotype cycle.

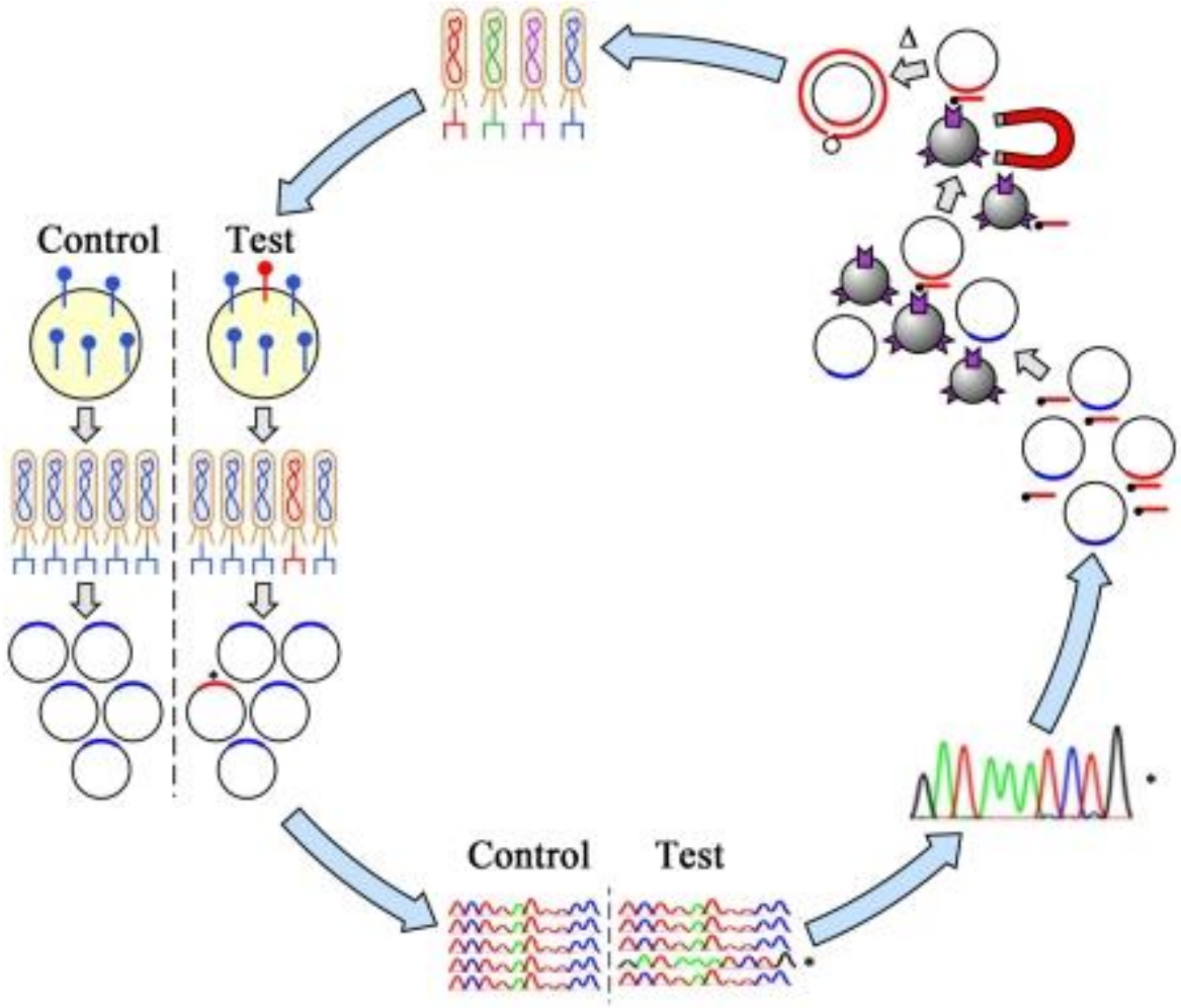

DNA-encoded chemical libraries,DECL

Proc. Natl. Acad. Sci. USA
Vol. 89, pp. 5381–5383, June 1992
Chemistry

Encoded combinatorial chemistry

(chemical repertoire/encoded libraries/commaless code)

SYDNEY BRENNER AND RICHARD A. LERNER

Departments of Chemistry and Molecular Biology, The Scripps Research Institute

Contributed by Sydney Brenner, March 3, 1992

ABSTRACT **The diversity of chemical synthesis and the power of genetics are linked to provide a powerful, versatile method for drug screening. A process of alternating parallel combinatorial synthesis is used to encode individual members of a large library of chemicals with unique nucleotide sequences. After the chemical entity is bound to a target, the genetic tag can be amplified by replication and utilized for enrichment of the bound molecules by serial hybridization to a subset of the library. The nature of the chemical structure bound to the receptor is decoded by sequencing the nucleotide tag.**

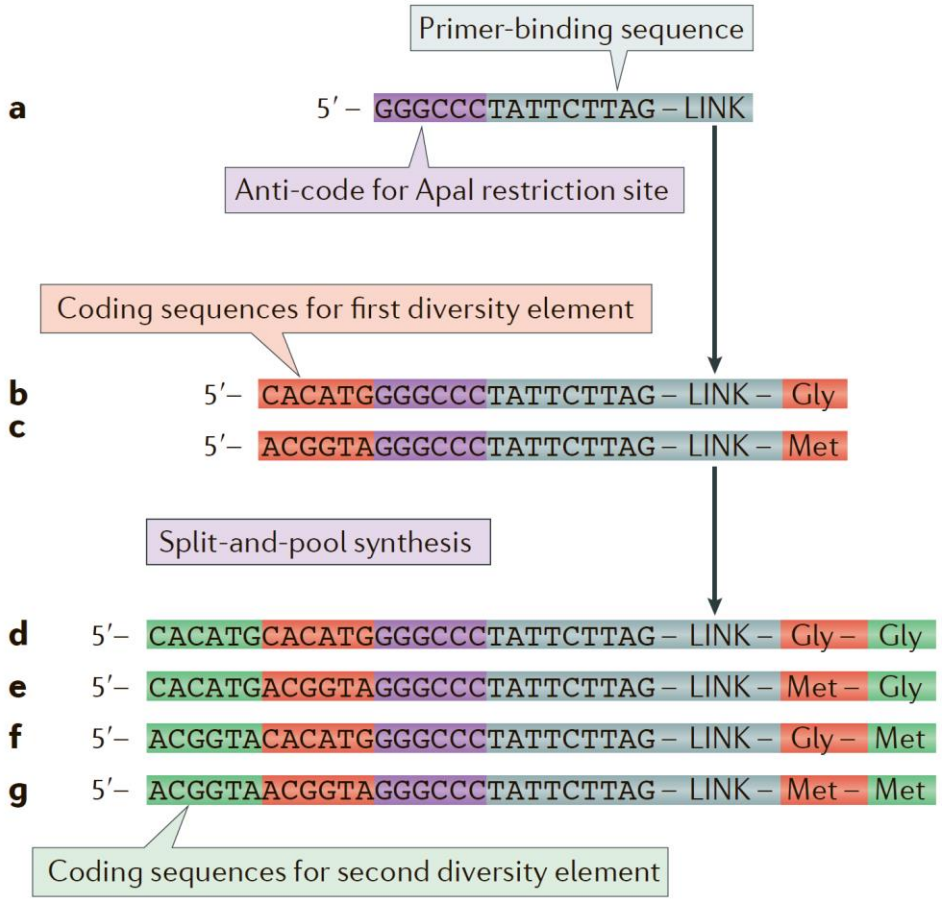

DECL:
Between Chemistry and Biology

Chemistry ⟷ **Biology**

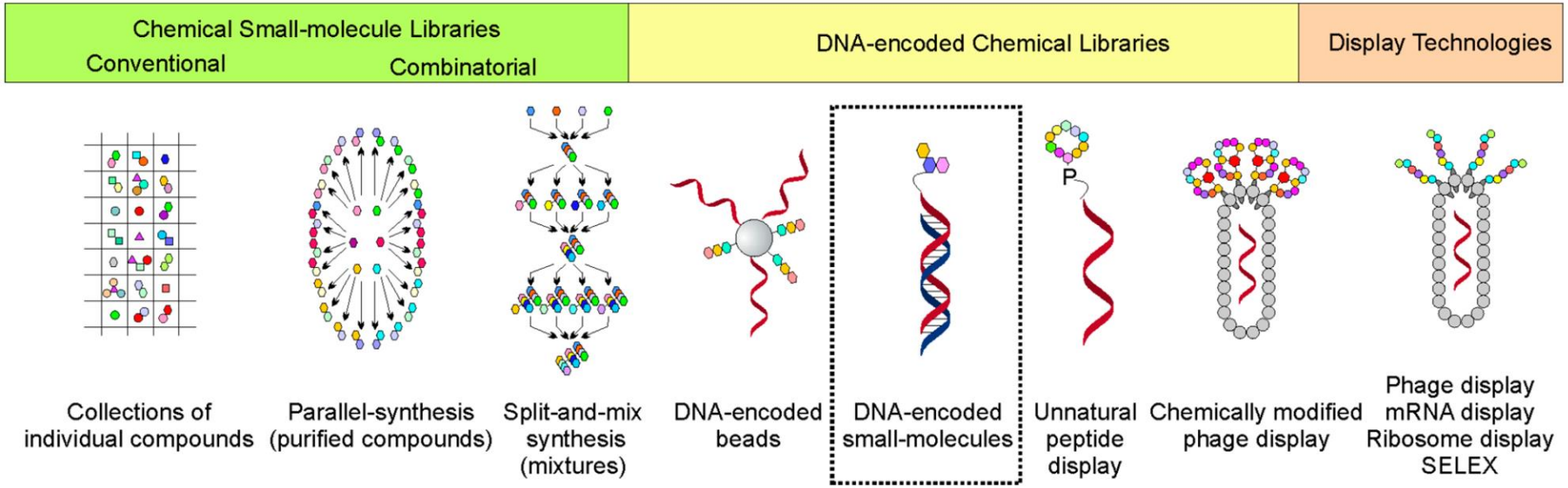

Franzini et al., Acc Chem Res., 2014

Chemical space

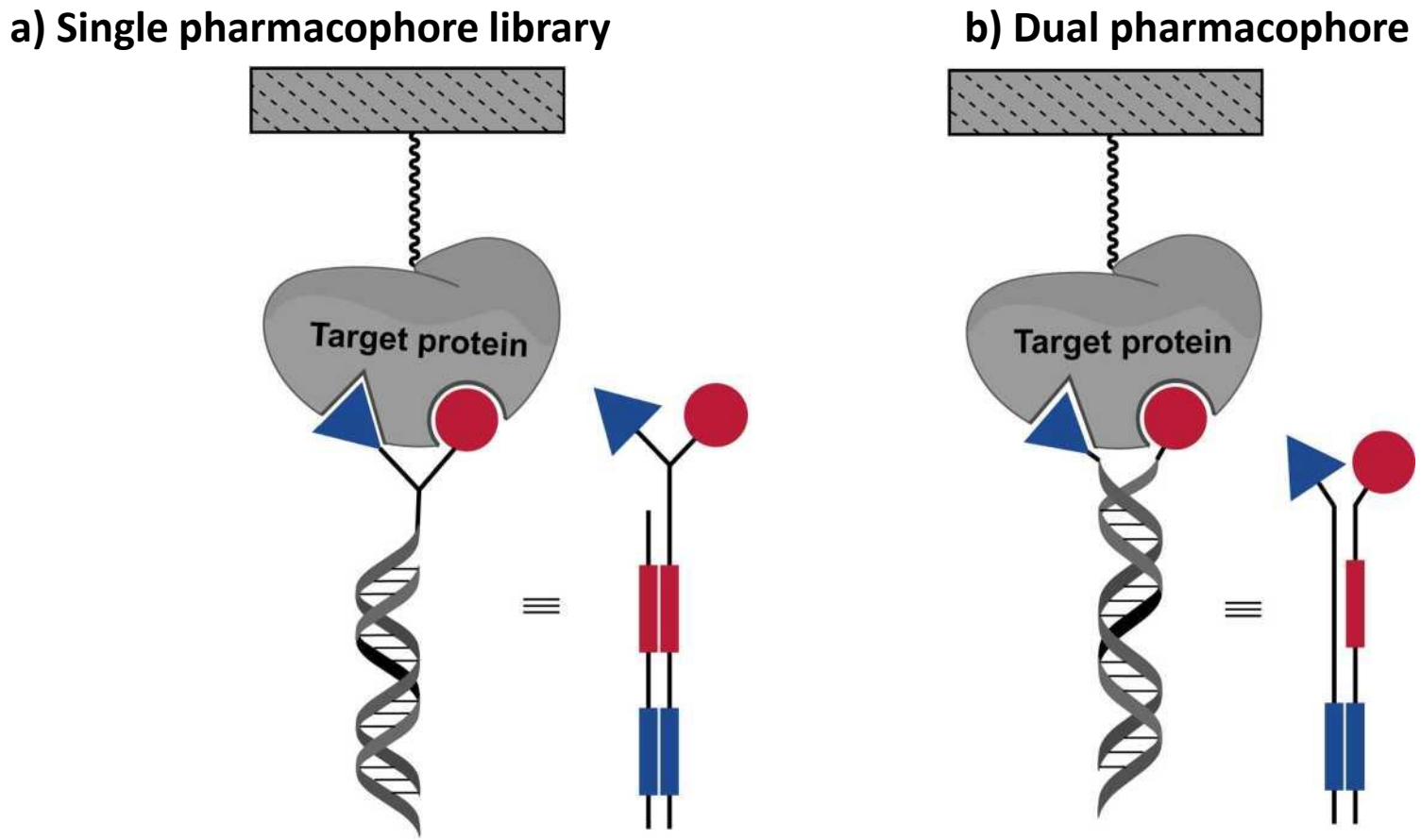

Schematic representation of (a) a single-pharmacophore DNA-encoded chemical library and (b) of a dual pharmacophore DNA-encoded chemical library. In the scheme, the building blocks (triangles and circles) and the corresponding DNA-barcodes (rectangles) are depicted using the same color.

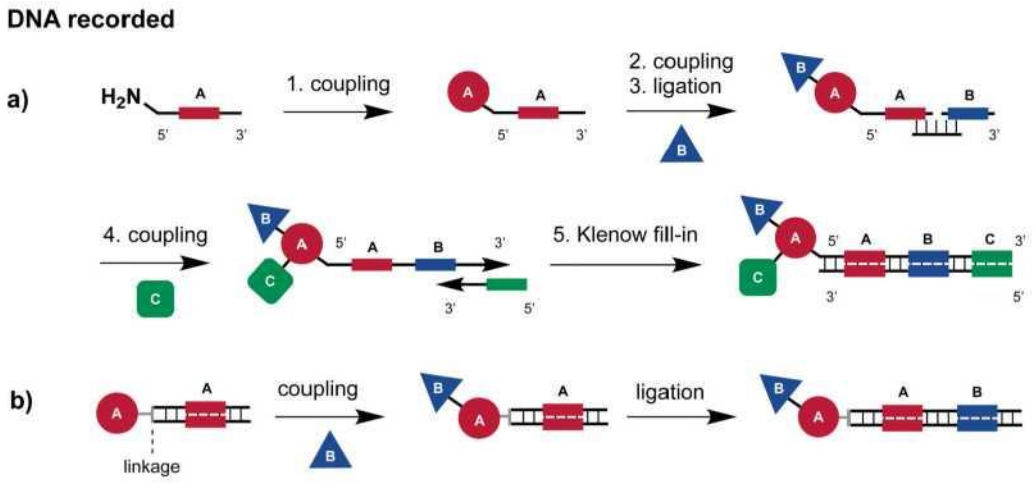

(a) Schematic representation of strategies for DNA-recorded synthesis.

(b) In variation of the encoding procedures described in (a)

(c) In DNA-templated synthesis, pre-formed DNA-template molecules containing coding parts are annealed with code-specific reagent oligonucleotides

(d) In a further implementation of this procedure, a template containing poly-inosine (poly-I) segments allows the annealing with various code-building block oligonucleotide conjugates.

(e) In the ESAC approach, two partially complementary sub-libraries A and B are combinatorially assembled.

Dual-display of small molecules enables the discovery of ligand pairs and facilitates affinity maturation

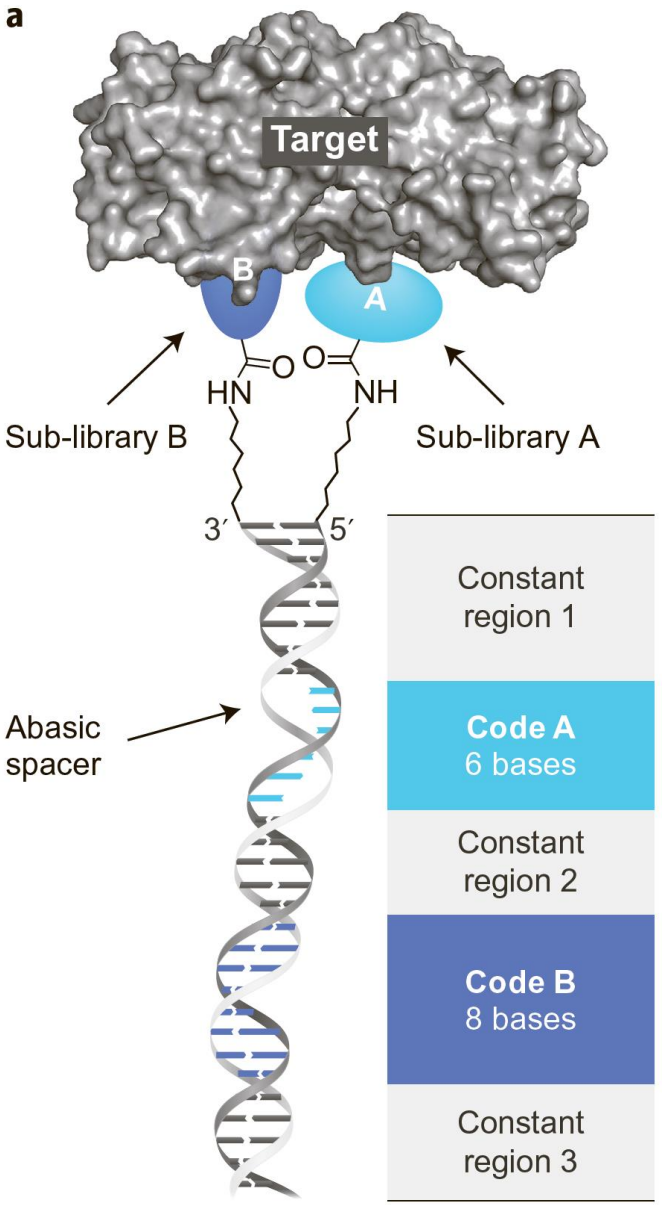

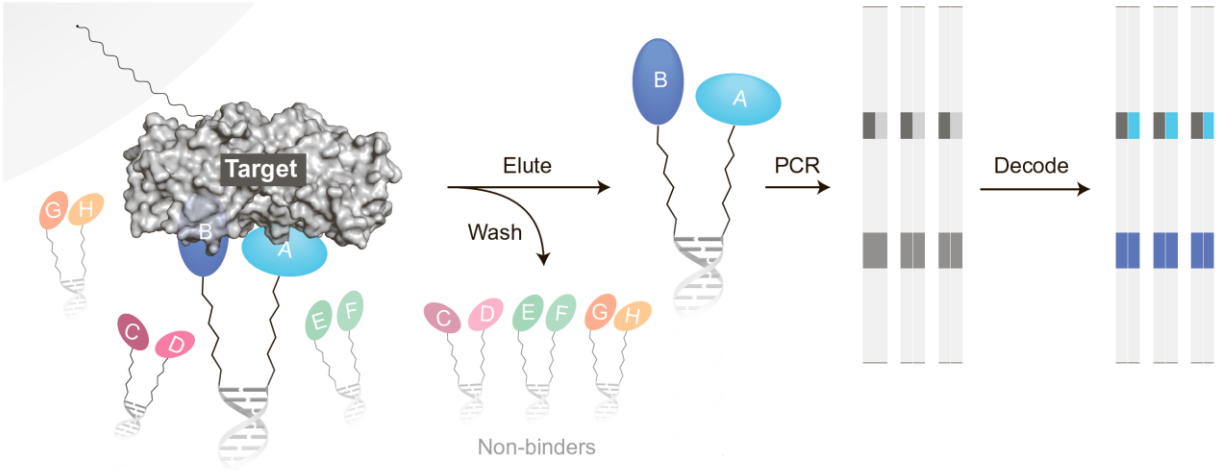

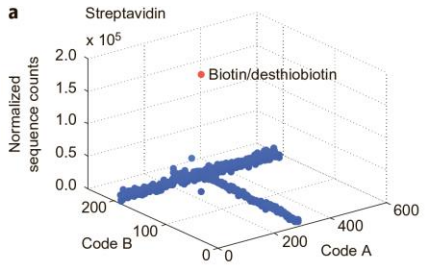

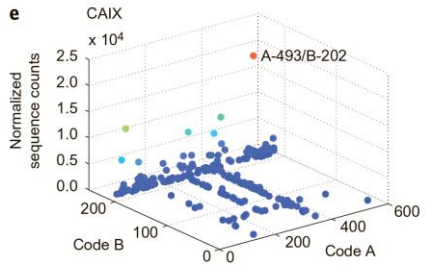

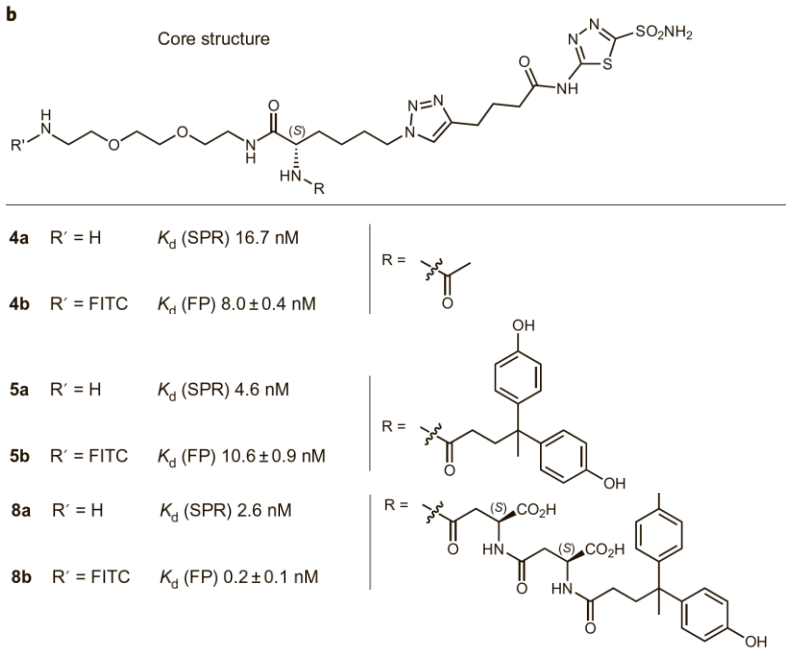

Wichert et al., Nat Chem., 2015

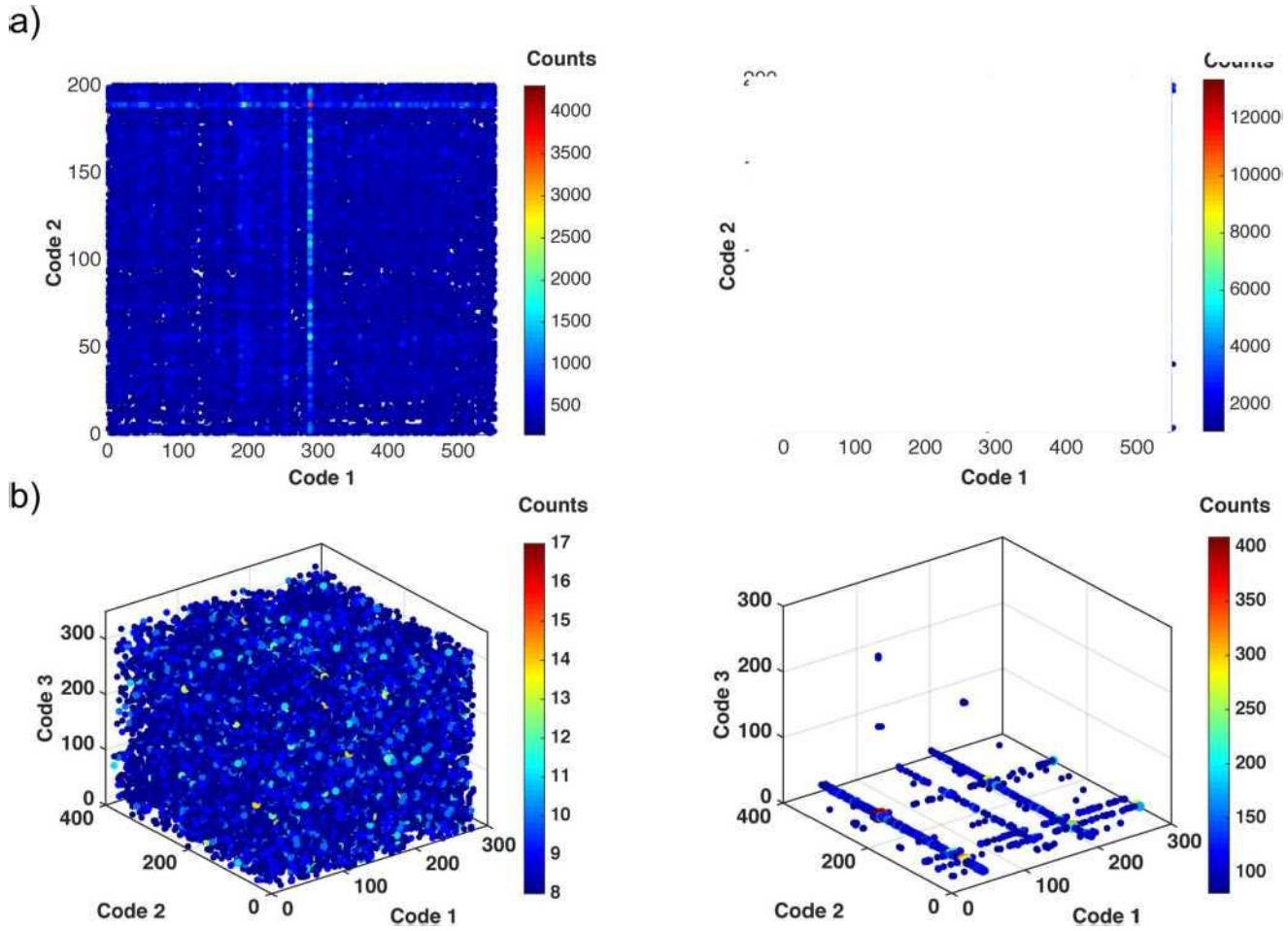

Fingerprints of Naive libraries (left panels) composed of (a) two sets of building blocks or (b) three sets of building blocks are compared with the same libraries selected against (a) horseradish peroxidase (HRP) or (b) carbonic anhydrase (CA) IX (right panels).

DECL research in academia and industry

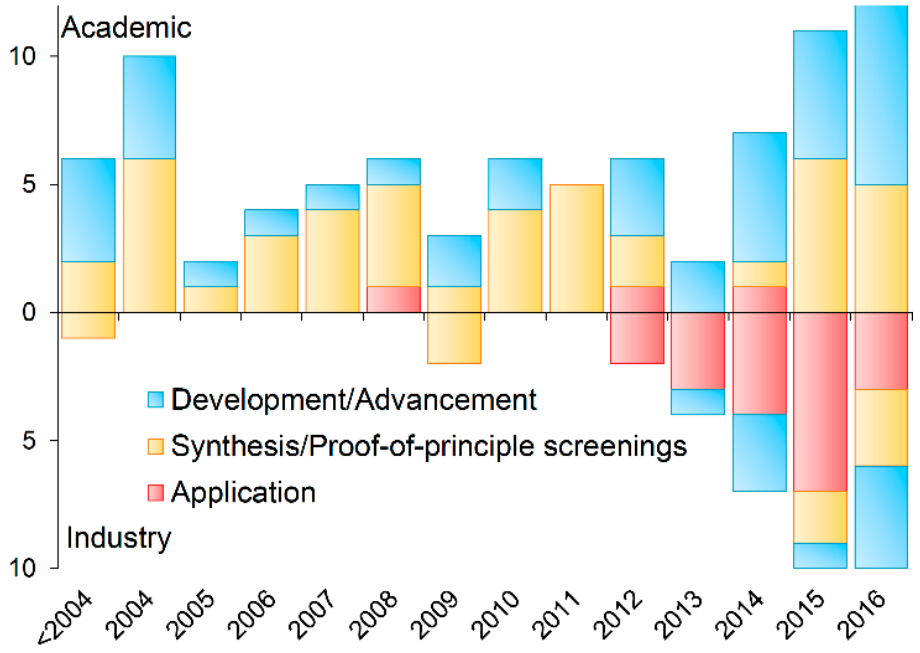

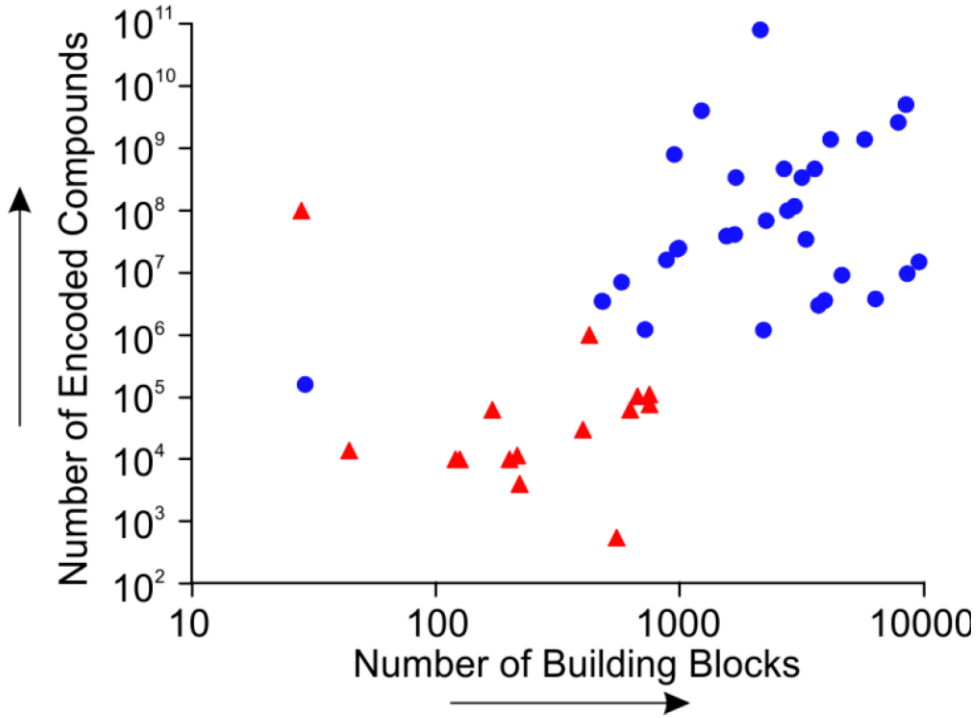

academic (▲) and industrial (●) research groups.

Yuen et al., ChemBioChem, 2016

DECL:
Between Chemistry and Biology

CISION PR Newswire

Send a Release

Scientific Advisory Board Announced for DELopen to Guide the Open Access DNA Encoded Library Interchange

NEWS PROVIDED BY
DELopen →
May 06, 2019, 01:37 ET

SHARE THIS ARTICLE

SHANGHAI and BOSTON, May 6, 2019 /PRNewswire/ -- DELopen, a new platform dedicated to the hit generation of drug discovery of DNA Encoded Library (DEL) Technology, has announced the formation of its Scientific Advisory Board.

The board, chaired by Dr. Richard Lerner, Institute Professor of Scripps Research, and composed of diverse members from prestigious research institutions and industry globally, will set the direction and guide the development of DELopen in its vision to advance the adoption of DNA encoded library technology in new drug discovery.

Directed evolution

Rational design

Combinatorial approach

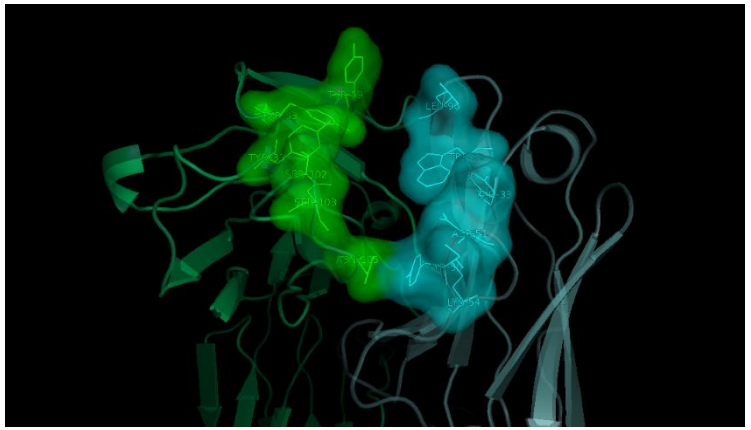

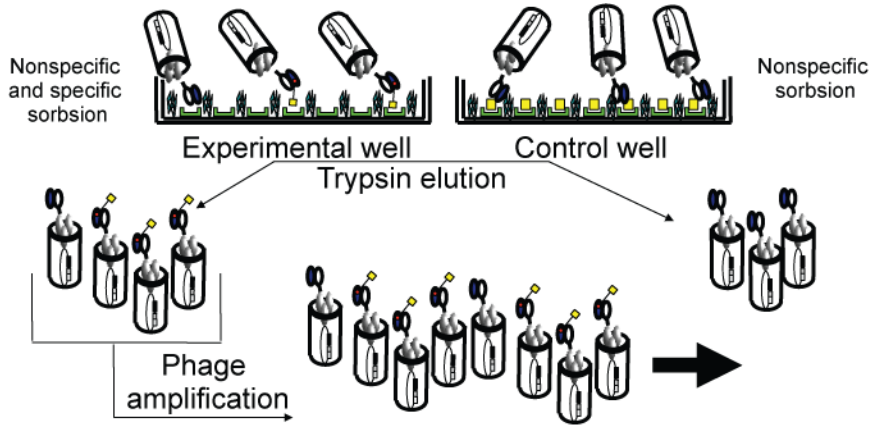

High resolution 3D

Effective screening

KUNGL. VETENSKAPS AKADEMIEN
THE ROYAL SWEDISH ACADEMY OF SCIENCES

The Nobel Prize in Chemistry 2018
Nobelpriset i kemi 2018

Med ena hälften till
With one half to

Frances H. Arnold, USA

"för riktad evolution av enzymer"

"for the directed evolution of enzymes"

och med den andra hälften gemensamt till
and with the other half jointly to

George P. Smith, USA

Sir Gregory P. Winter, UK

"för fagdisplay av peptider och antikroppar"

"for the phage display of peptides and antibodies"

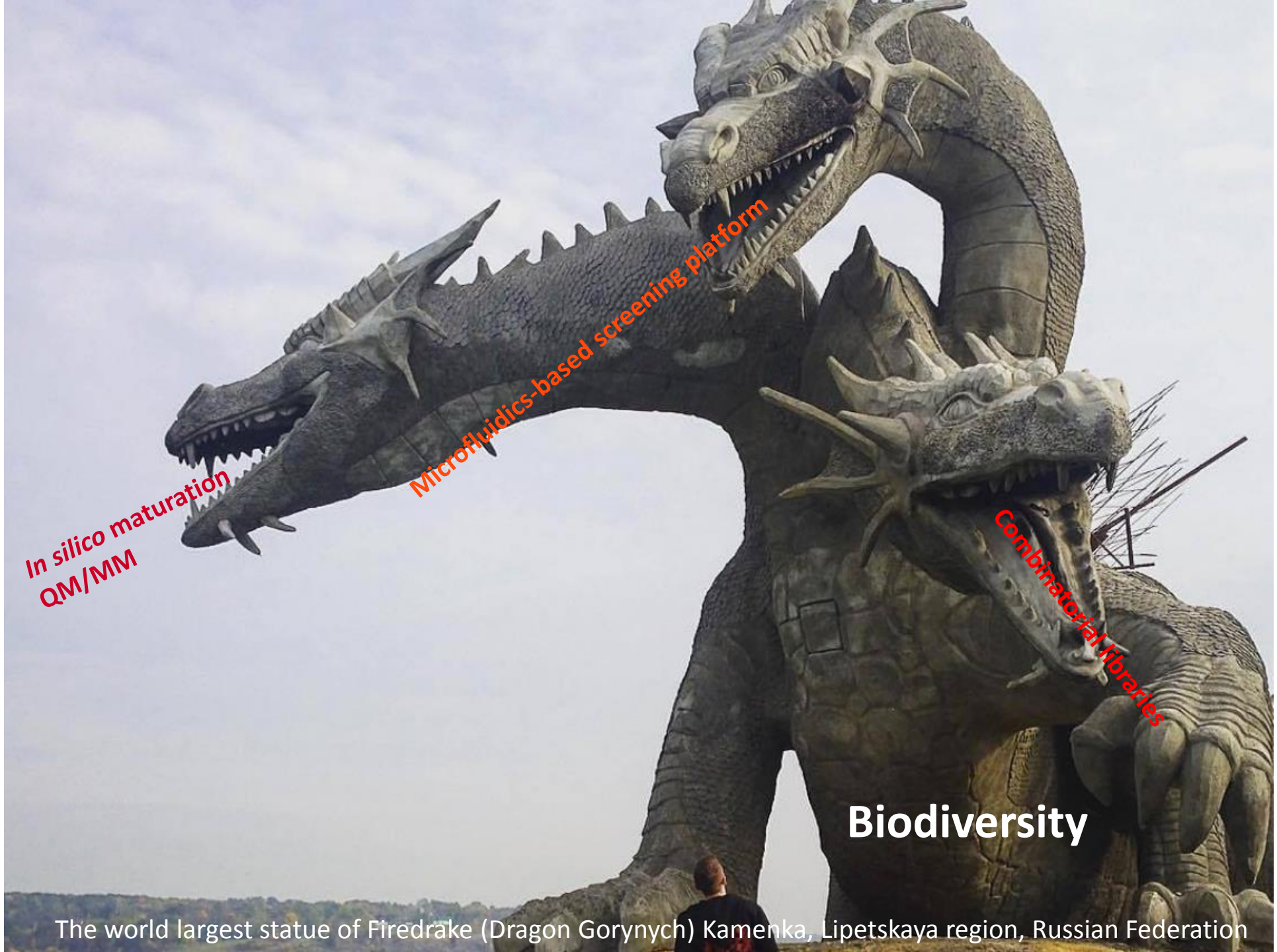

The world largest statue of Firedrake (Dragon Gorynych) Kamenka, Lipetskaya region, Russian Federation

MESSAGE

BioCat Lab

B cell diversity allows to design proteins with novel functionality:

Evolution in test –tube

To analyze Phenotype - Genotype

Edward Jenner "the father of immunology"

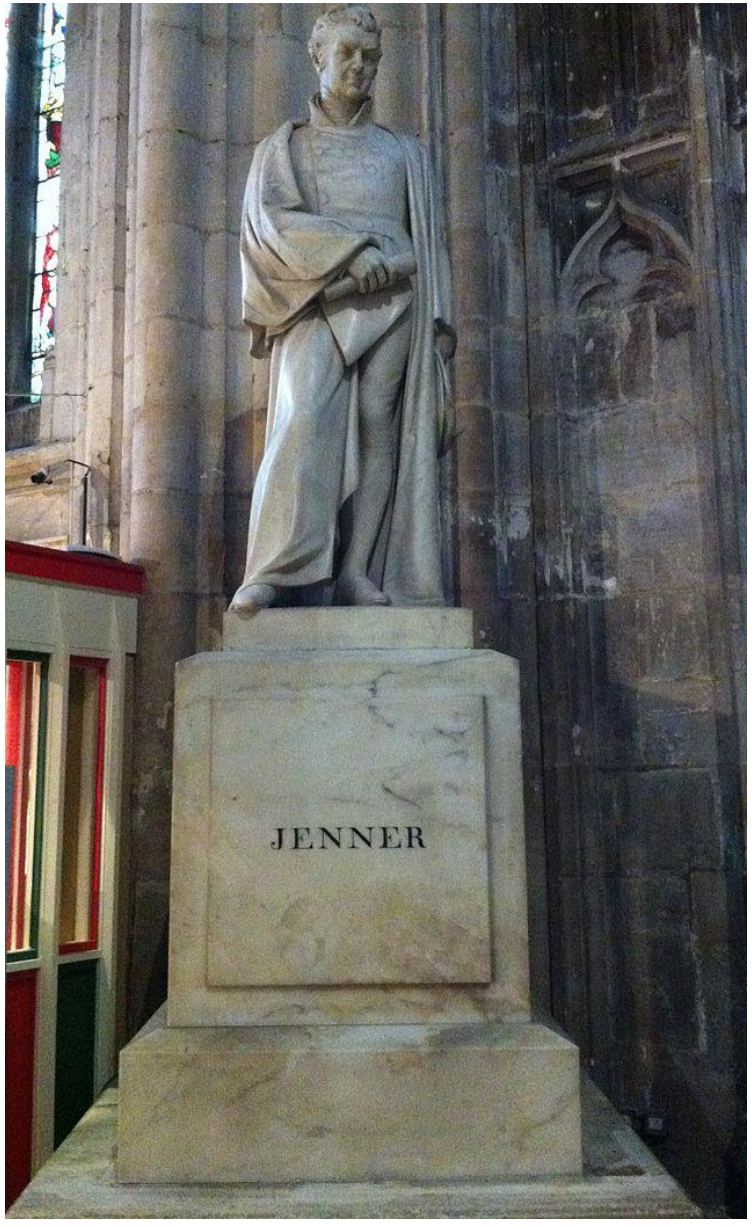

smallpox vaccine, the world's first vaccine.

Nobel Prize of 1908
Physiology or Medicine

Ilya Mechnikov
1845-1916

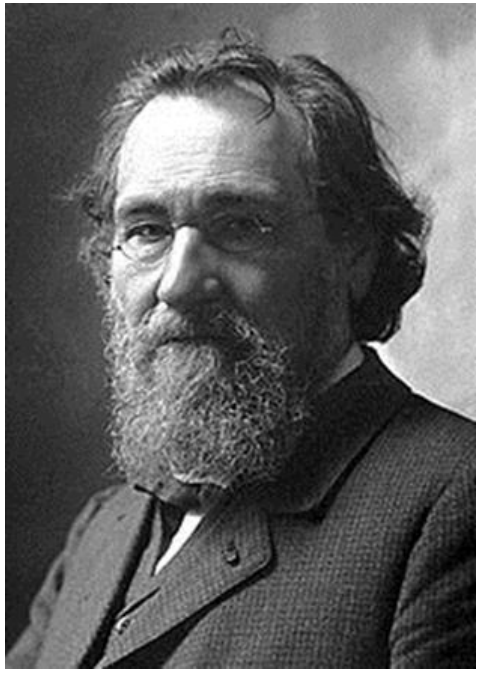

Discovered macrophage in 1882
Grand father of Modern
"Innate Immunity"

Paul Ehrlich
1854-1915

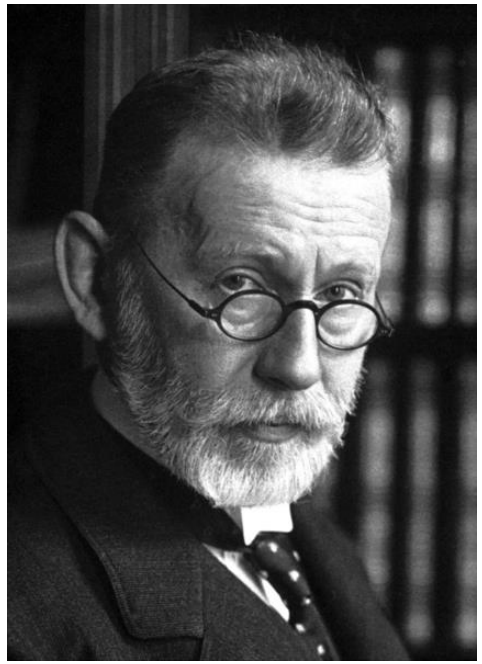

Grand father of Modern hematology, immunology and chemotherapy & pharmacoloy.

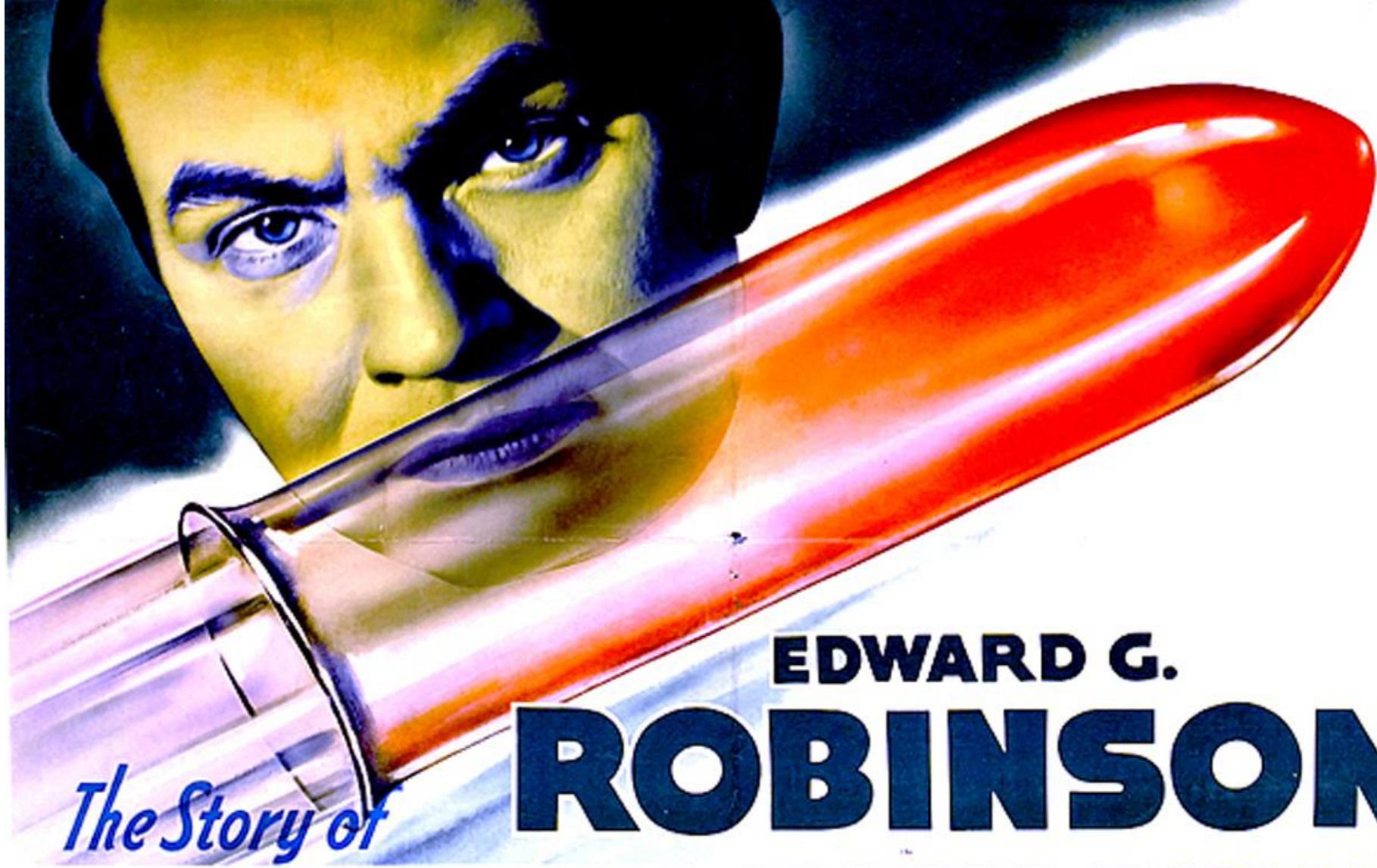

EDWARD G.

ROBINSON

The Story of

Dr. EHRLICH'S MAGIC BULLET

with RUTH GORDON · OTTO KRUGER · DONALD CRISP

Directed by WILLIAM DIETERLE • A WARNER BROS.-First National Picture

Presented by

WARNER BROS.

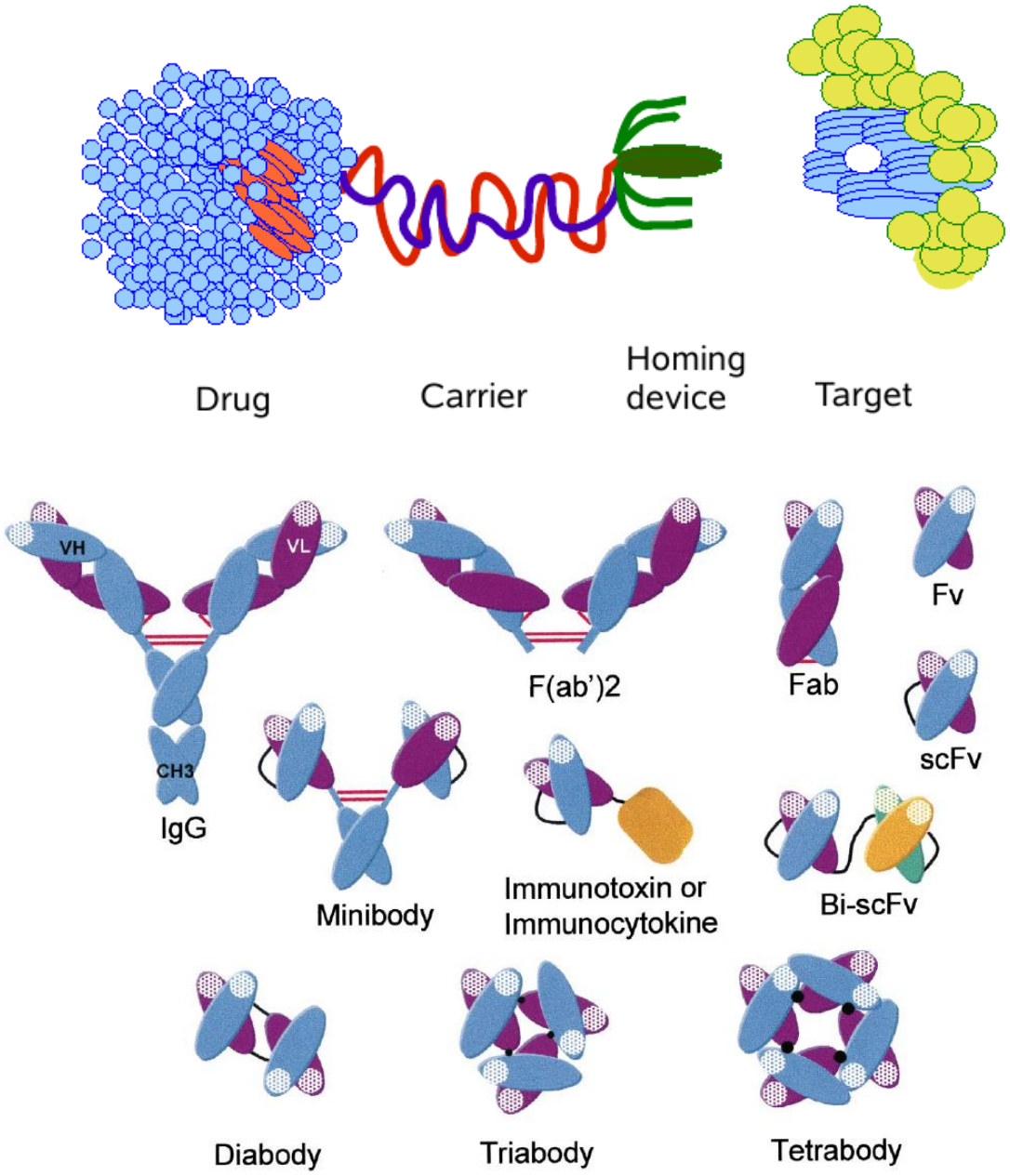

Magic bullet

Ehrlich reasoned that if a compound could be made that selectively targeted a disease-causing organism, then a toxin for that organism could be delivered along with the agent of selectivity. Hence, a "magic bullet" (*magische Kugel*, his term for an ideal therapeutic agent) would be created that killed only the organism targeted. The concept of a "magic bullet" was to some extent realized by the invention of monoclonal antibodies as they provide a very specific binding affinity.

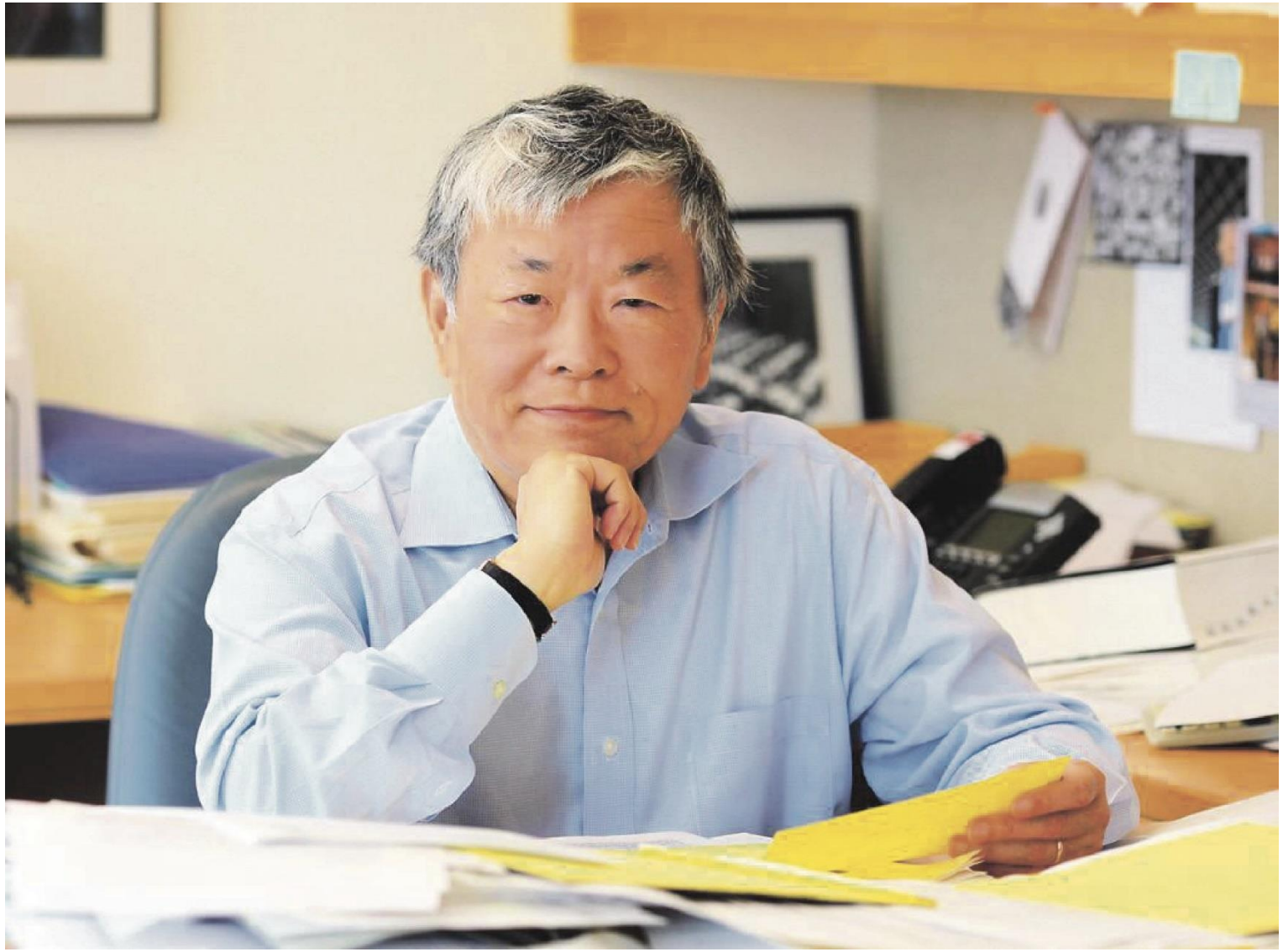

Susumu Tonegawa
Nobel prize 1987

BioCat Lab

MESSAGE

What antibody may do?

-To bind antigen/pathogen

-To destroy

Linus Pauling
Nobel prize 1954, 1962

Теория переходного состояния

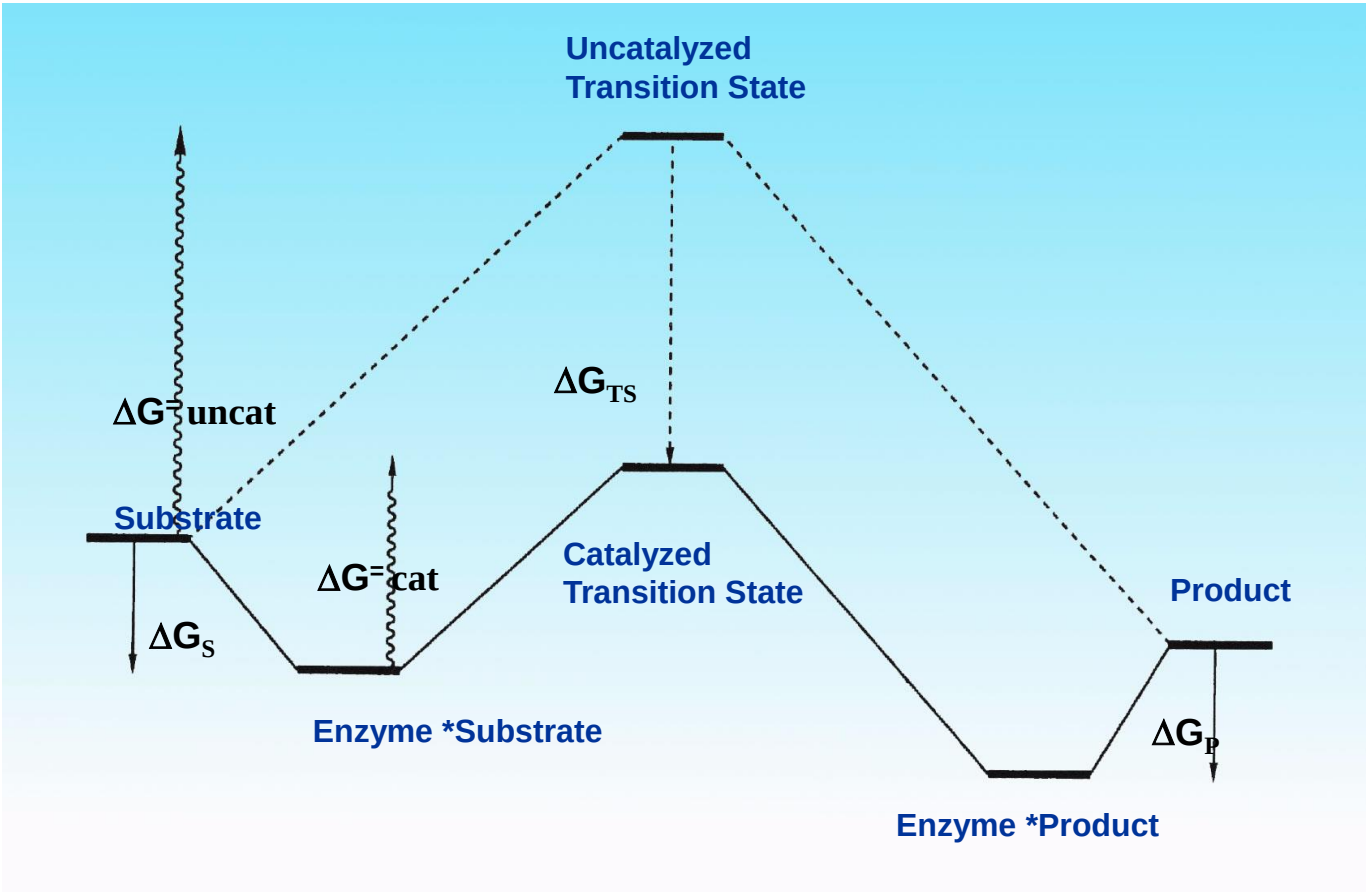

DG= uncat-DG‡ cat = DG_{TS}-DG_S

or $k_{cat}/k_{uncat} = K_M/K_i$

Proc. Natl. Acad. Sci. USA
Vol. 92, pp. 2145–2149, March 1995
Immunology

Unexpectedly high occurrence of catalytic antibodies in MRL/*lpr* and SJL mice immunized with a transition-state analog: Is there a linkage to autoimmunity?

DAN S. TAWFIK*†, RACHEL CHAP†, BERNARD S. GREEN†, MICHAEL SELA*, AND ZELIG ESHHAR*‡

*Department of Chemical Immunology, The Weizmann Institute of Science, Rehovot 76100 Israel; and †Department of Pharmaceutical Chemistry, The Hebrew University, Faculty of Medicine, P.O. Box 12065, Jerusalem 91120, Israel

Contributed by Michael Sela, November 14, 1994

ABSTRACT **Upon testing the ability of several strains of mice to elicit esterolytic antibodies after immunization with a *p*-nitrobenzyl phosphonate hapten, we have found that the occurrence of catalytic antibodies in SJL and MRL/*lpr* autoimmune mice is dramatically higher than in normal mouse strains (e.g., the wild-type MRL/++ or BALB/c). Fewer than 10 catalytic clones are usually obtained from a single fusion of lymphocytes taken from normal mice, whereas several hundred catalytic clones are obtained in SJL or MRL/*lpr* mice. Differences in the numbers of hapten-binding clones do not account for the high occurrences of catalytic clones in these strains. This phenomenon prevailed in the early responses; in both SJL and MRL/*lpr* mice a significant decline in the appearance of catalytic clones was observed after multiple immunizations. Esterolytic antibodies were not found in MRL/*lpr* mice immunized with haptens that do not mimic the transition state for the hydrolysis of the ester substrate (e.g., with a substrate analog). The catalytic antibodies manifest high specificity to the antigen and variability in their binding and catalytic properties. The use of autoimmunity-prone mice may greatly expand the repertoire of catalytic clones elicited against a transition-state analog hapten. More intriguing is the possible linkage between autoimmunity and the appearance of catalytic antibodies. These results suggest that there is normally a selection against the expression of certain variable genes encoding antibodies with catalytic activity.**

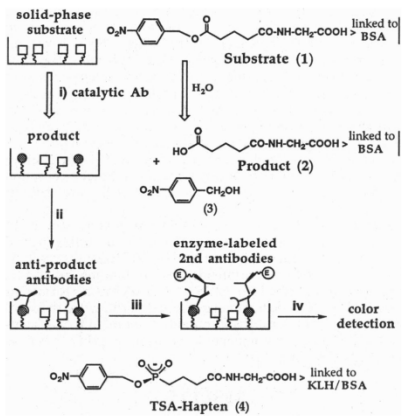

V. A. Engelhardt Institute of Molecular Biology, Academy of Sciences of Russia, Vavilov str., 32, 117984 Moscow, B-334, Russia.

*To whom correspondence should be addressed.

esterase and
amidase

drolyzing Autoantibodies

Shuster, Gennady V. Gololobov,
ashuk, Anastasiya E. Bogomolova,
nirnov, Alexander G. Gabibov*

tected in the sera of patients with various autoimmune
be a property of autoantibodies. The DNA hydrolyzing
affinity and high-performance liquid chromatography, cor-
lobulin M (IgM) and IgG and had a positive response to
NA hydrolyzing autoantibodies were stable to acid shock
pattern that was different from that of deoxyribonuclease

iseases pro-
rotein com-
nzymes that
bolism (2).

In autoimmune diseases, there can be spontaneous induction of anti-idiotypic antibodies (Abs), which are Abs elicited by a primary antigen. These anti-idiotypic Abs may have characteristics of the primary antigen, including catalytic activity. In some cases, the sera of patients with scleroderma, systemic lupus erythematosus (SLE), or rheumatoid arthritis have an

β-elimin

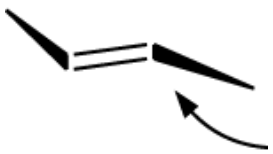

formation and opening of the oxirane ring

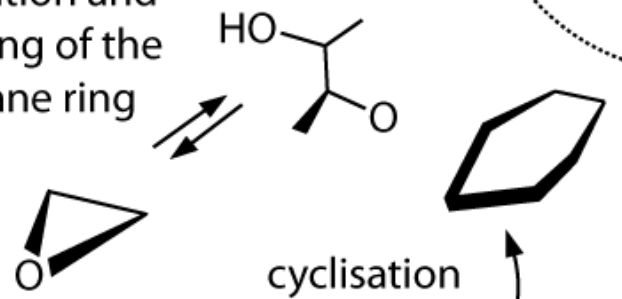

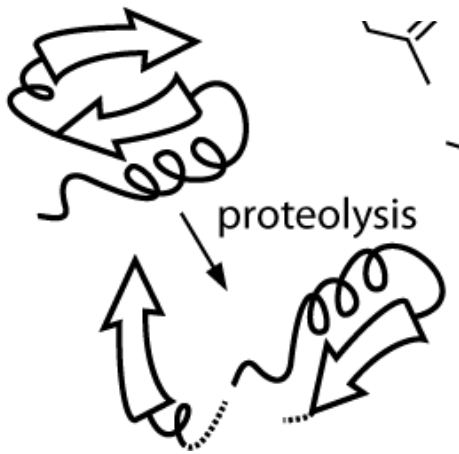

antibodies

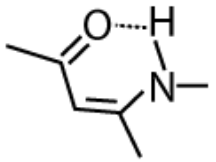

Enzyme Catalysis in Organic Synthesis. Chapter 14. Catalytic antibodies. Smirnov I., Belogurov A., Gabibov A. Wiley-VCH, 2012

Structural Similarity Between BV04-01 and MRL-4 anti-DNA Autoantibodies: DNA-binding and DNA-cleaving Activities are Germline-Encoded

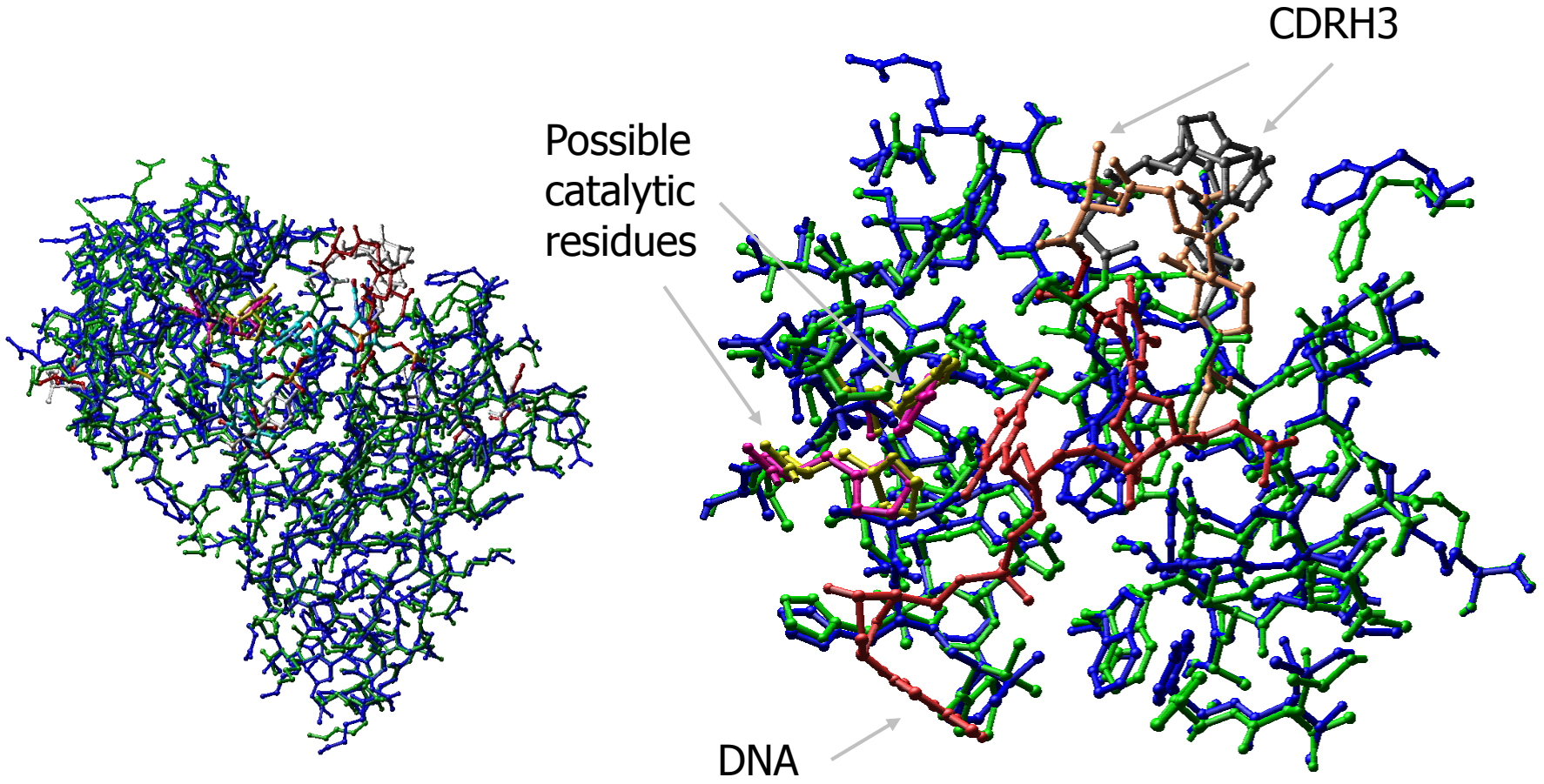

Schuster et al,Science, 1992, Gololobov et al,PNAS, 1995; Gololobov et al.Mol Immunol. 1997.

Abzymes as a two-sided sword

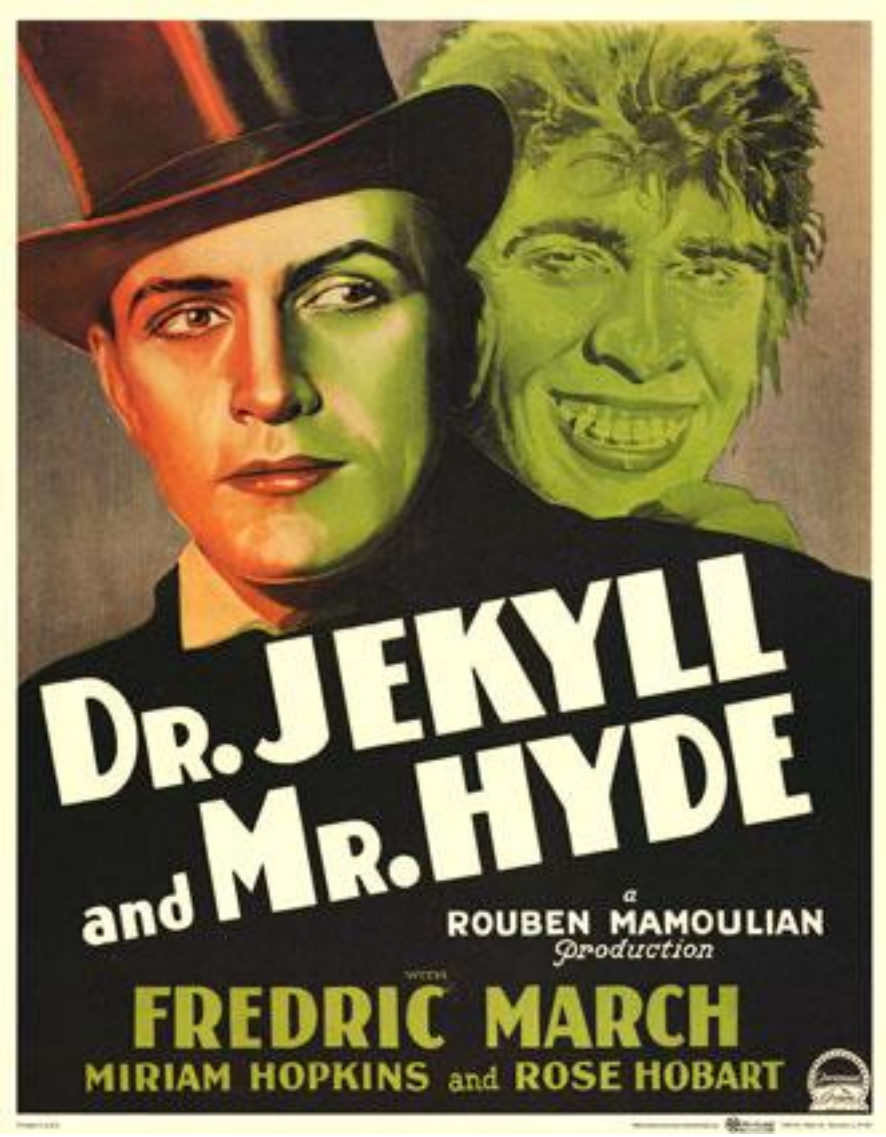

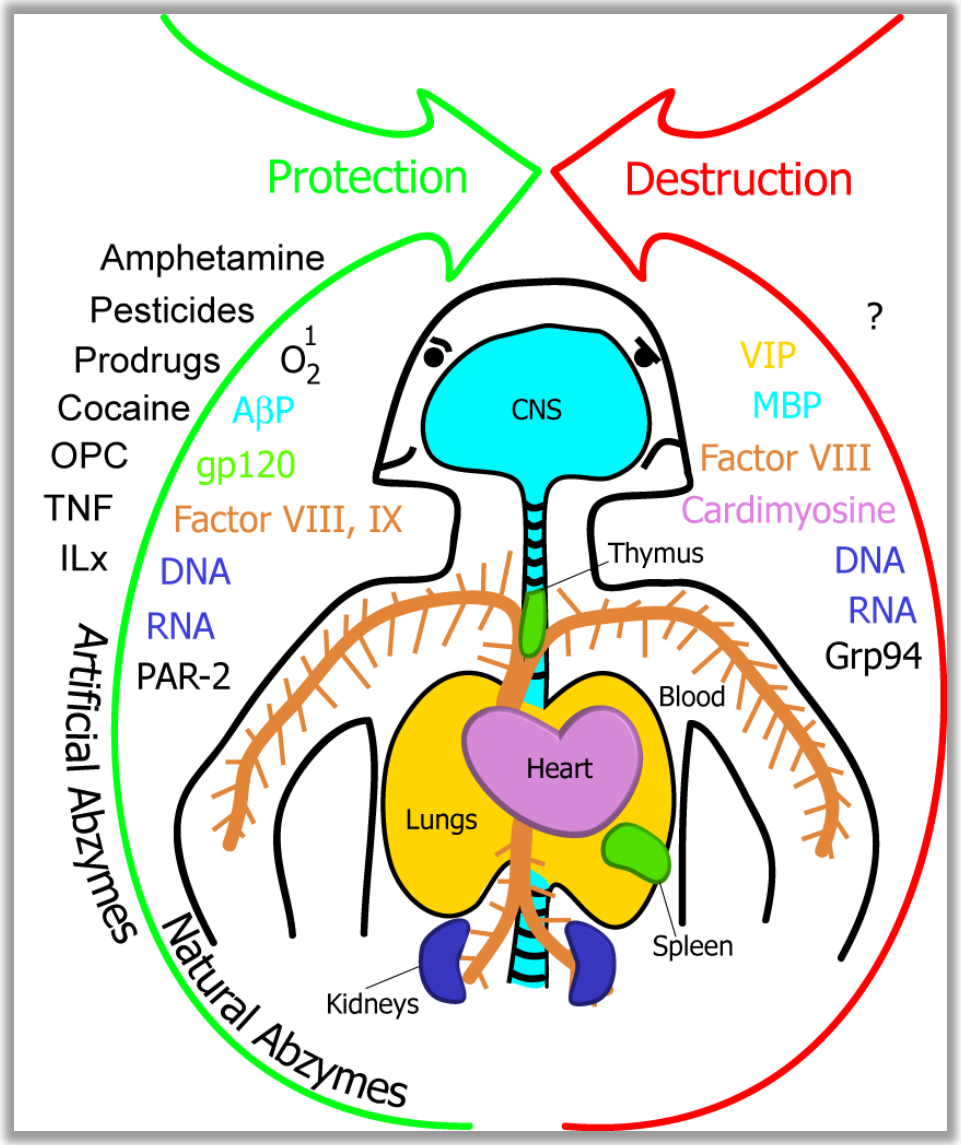

Belogurov et al, BioEssays 2009

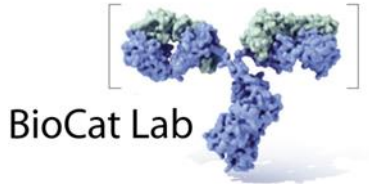

MESSAGE

To make *de novo* functional binder/biocatalyst using Ig template we have to:

- enlarge the repertoire for combinatorial screening

- propose the "vector" for selection strategy

For these purposes we may use:

- phage-display or other libraries ("immunization" and screening in vitro),

- autoimmune repertoires (in vivo)

BioCat Lab

MESSAGE

Limited opportunity to accelerate reactions by mimicking unique transition state to generate active site

Antidotes toward chemical weapons: promiscuity of catalytic sites.

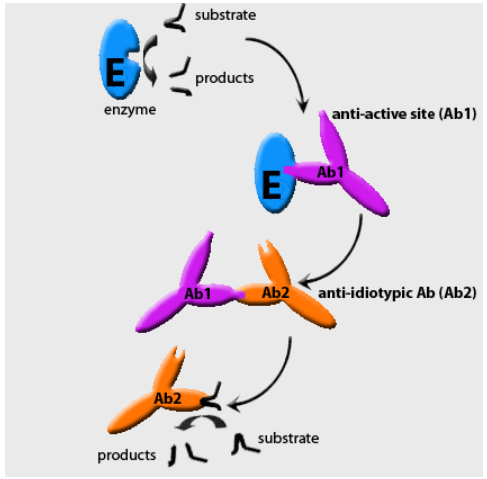

3D Structure of the 9A8 Antiidiotypic Antibody Active Site

- Superposition of the active sites of esterolytic abzymes 9A8 (green) and 17E8 (blue).
- Ser99 - His35 diades are indicated.
- Hydrogene bonds are indicated by dashed lines.

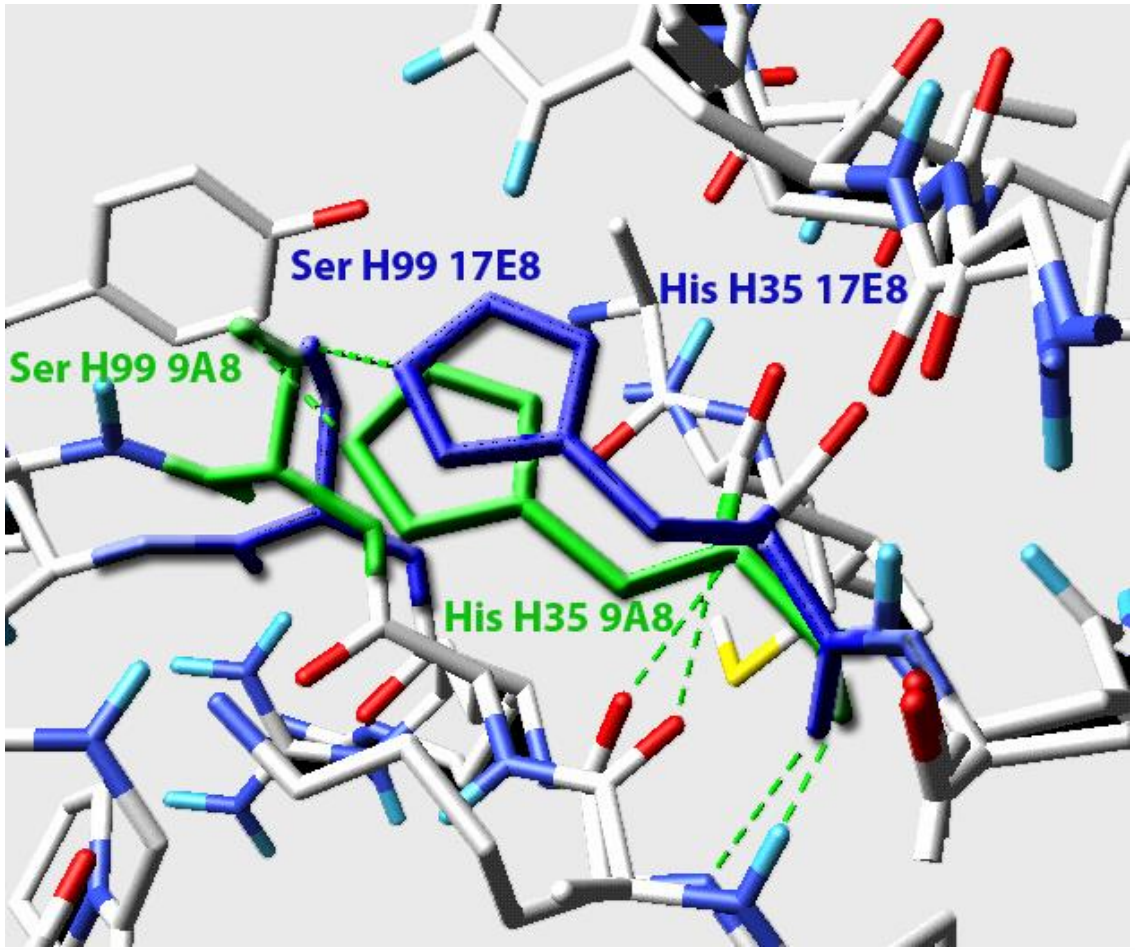

9A8 may covalently accept and anti-acetylcholine esterase poisons

Kolesnikov et al, PNAS 2000

Poisoning of OPC leads to collapse nervous system

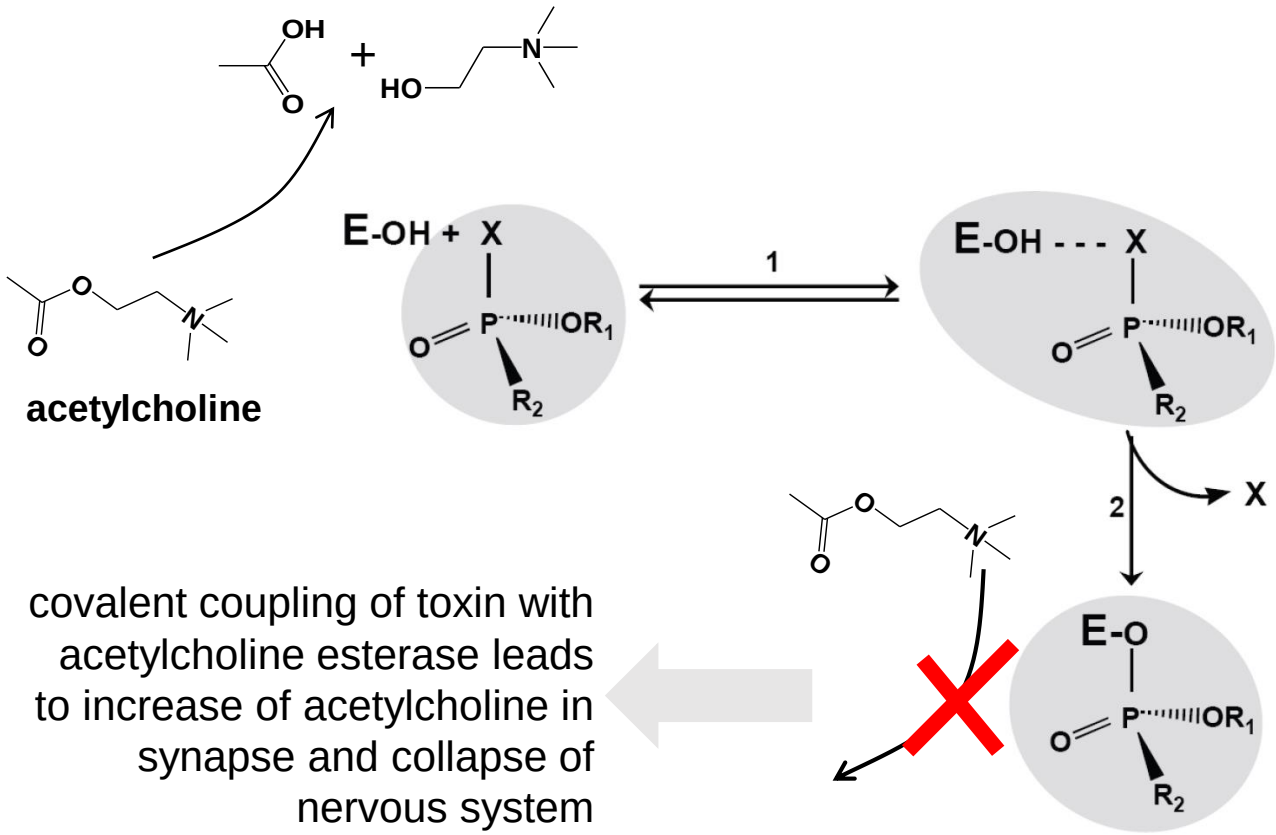

covalent coupling of toxin with acetylcholine esterase leads to increase of acetylcholine in synapse and collapse of nervous system

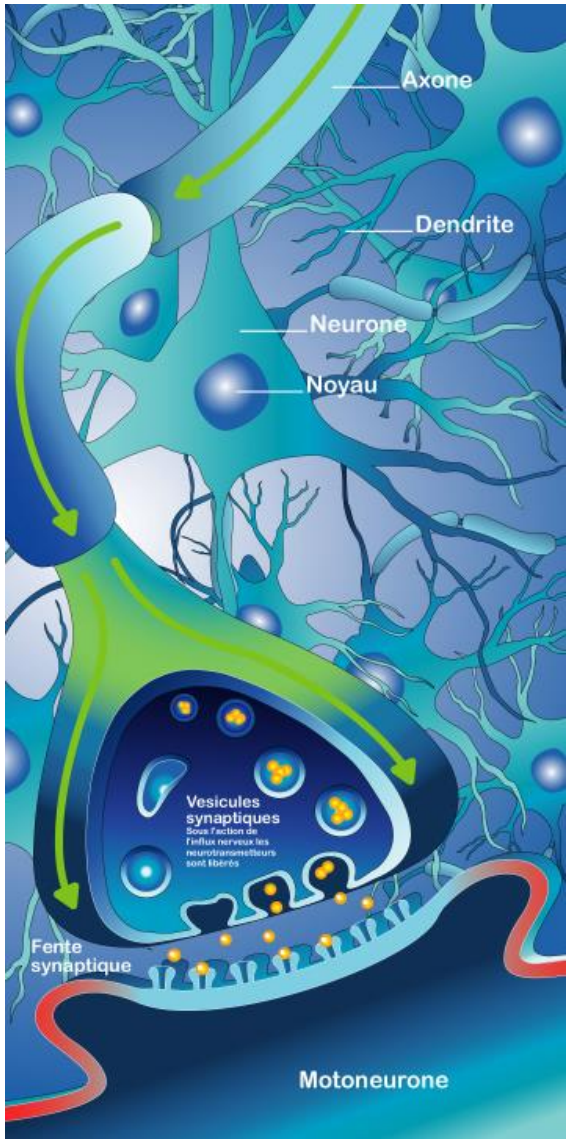

Reactive immunization and kinetic selection as combinatorial approaches to rise novel artificial biocatalysts

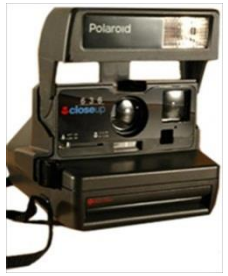

Reactive immunization

Immunization of mice

Proliferation of B-cells, carrying BCR with covalent bound reactive ligand

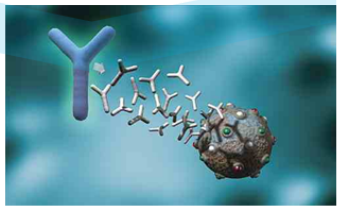

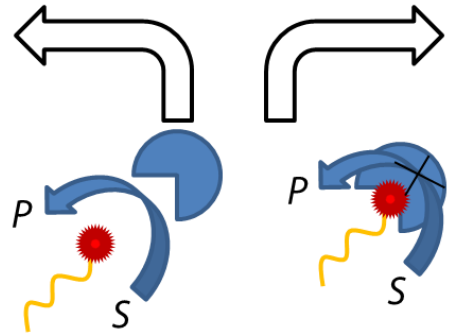

ENZYME CATALYSIS

ANTIBODY CATALYSIS

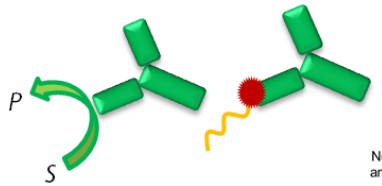

Kinetic selection

Incubation with phage of combinatorial library

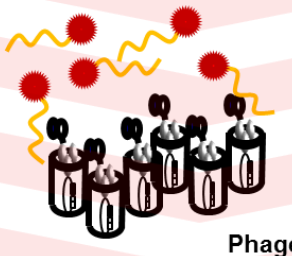

Phage selection with covalent bound reactive ligand

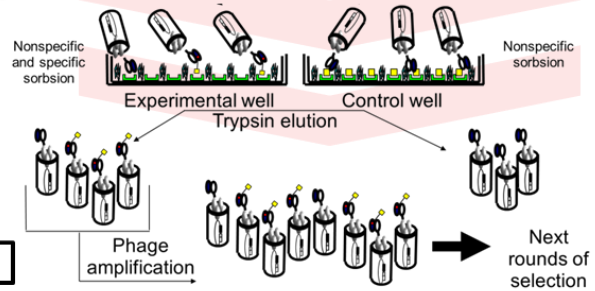

Kinetic selection analysis revealed close family relationship of the reactive clones with preferred pairing of lambda V_L and V_H chains with conserved CDR-H3 sequences

+

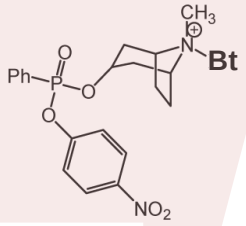

Clone	Light chain: Family/Segment	Light chain:	Light chain: CDR3	Heavy chain: Family/Segment	Heavy chain:	Heavy chain: CDR3	Phosphonate reactivity constant k_2/K_D, $M^{-1}min^{-1}$
Nonselected clones							
N4		A23*	MQATQFP**RP**	VH6	DP-74	FNTPTFDY	
N6	Vλ7	DPL19	LLSYSGA**NV**	VH7	DP-21	SAMVNPV	
N7	Vλ4	DPL24	GESHTI**DGQV**	VH4	DP-66	TSMHFRRWR	
N8	Vλ1	DPL3	AAWDDSL**TPT**	VH2	DP-27	REGRVTDY	
N9	Vλ3	DPL16	NSRDSSG**NH**	VH1	DP-10	SMNPTFDY	
N17	Vλ9	DPL22	GADHGSGS**SF**	VH4	DP-68	VLFVTFDY	
N43		A19*	MQALQ**ALC**	VH6	DP-74	TLGDPFDY	
N48	Vλ4	DPL24	GESHTIGGQ**VS**	VH4	DP-71	CPRPTH	
N55	Vλ1	DPL2	AAWDDSL**TCC**	VH1	DP-14	NVRNMWMW	
Binding clones							
S.1	Vλ1	DPL-3	AAWDDSL**V**	VH1	DP-14	NLNVVDS	220
S.3	Vλ1	DPL-3	AAWDDSL**GA**	VH3	DP-45	ESGAPDS	240
S.7	Vλ1	DPL-3	AAWDDSL**QG**	VH1	DP-7	DHLGAGG	1000
S.9	Vλ3	DPL-16	NSRDSSG**Y**	VH4	DP-67	RVRDRVL	210
S.11	Vλ1	DPL-2	AAWDDSL**SAP**	VH3/VH4	DP-47/ DP-67	STEGEQS	170
S.14	Vλ1	DPL-3	AAWDDSL**LSP**	VH1	DP-10	MYDMQKS	210
Reactive clones							
A.1	Vλ1	DPL-3	AAWDDSL**DAF**	VH4	DP-66	FDAPNTRA	450
A.46	Vλ1	DPL-3	AAWDDSL**FSP**	VH4	DP-66	FGGQQVP	2120
A.5	Vλ1	DPL-3	AAWDDSL**GT**	VH4	DP-65	FGTRGNTH	
A.43	Vλ1	DPL-3	AAWDDSL**SAL**	VH4	DP-65	WMDNT	
A.7	Vλ1	DPL-3	AAWDDSL**GGP**	VH4	DP-71	FGGQQVP	
A.49	Vλ1	DPL-3	AAWDDSL**GT**	VH4	DP-71	HEGPLSAAQ	
A.21	Vλ1	DPL-3	AAWDDSL**RSP**	VH1	DP-3	DREL	
A.17	Vλ1	DPL-5	GTWDSSL**NP**	VH4	DP-67	LTQSSHNDAN	

Covalent selection of reactibody molecule against organophosphorus nerve agents

Griffin.1 scFv library

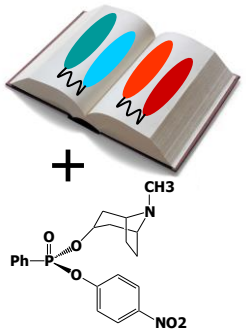

X-phosphonate

Phage-display screening.
Reshetnyak et al, JACS 2007

Conversion of scFv antibodies into full-size antibody
Kurkova IN et. al. Dokl Biochem Biophys. 2009.

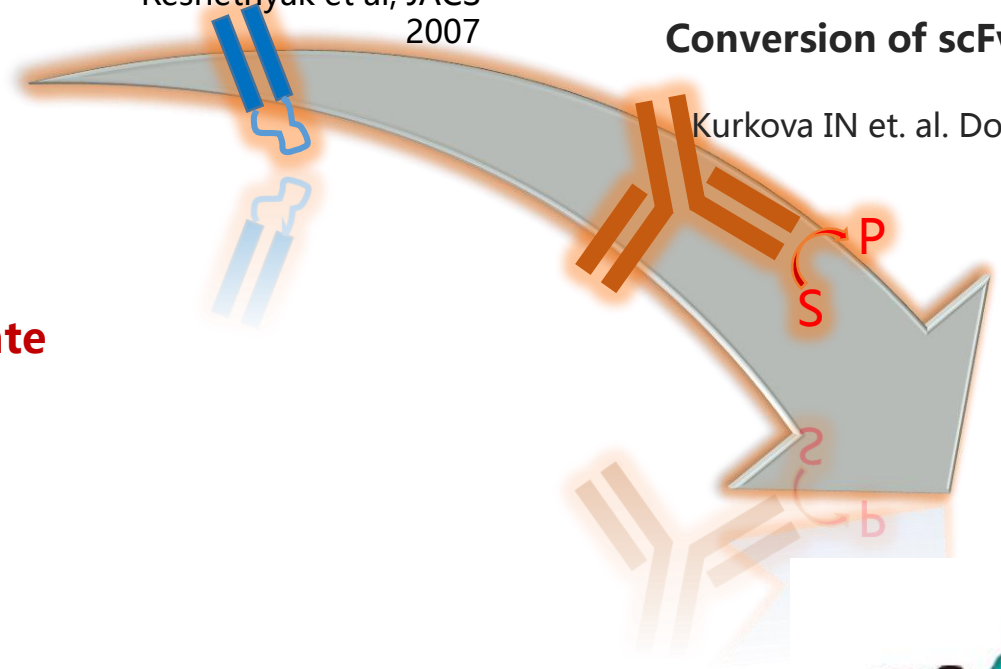

Crystallization and structural

Reactibody A17 forms enzyme-like active center with deep cavity and nucleophilic tyrosine residue on the bottom of the pocket

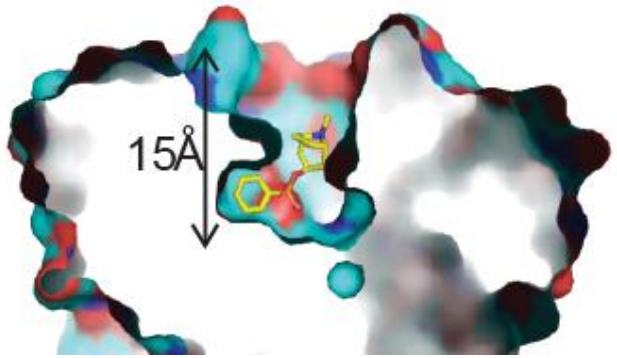

Smirnov et al. PNAS. 2011

Reactibody A17 is predisposed for covalent catalysis.

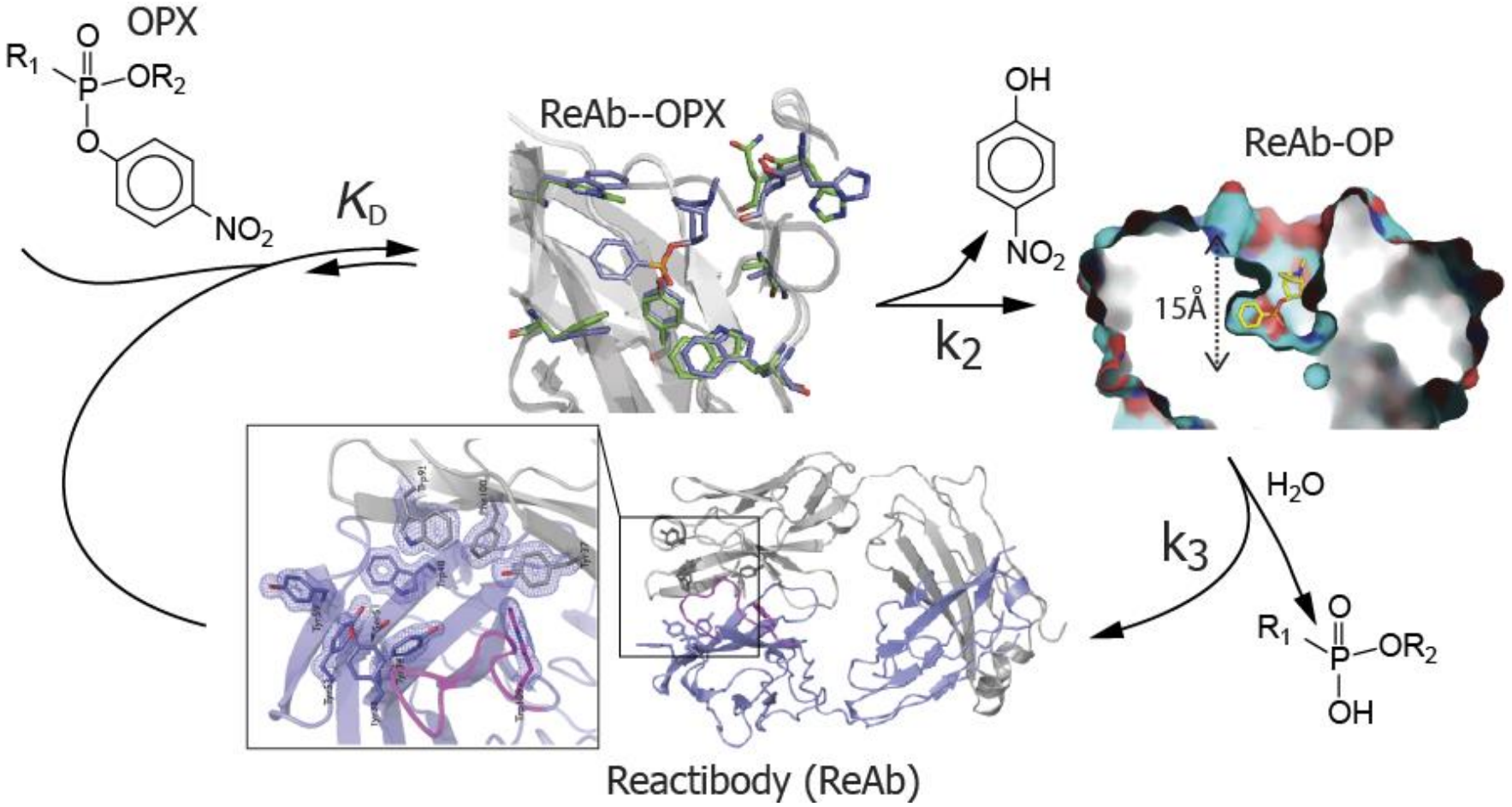

Ponomarenko et al. Acta Chrystal. D, 2014; Smirnov et al., PNAS, 2011

A.17 antibody has unusual deep cavity with nucleophilic tyrosine at its base

I. Smirnov, I. Kurkova et al, PNAS 2011

The pre-existing primitive active site of the A.17 antibody stereo-selectively interacts with P(R)-isomer of the phosphonate molecule

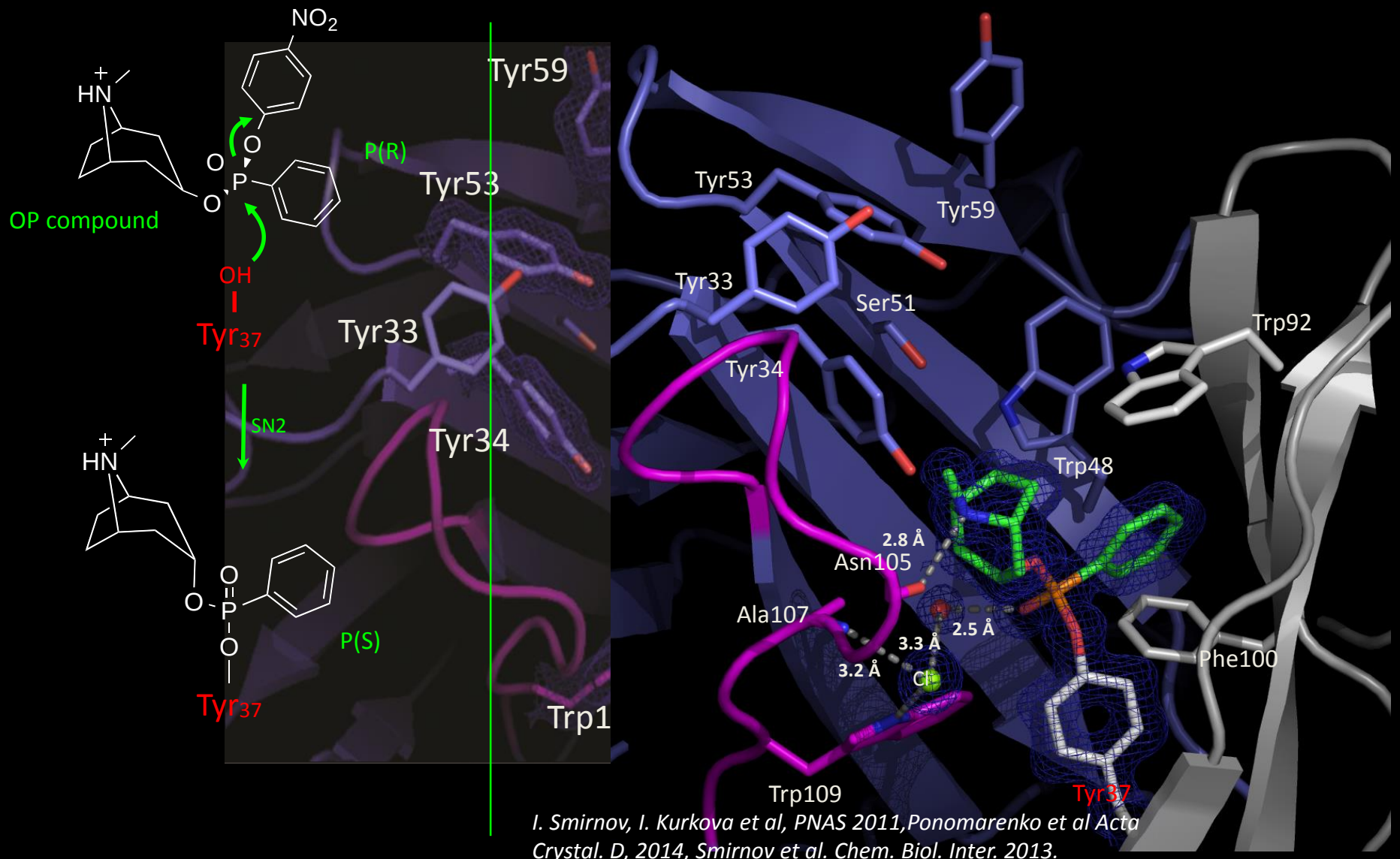

I. Smirnov, I. Kurkova et al, PNAS 2011,Ponomarenko et al Acta Crystal. D, 2014, Smirnov et al. Chem. Biol. Inter. 2013.

MATURATION
IN SILICO

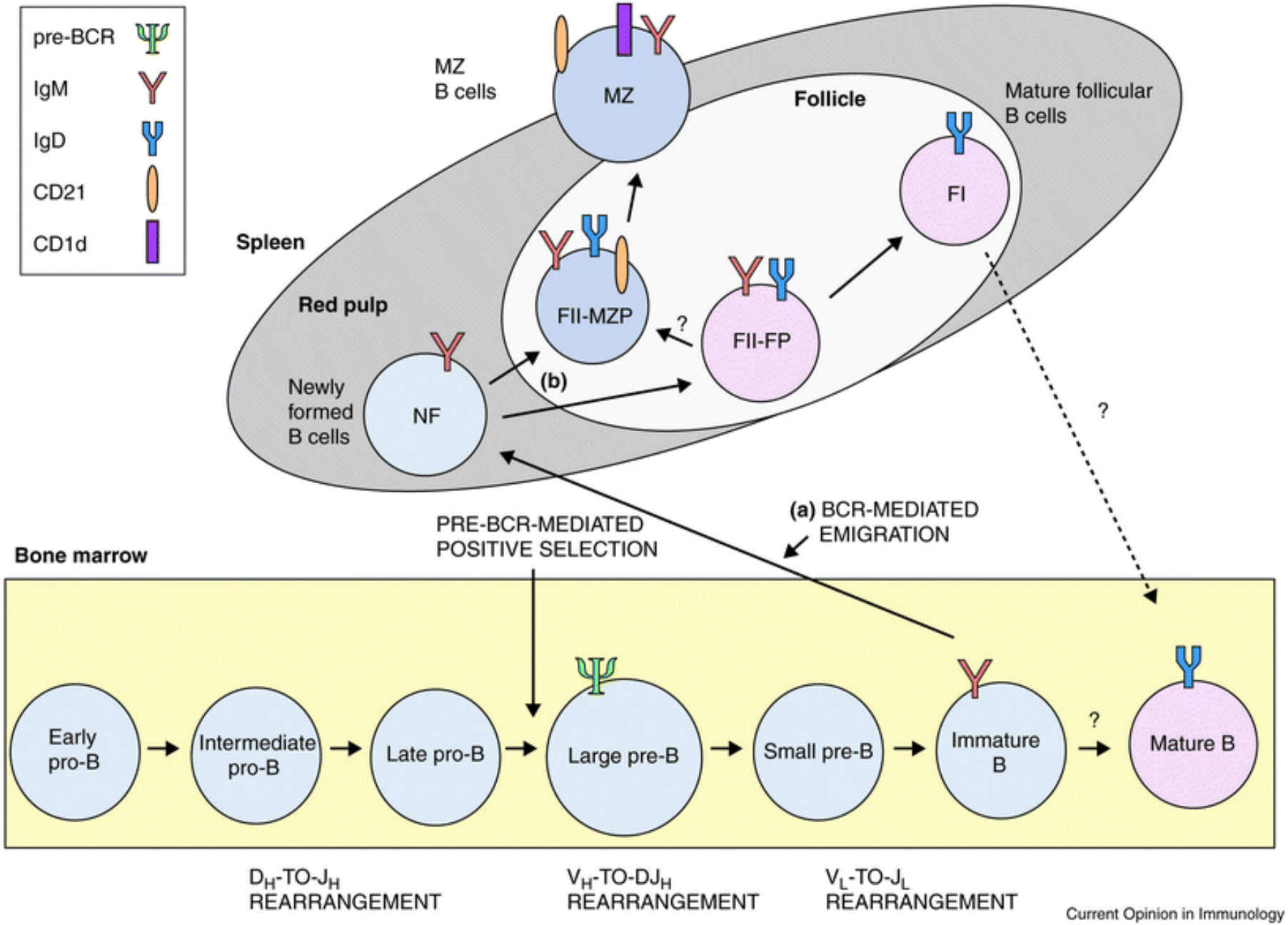
pre-BCR
IgM
IgD
CD21
CD1d
MZ
B cells
MZ
Follicle
Mature follicular
B cells
FI
Spleen
Red pulp
FII-MZP
?
FII-FP
Newly
formed
B cells
NF
(b)
?
PRE-BCR-MEDIATED
POSITIVE SELECTION
(a) BCR-MEDIATED
EMIGRATION
Bone marrow
Early
pro-B
Intermediate
pro-B
Late pro-B
Large pre-B
Small pre-B
Immature
B
?
Mature B
D_H-TO-J_H
REARRANGEMENT
V_H-TO-DJ_H
REARRANGEMENT
V_L-TO-J_L
REARRANGEMENT
Current Opinion in Immunology

BioCat Lab

MESSAGE

Expanded opportunity to mimic several transition states and select optimal substrate and product orientations

MESSAGE: Combination of instrumental and computational methods may be regarded as an efficient strategy to obtain artificial biocatalysts/binders *de novo*

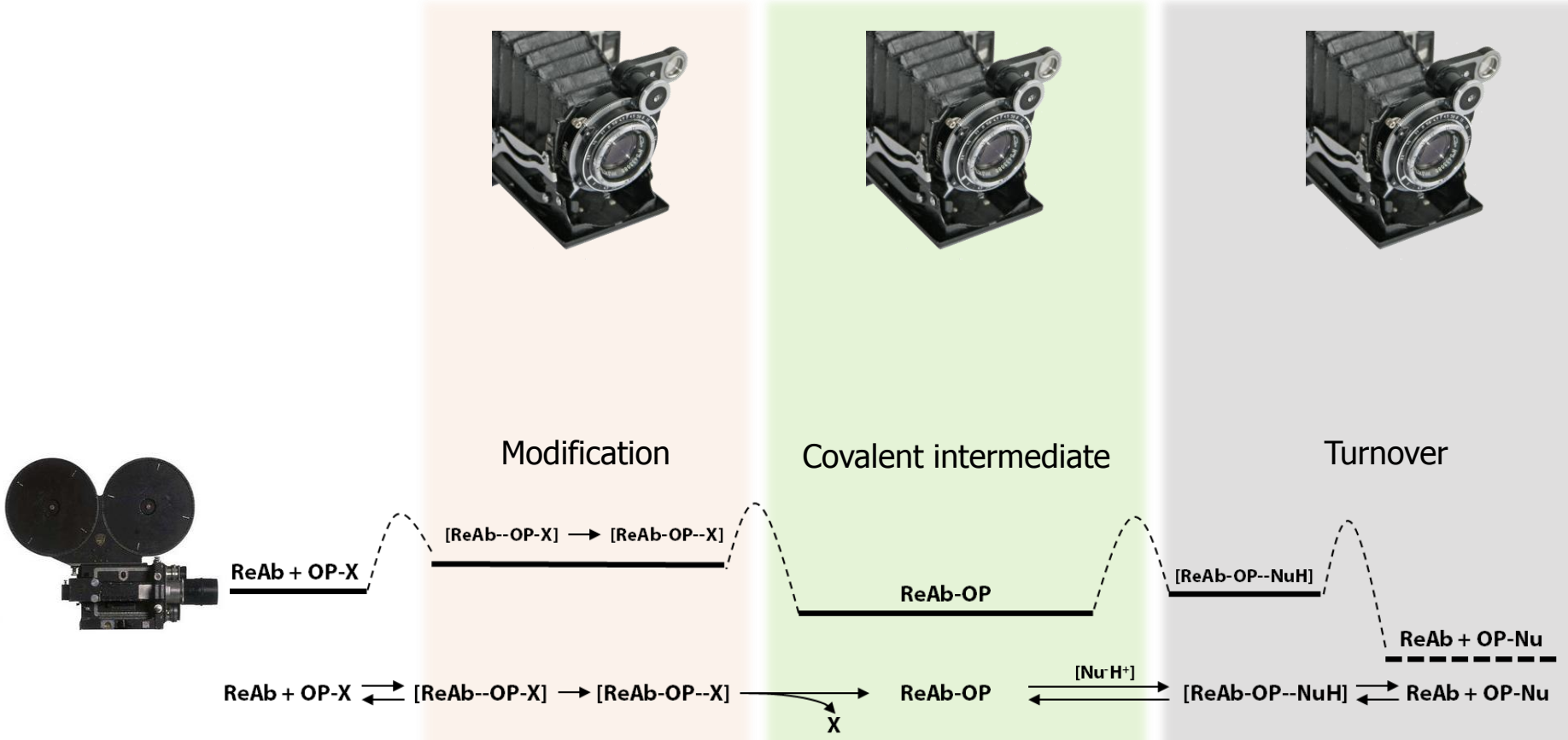

Hybrid QM/MM and MD approach

The *in silico* maturation scheme

We selected 23 amino acids which when mutated to Arg could form a H-bond (≤3.2 Å) with the phosphate moiety of paraoxon

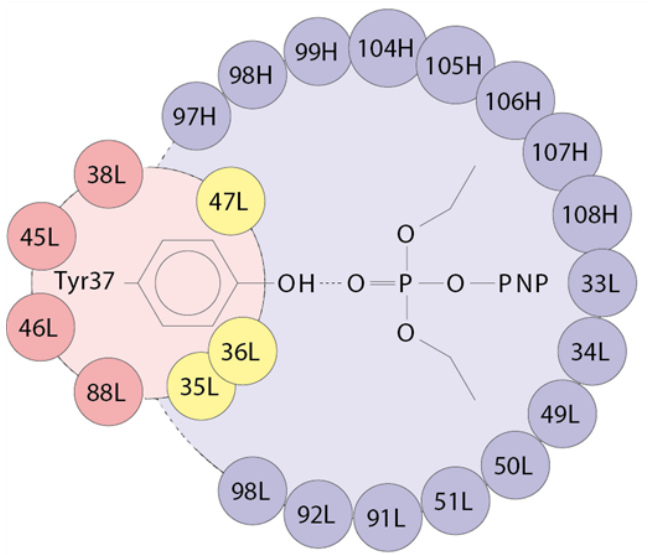

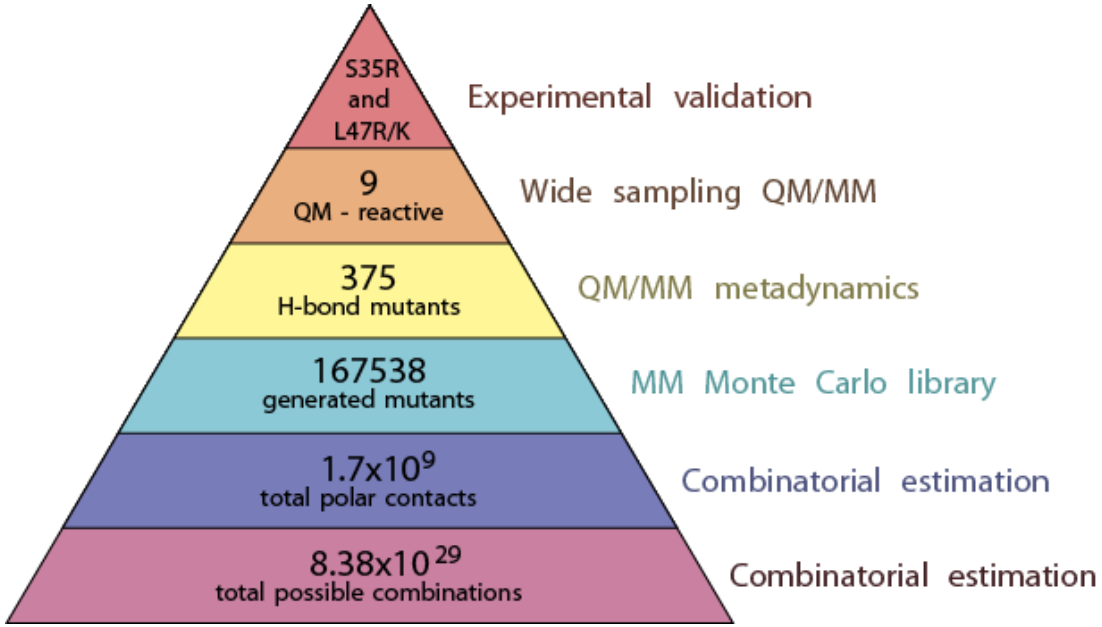

Stages of rational restriction of library size:

1. Limiting to 11 polar residues and restricting permutations to four-at-a-time
2. Programming of 7 H-bond-donor amino acids (Arg, His, Lys, Ser, Thr, Trp, Tyr) and 3 of Glu, Asp, and Ser mutations to provide general acid-base catalysis for Tyr37

The QM/MM calculations revealed:

(i) systems with an anionic amino acid mutation did not deliver covalent reaction

(ii) the best successful runs resulted from Arg, Lys and His in positions 35, 47 of the light chain

Smirnov et al. Science Adv. 2016

Synergy of QMMM and funnel metadynamics allows to generate catalytic antibody variants with high reactivity and stereospecificity

QMMM

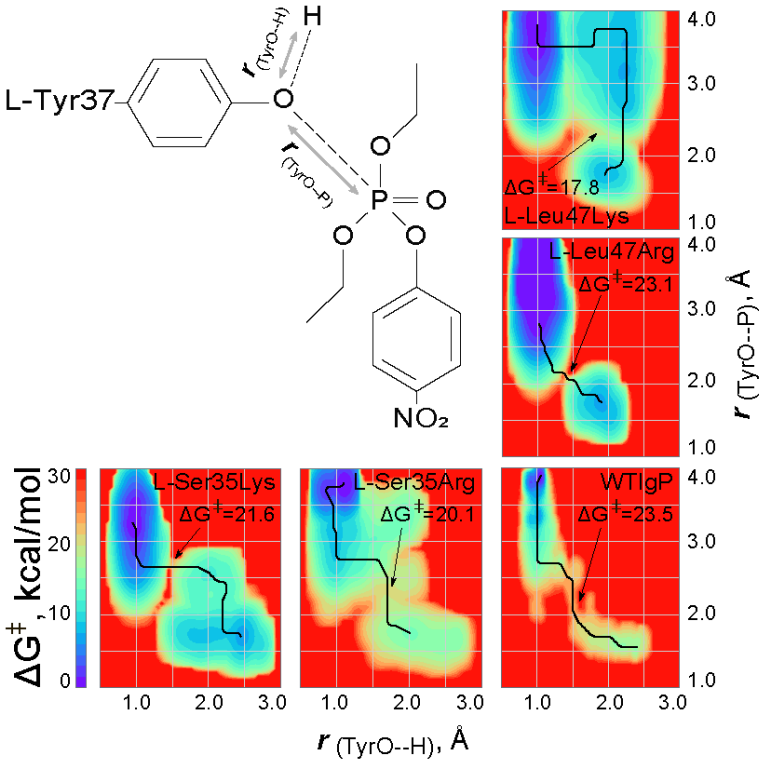

Funnel metadynamics

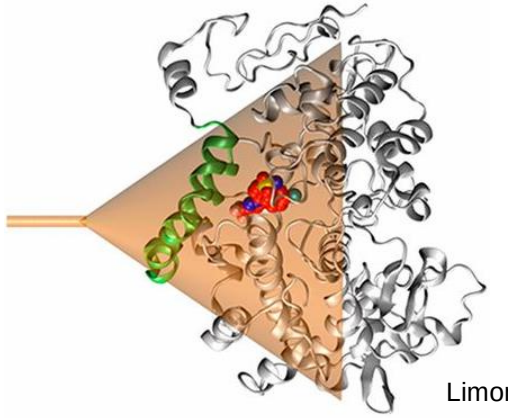

Limongelli et al., PNAS 2013

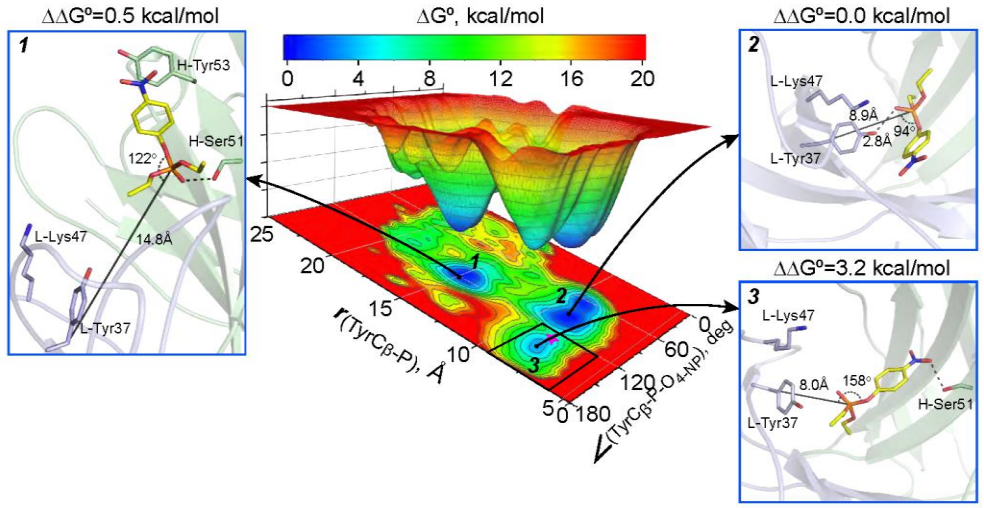

Mokrushina et al., PNAS 2020

Mechanism of paraoxon hydrolysis by Ig-paraoxonase.

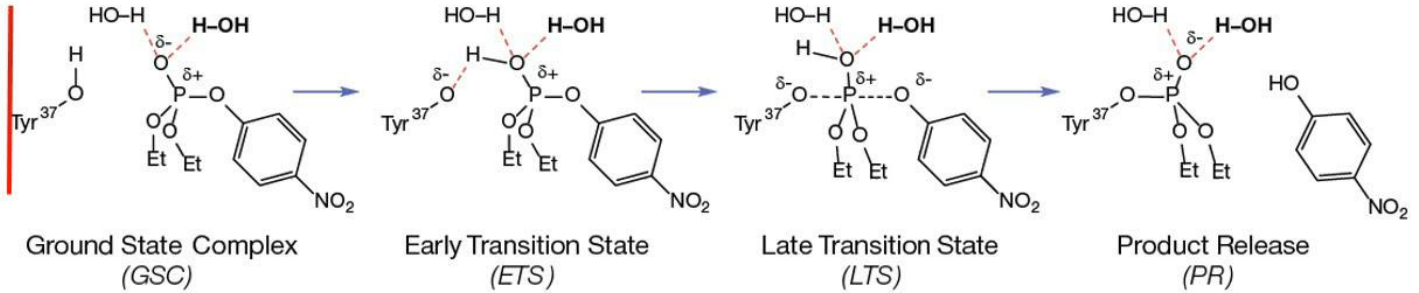

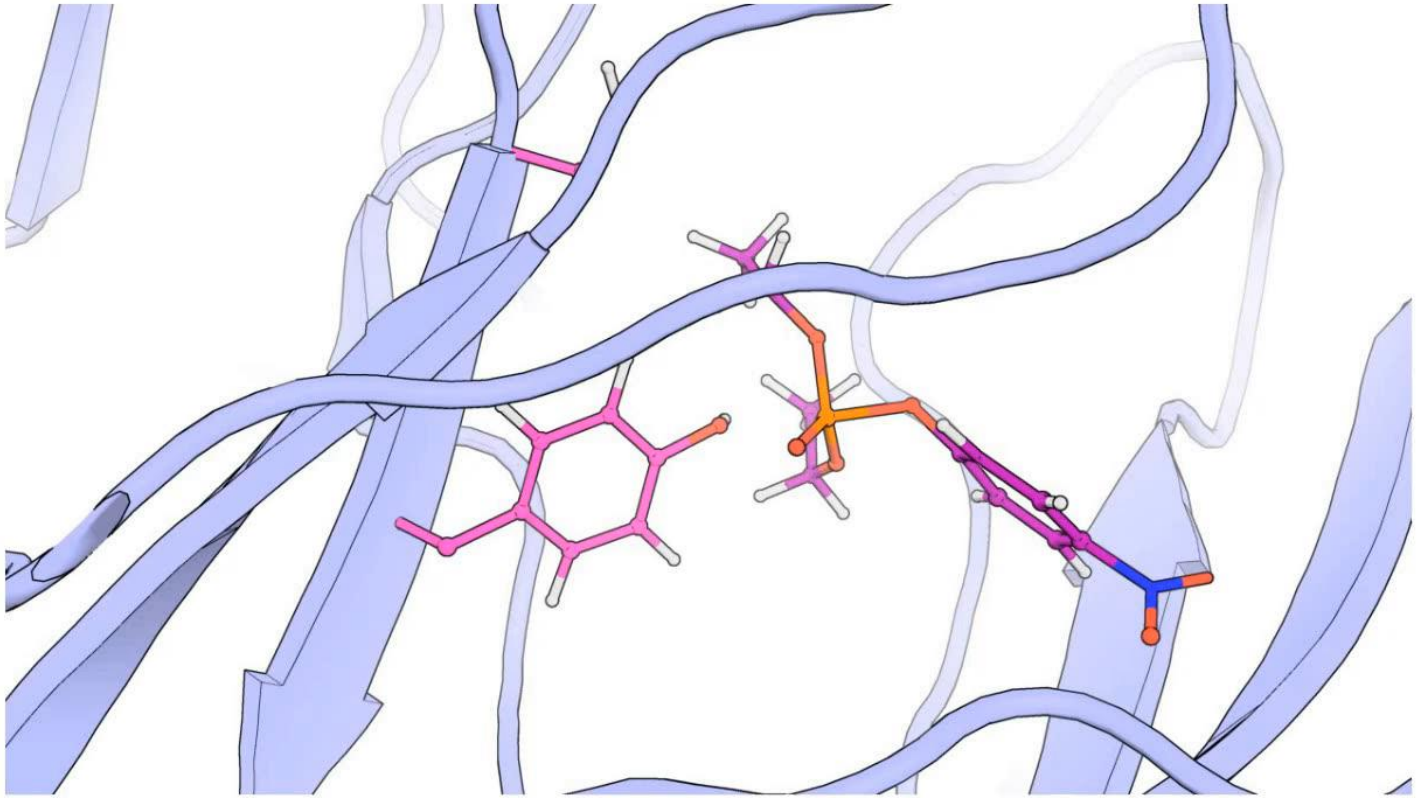

The QM computed mechanism of TS development for step 1 of WTIgP reaction with paraoxon; the classic $S_N2(P)$ mechanism with tbp geometry is initiated by early proton transfer followed in 5-20 fs by late TS O–P bond formation.

Directed evolution of novel biocatalysts

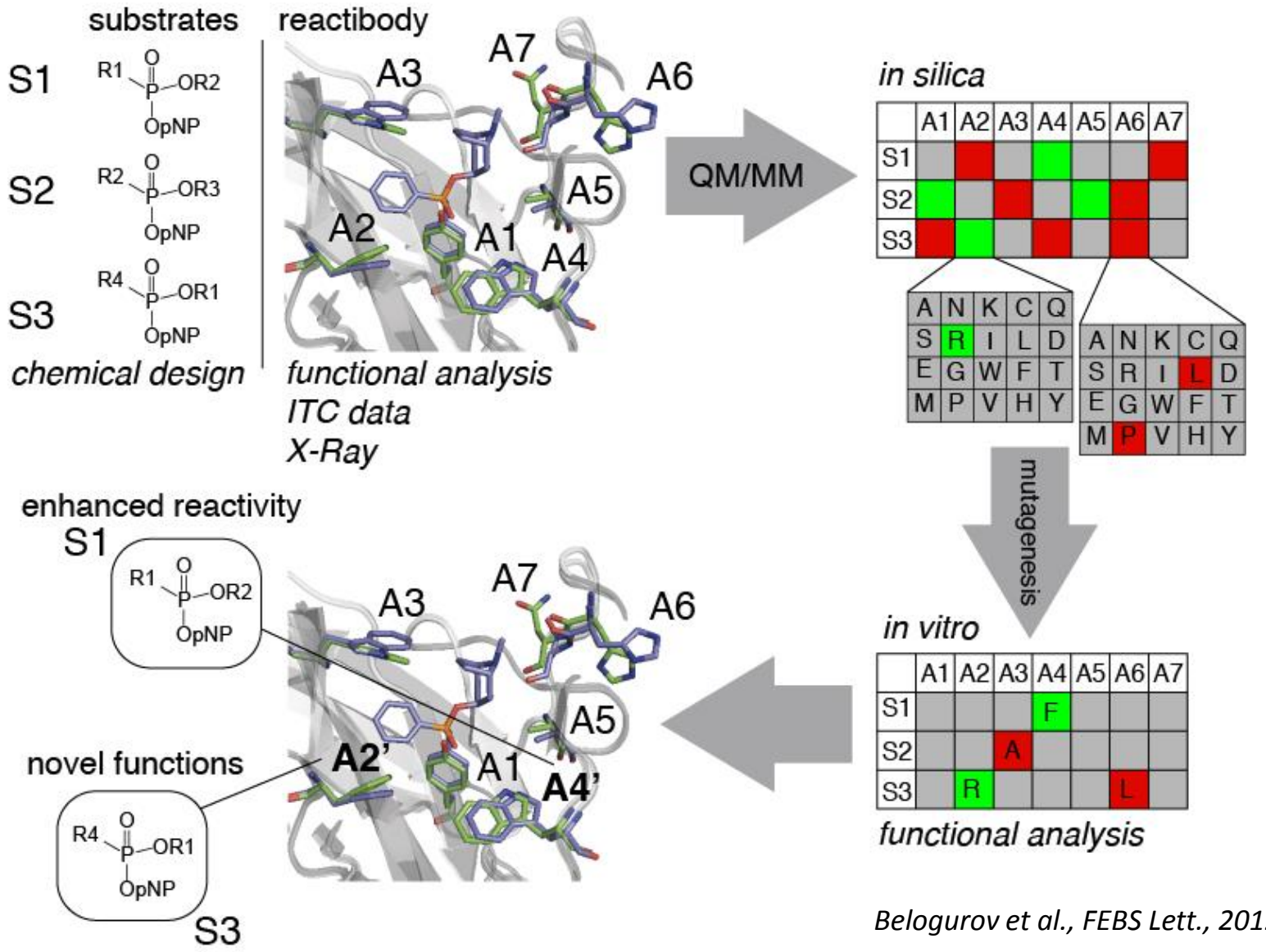

Belogurov et al., FEBS Lett., 2012

Microfluidic platform for ultrahigh-throughput screening of biodiversity

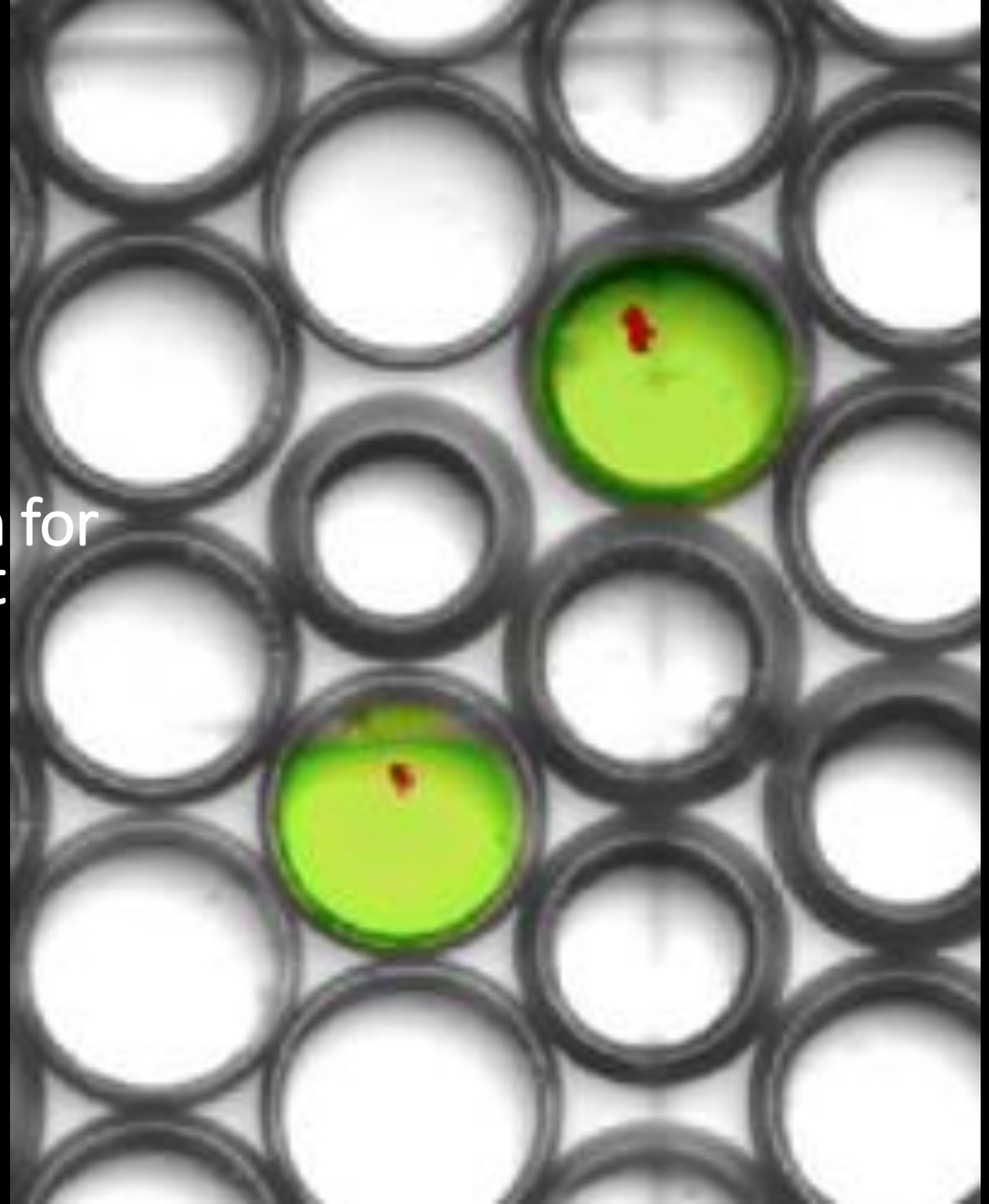

Universal screening techniques

Binding

(Phenotype – formation of complex)

1. SELEX
2. Ribosome display
3. mRNA display
4. Phage display
5. Cell display

Genotype

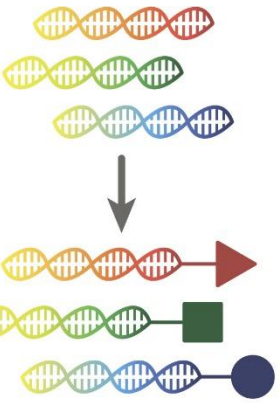

(Phenotype – any product)

***In vitro* compartmentalization**

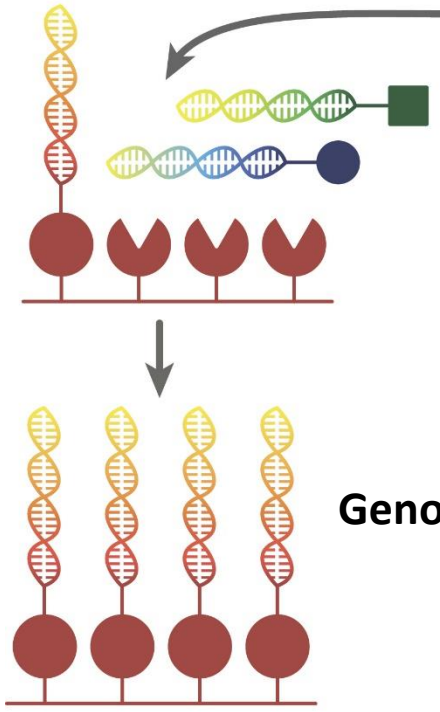

Genotype-phenotype linkage

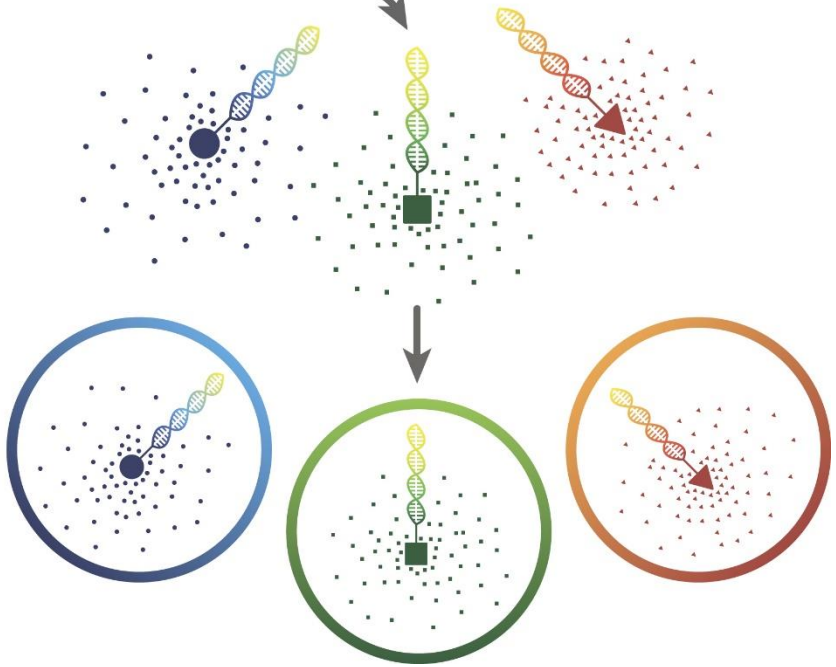

Скрининг в «каплях» – искусственных клетках

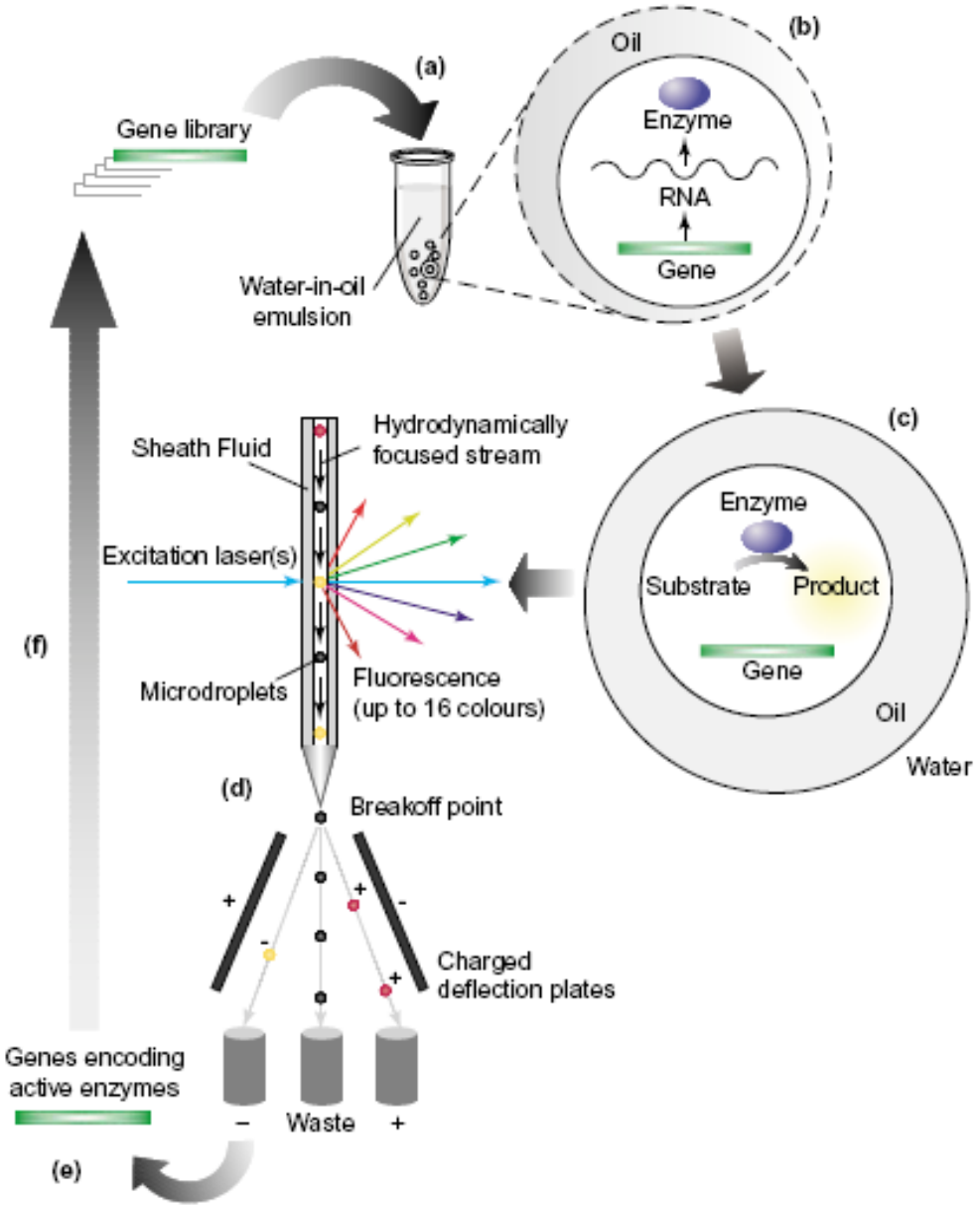

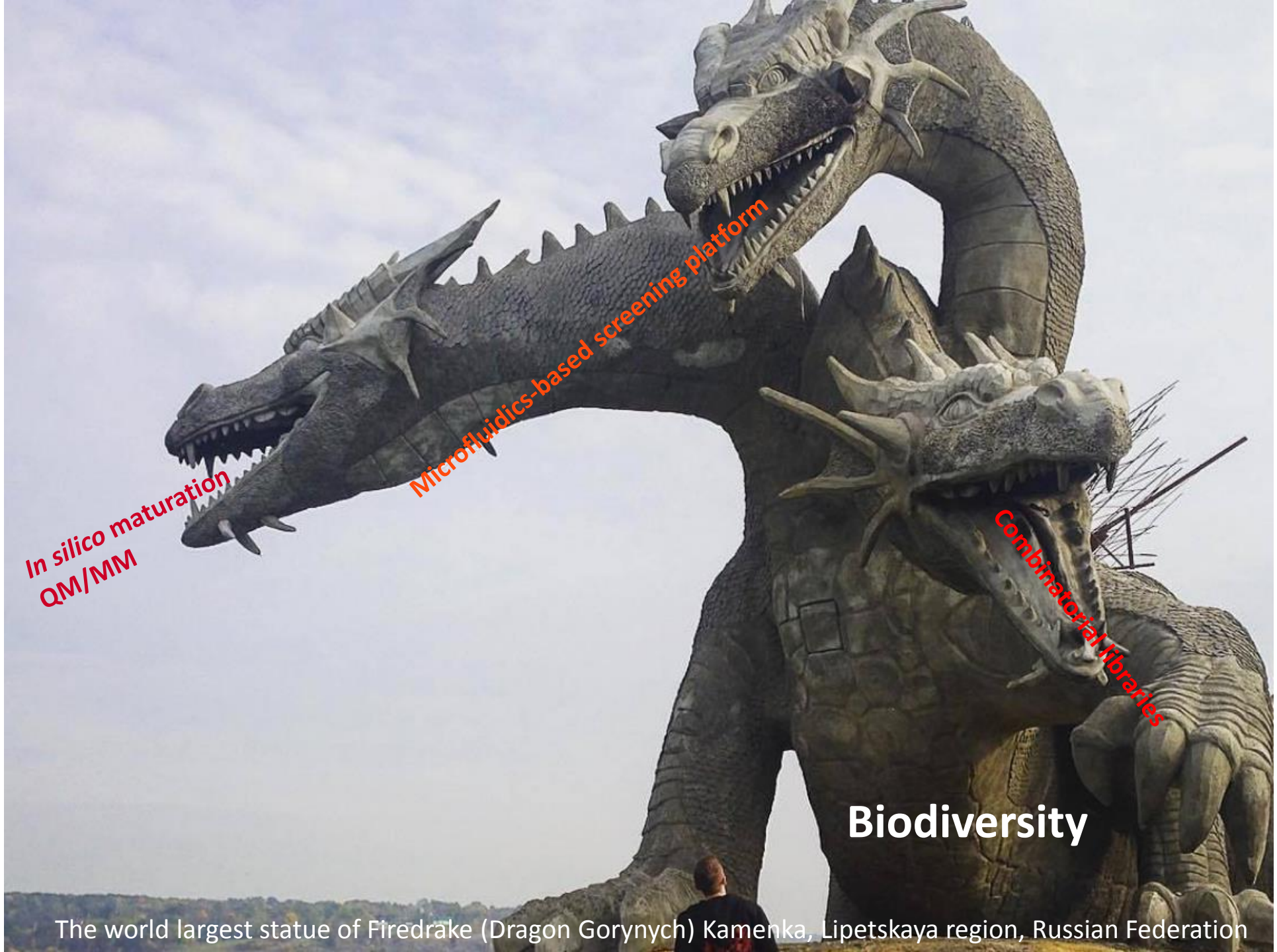

The world largest statue of Firedrake (Dragon Gorynych) Kamenka, Lipetskaya region, Russian Federation

Microfluidic platform for ultrahigh-throughput screening

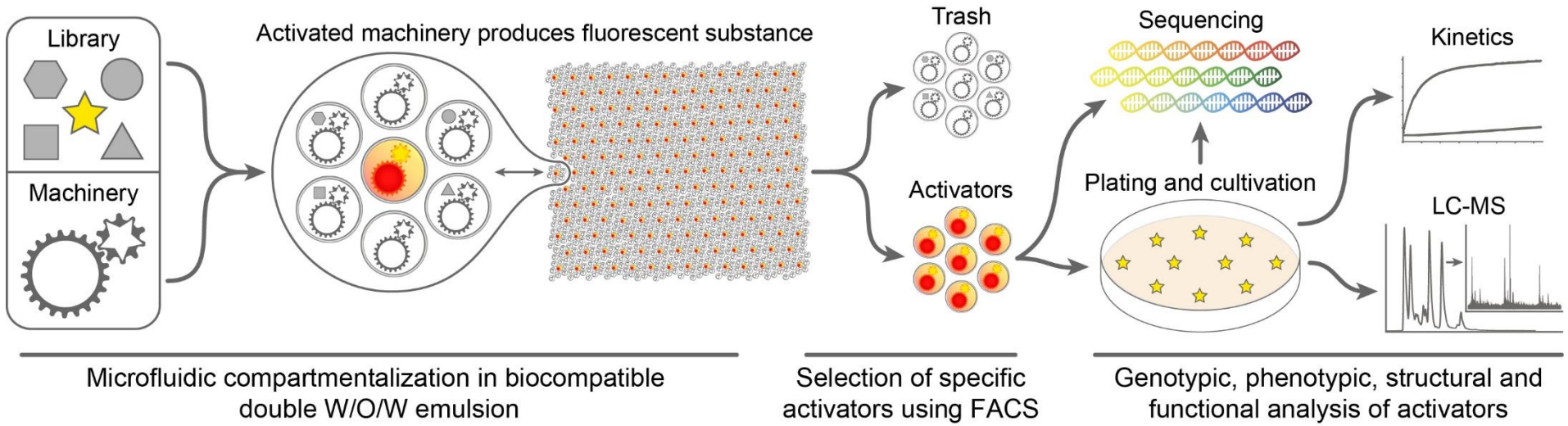

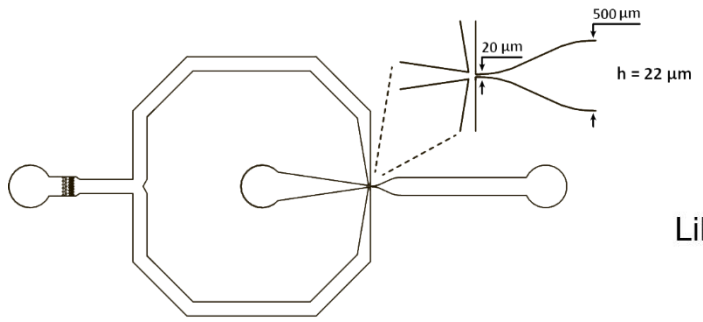

20 µm microfluidic chip

Terekhov et al., PNAS 2017

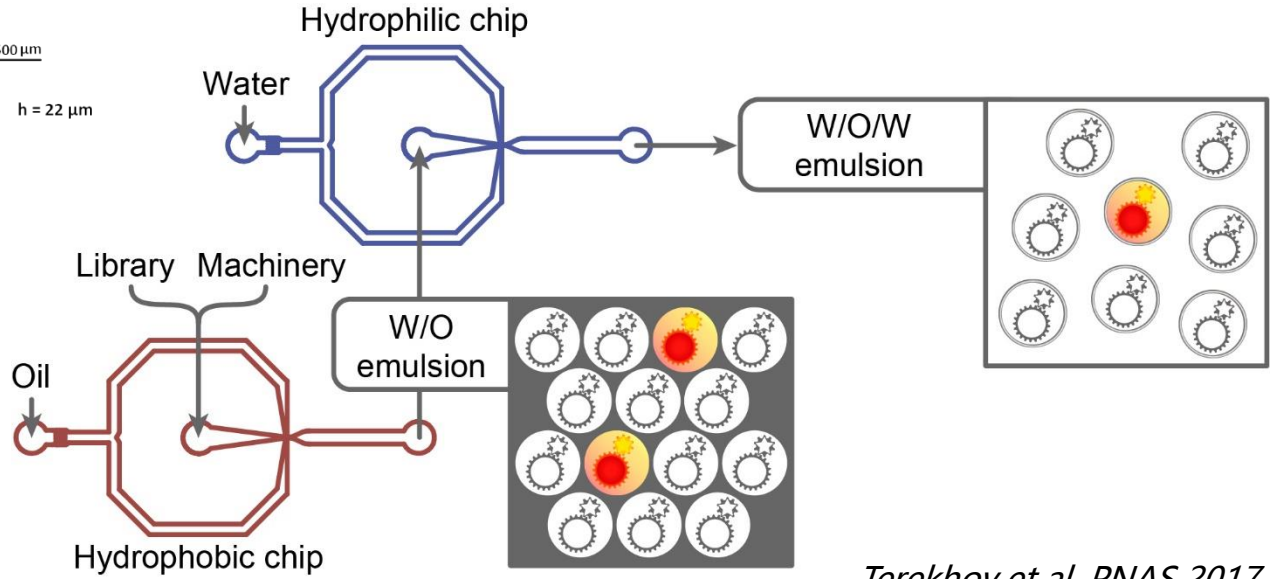

Terekhov et al. PNAS 2017

MESSAGE

Ultrahigh-throughput screening (uHTS) techniques can identify unique functionality from millions of variants.

Selection of novel BChE mutants with artificial activity

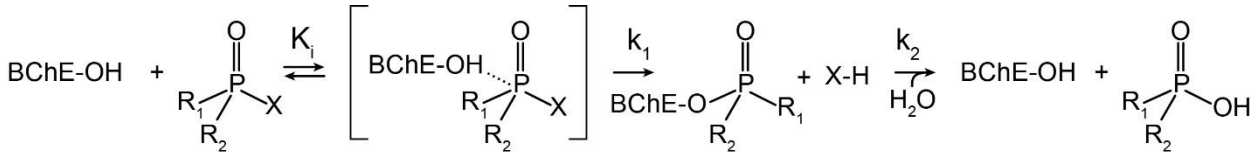

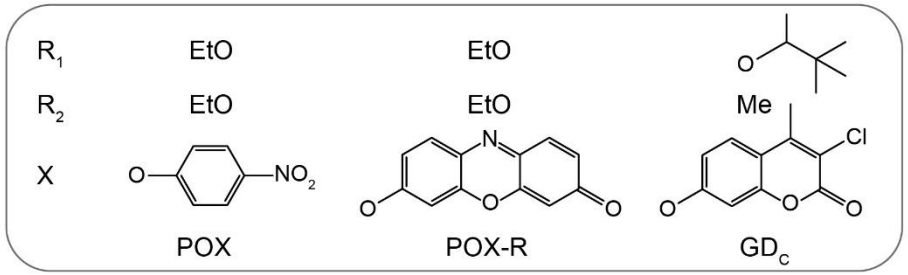

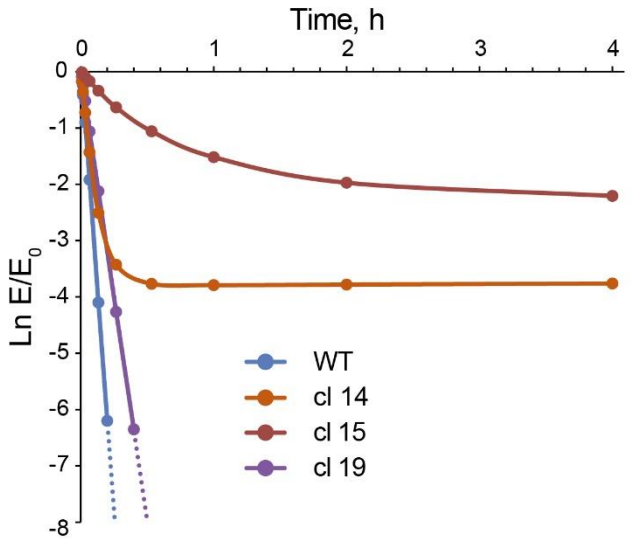

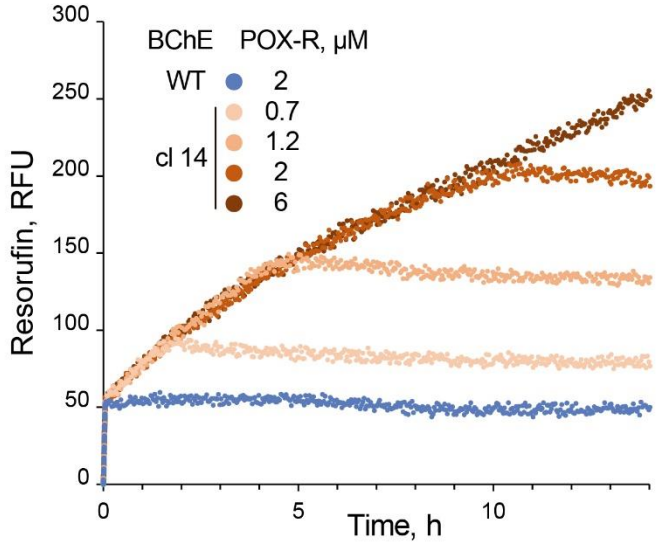

OP	POX				GD_C			
BChE	WT	Selected		Negative control	WT	Selected		Negative control
		cl 14	cl 15	cl 19		cl 14	cl 19	cl 15
k_1/K_i x10^{-1}, $M^{-1}c^{-1}$	290±30	260±40	25±4	140±20	3±1	0.5±0.1	0.05±0.01	2.0±0.5
k_2 x10^4, c^{-1}	-	1.0±0.1	1.1±0.1	-	-	-	-	-

Terekhov et al. PNAS 2017

Selection of *S. aureus* killers from oral microbiota

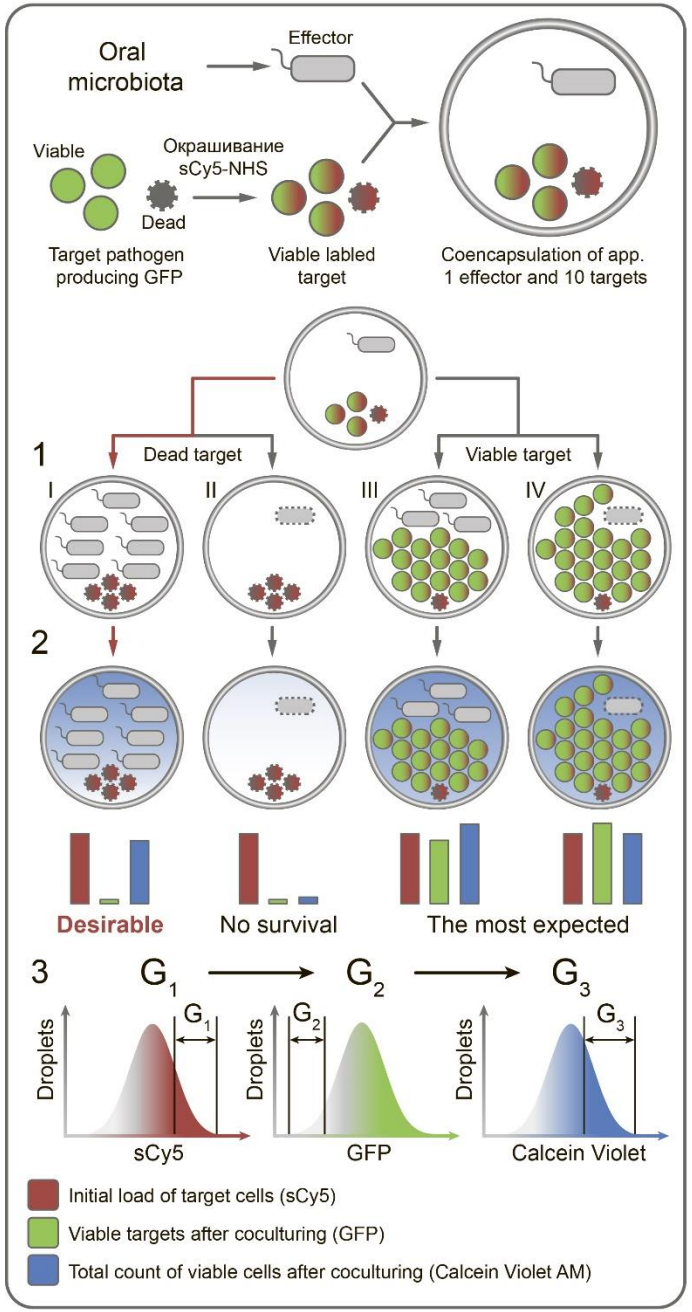

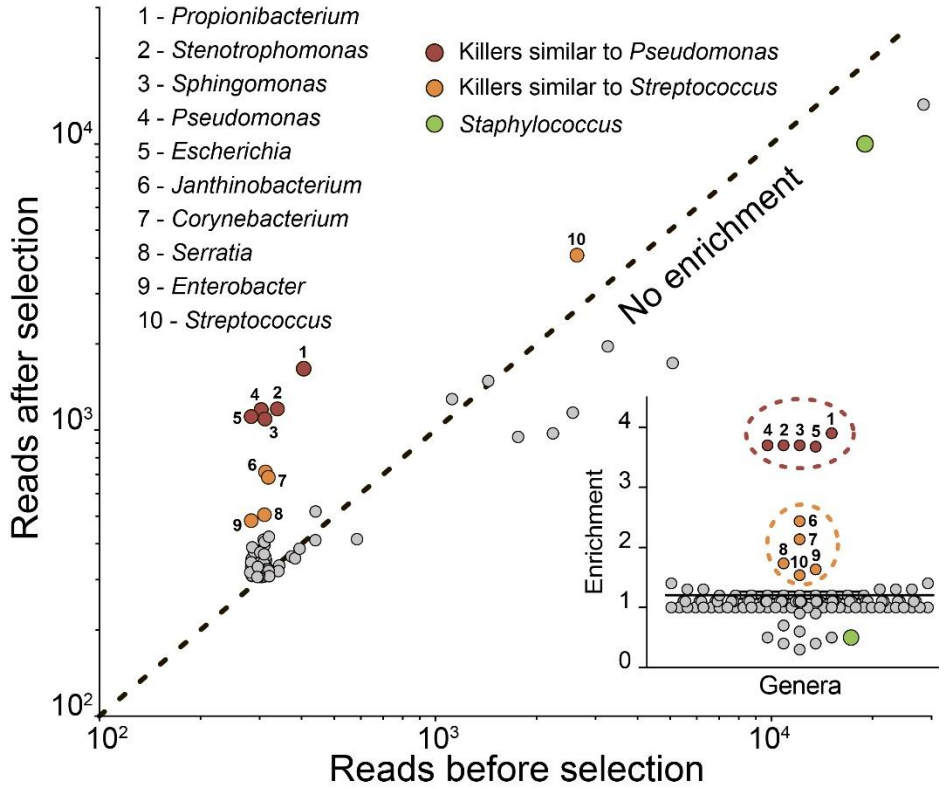

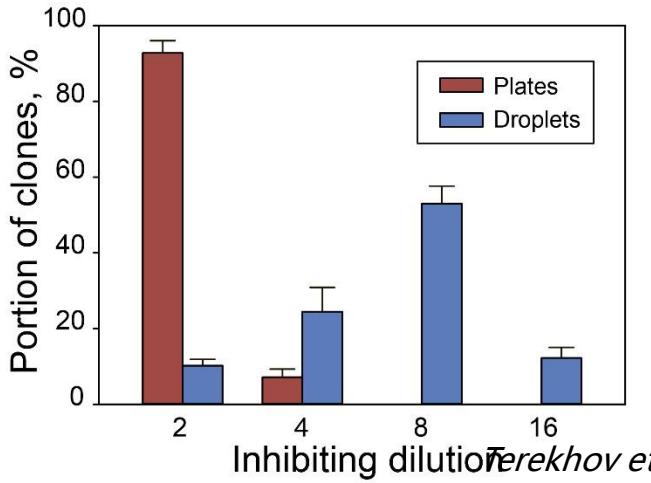

Terekhov et al. PNAS 2017

Oral microbiota of Siberian bear as an alternative source of *S. aureus* killers and antibiotic producers

New bacterial strains efficiently inhibiting *S. aureus* growth were selected using the developed microfluidic platform

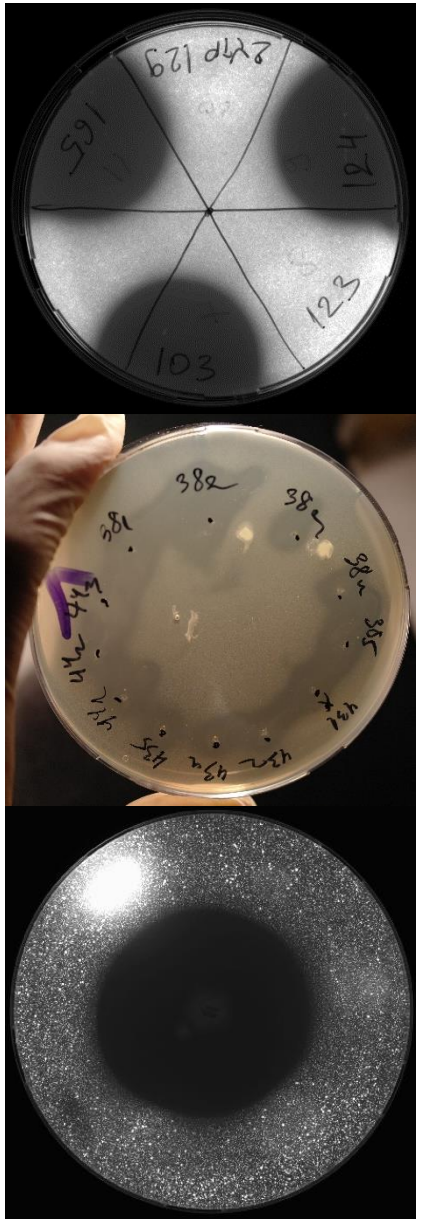

Oral microbiota of Siberian bear as an alternative source of *S. aureus* killers and antibiotic producers

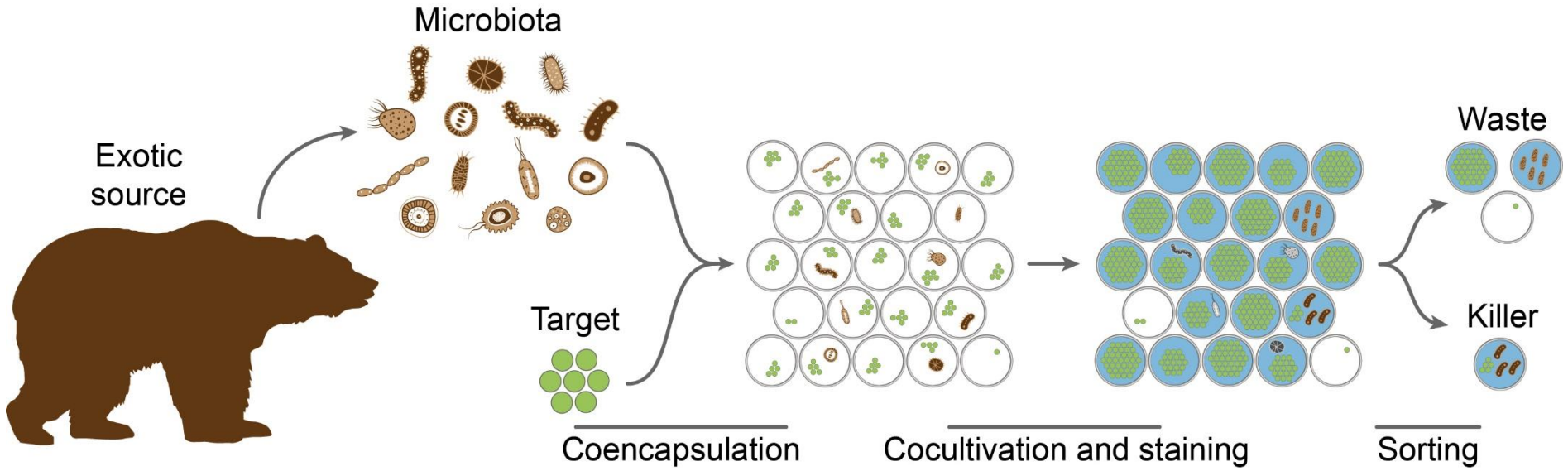

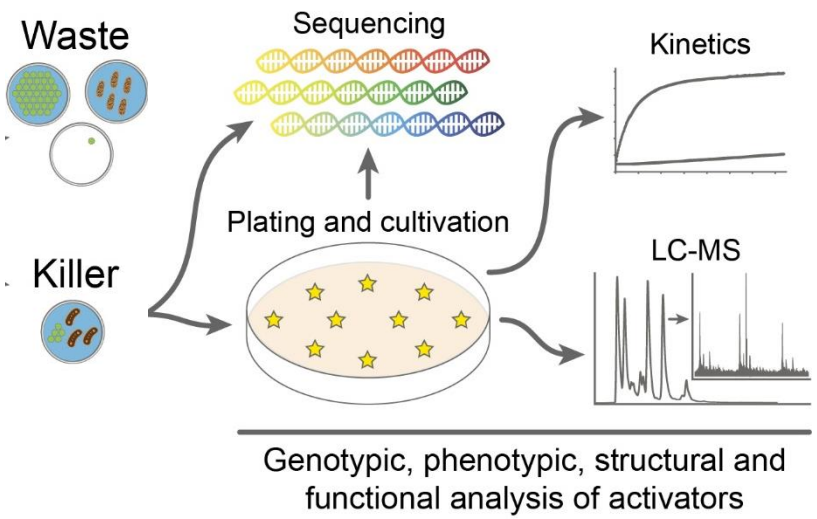

Terekhov, Smirnov et al., PNAS 2018

Multi-omics approach that was applied for discovery of regulation of Ami production

Genome analysis

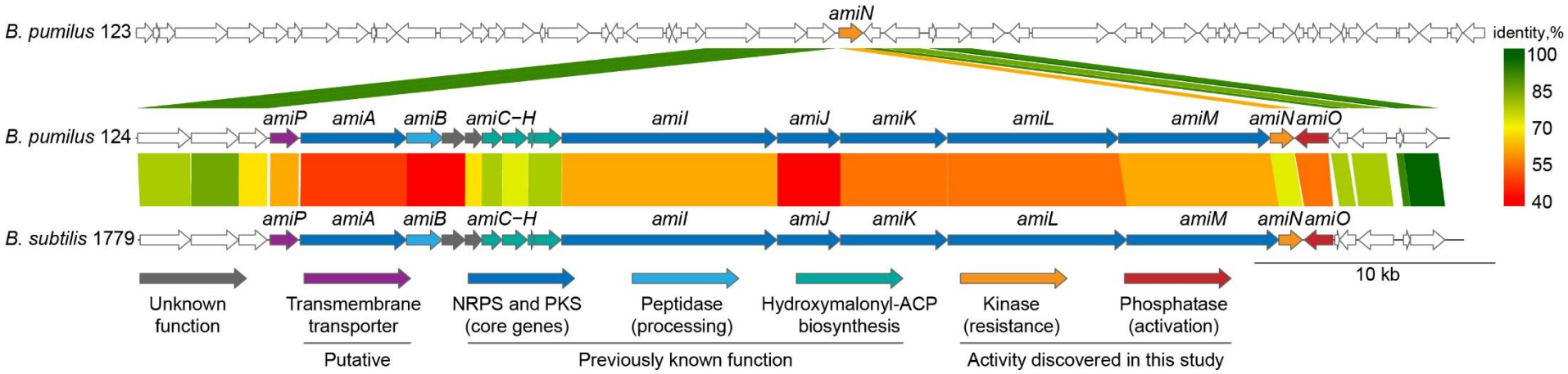

Proteome analysis

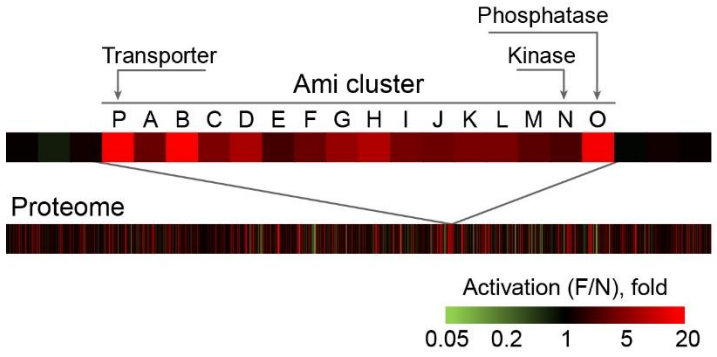

Terekhov, Smirnov et al., PNAS 2018

Amicoumacin A activity regulation

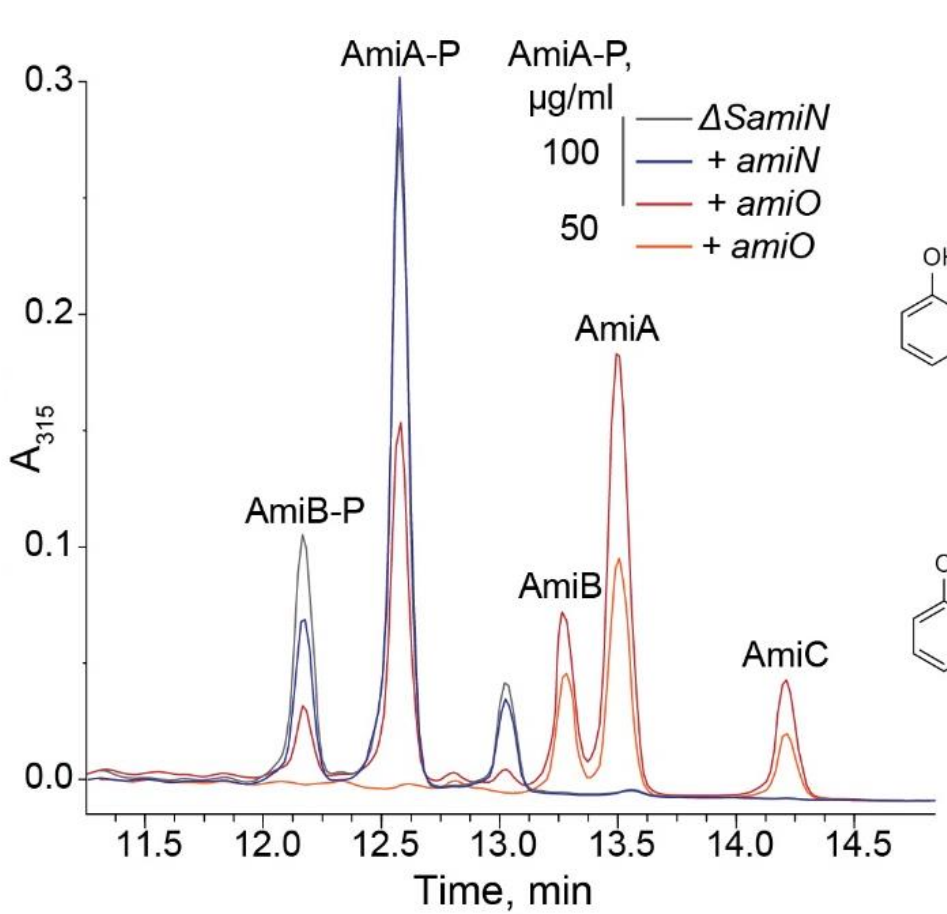

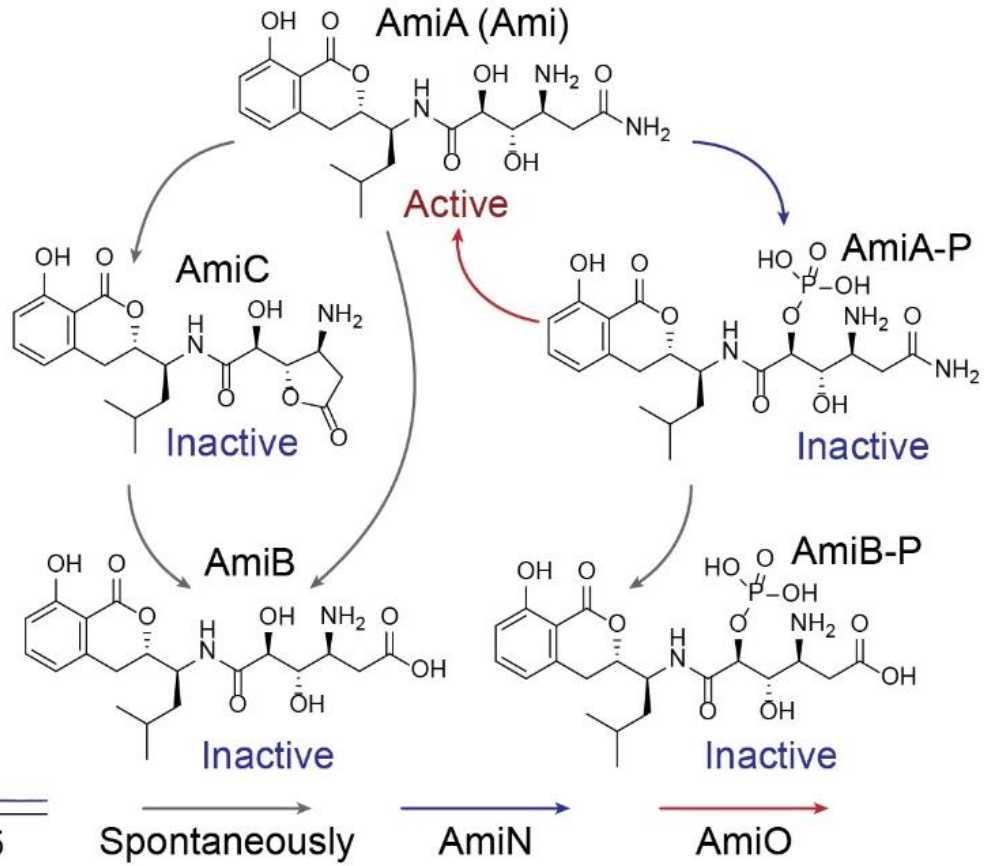

Terekhov, Smirnov et al., PNAS 2018

Amicoumacin kinases are very fast enzymes

Enzymes	k_{cat}, sec^{-1}	K_M, μM	k_{cat}/K_M, $sec^{-1}M^{-1}\times10^6$
AmiN	1.3±0.25	0.005±0.001	270±120
hAmiN	0.4±0.09	0.004±0.002	90±60
SubAmiN	1.5±0.2	0.05±0.008	30±9
3′-aminoglycoside O-phosphotransferase type IIIa (Kanamycin-kinase)	1.8±0.1	13±3	0.14±0.04
3′-aminoglycoside O-phosphotransferase type IIa (Amikacin-kinase)	0.5±0.2	720±300	0.0007±0.0.0005
Aminoglycoside-2″-O-nucleotidyltransferase	2.5±0.3	1.0±0.4	2.5±1.3
3’-Aminoglycoside N-acetyltransferase I	1.0±0.3	2.1±0.5	0.5±0.2
Penicillinase (Benzylpenicillin)	2000±800	50±15	40±28

Reaction conditions: 20 mM HEPES, 50 mM NaCl, 1 mM $MgCl_2$

Terekhov at all Science adv 2020

There is NO reaction in presence EDTA or Ca^{2+}

Reaction of amicoumacin kinases with substrate leads to close conformation of enzyme

Front

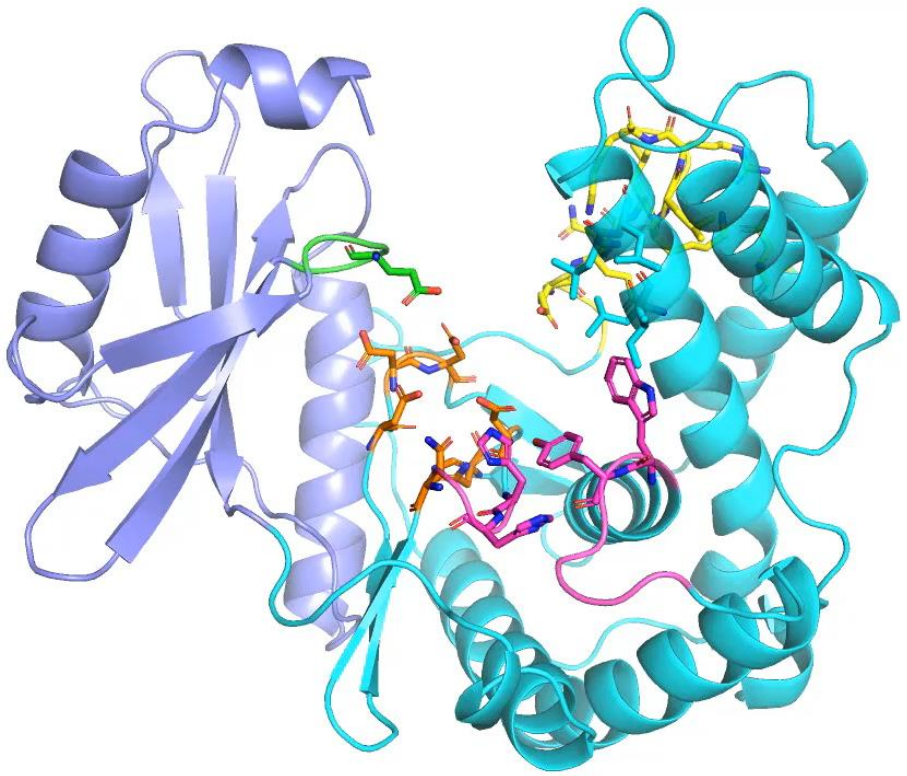

Up

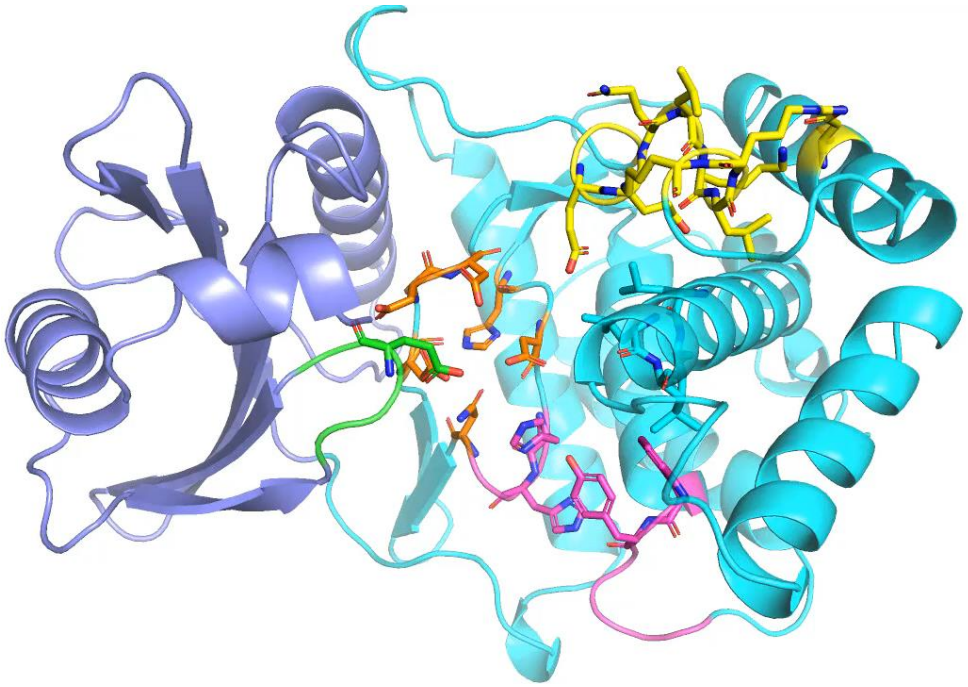

AmiN QM/MM simulations

Terekhov et al., Sci Adv. 2020

Atomistic details of the reaction

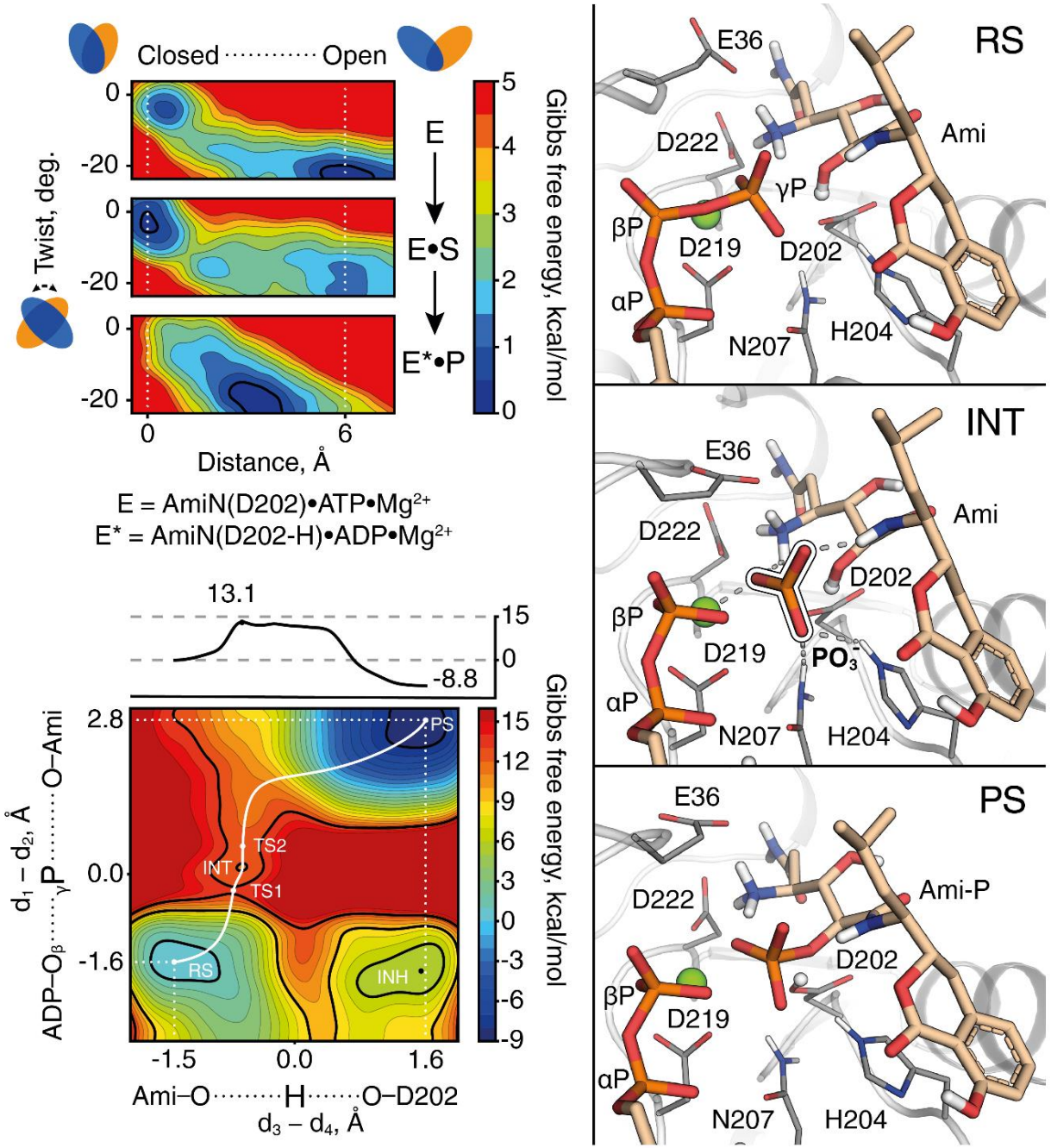

Terekhov et al., Sci Adv. 2020

The kinetic restriction of substrate promiscuity stems from the substrate-driven closure in the case of small-molecule kinases

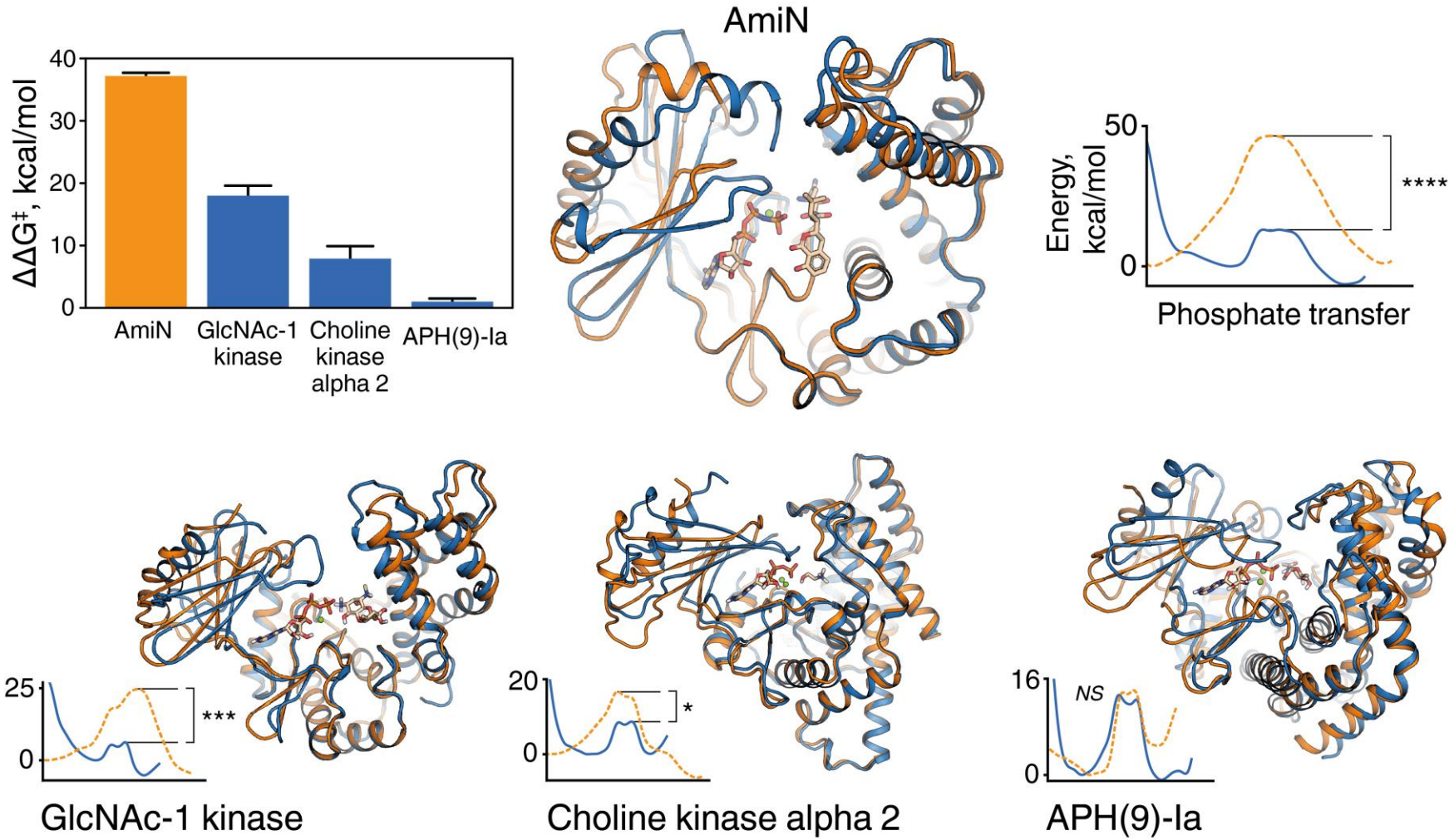

Terekhov et al., Sci Adv. 2020

Analysis of specificity of AmiN kinase

AmiN, hAmiN, SubAmiN were inactive against:

<u>Aminoglycosides</u>

- Kanamycin
- Gentamicin

<u>Macrolides</u>

- Erythromycin
- Tylosin

<u>Tetracycline class</u>

- Tetracycline
- Doxycycline

AmiN derived from protein kinase?

Peptides

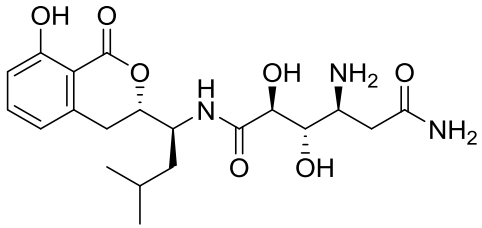

Ami

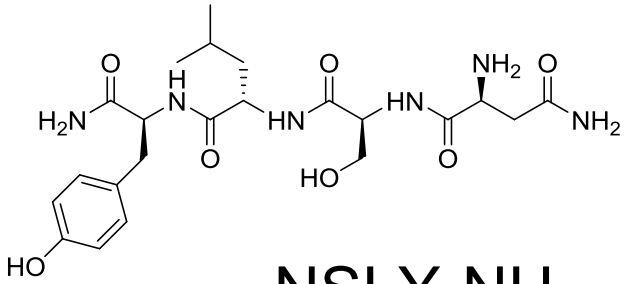

$NSLY\text{-}NH_2$

AmiN

No phosphorylation of

$NSLY\text{-}NH_2$ $NSL\text{-}NH_2$ $SLY\text{-}NH_2$ $SL\text{-}NH_2$

AmiN kinase is a protein kinase!

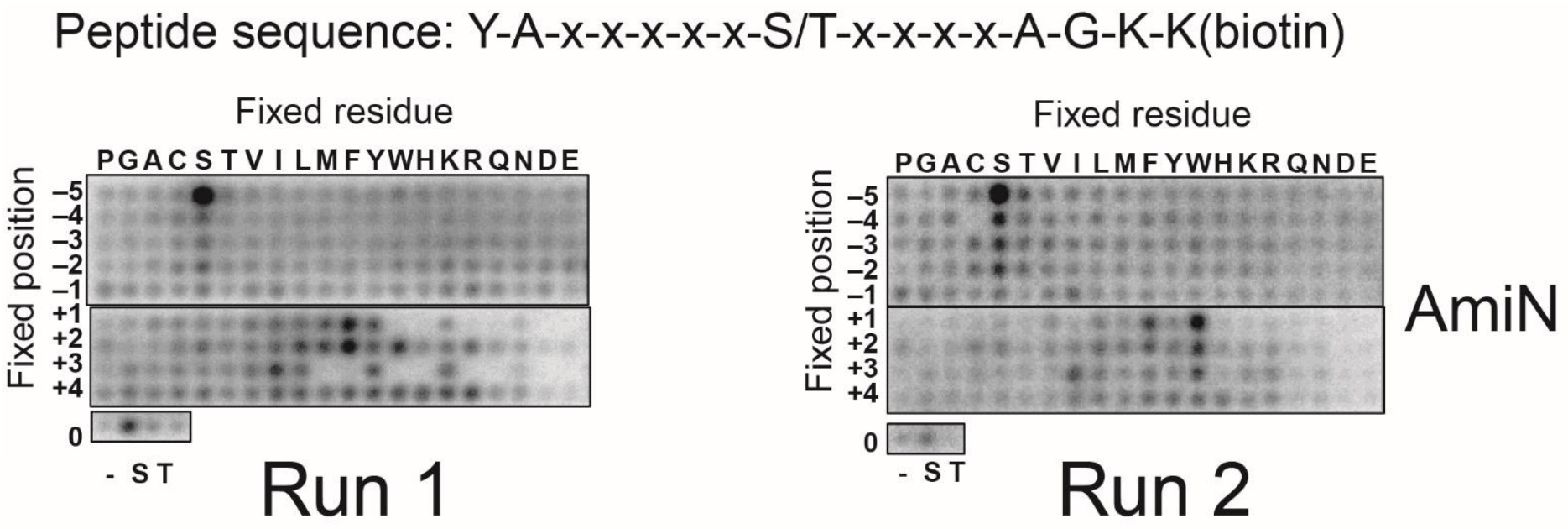

Potential peptide substrates: Y-A/L-S, P/R/I-S-W

Thanks to Benjamin Turk, Yale University

Rational design of semisynthetic antibiotics

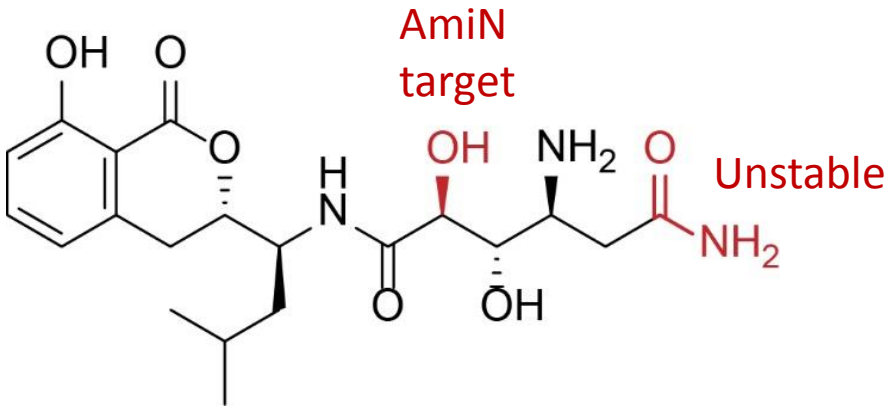

Identification of Ami weak points

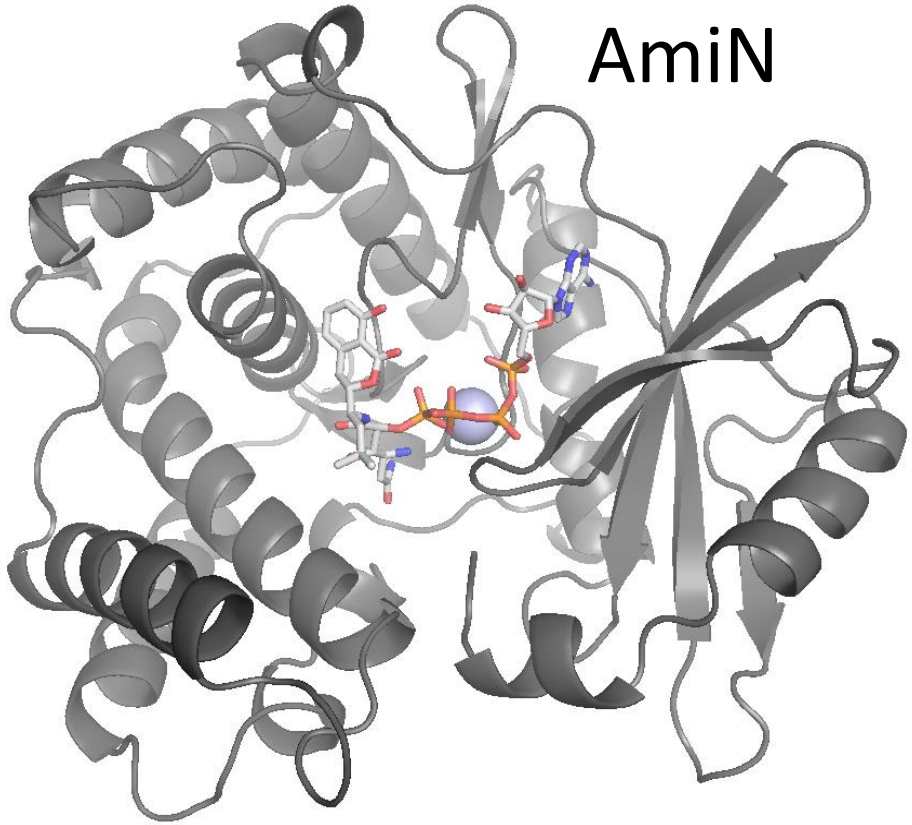

Total synthesis and SAR analysis of analogs

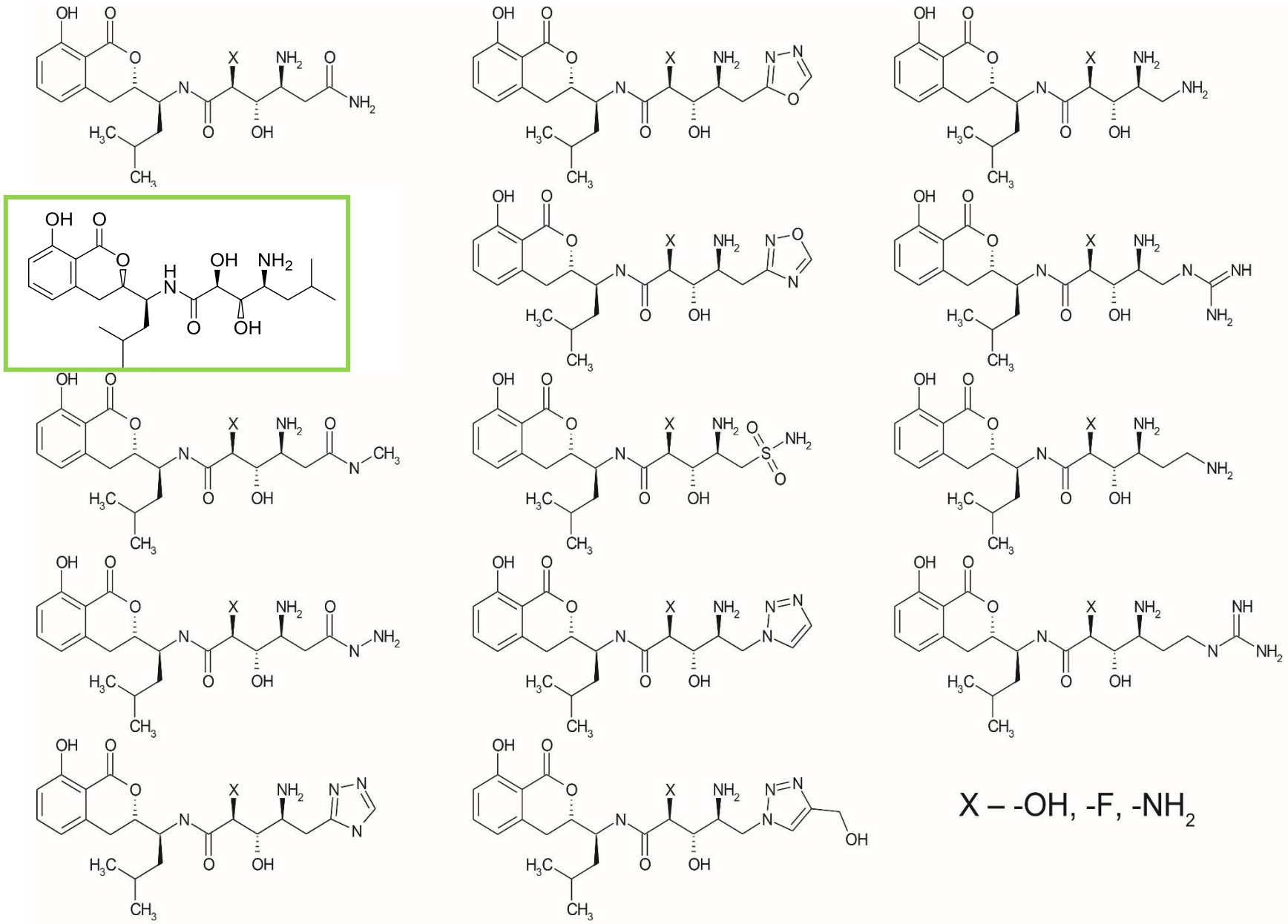

X – -OH, -F, -NH_2

“Deep functional profiling” of microbiomes for antibiotic activity/resistance screening

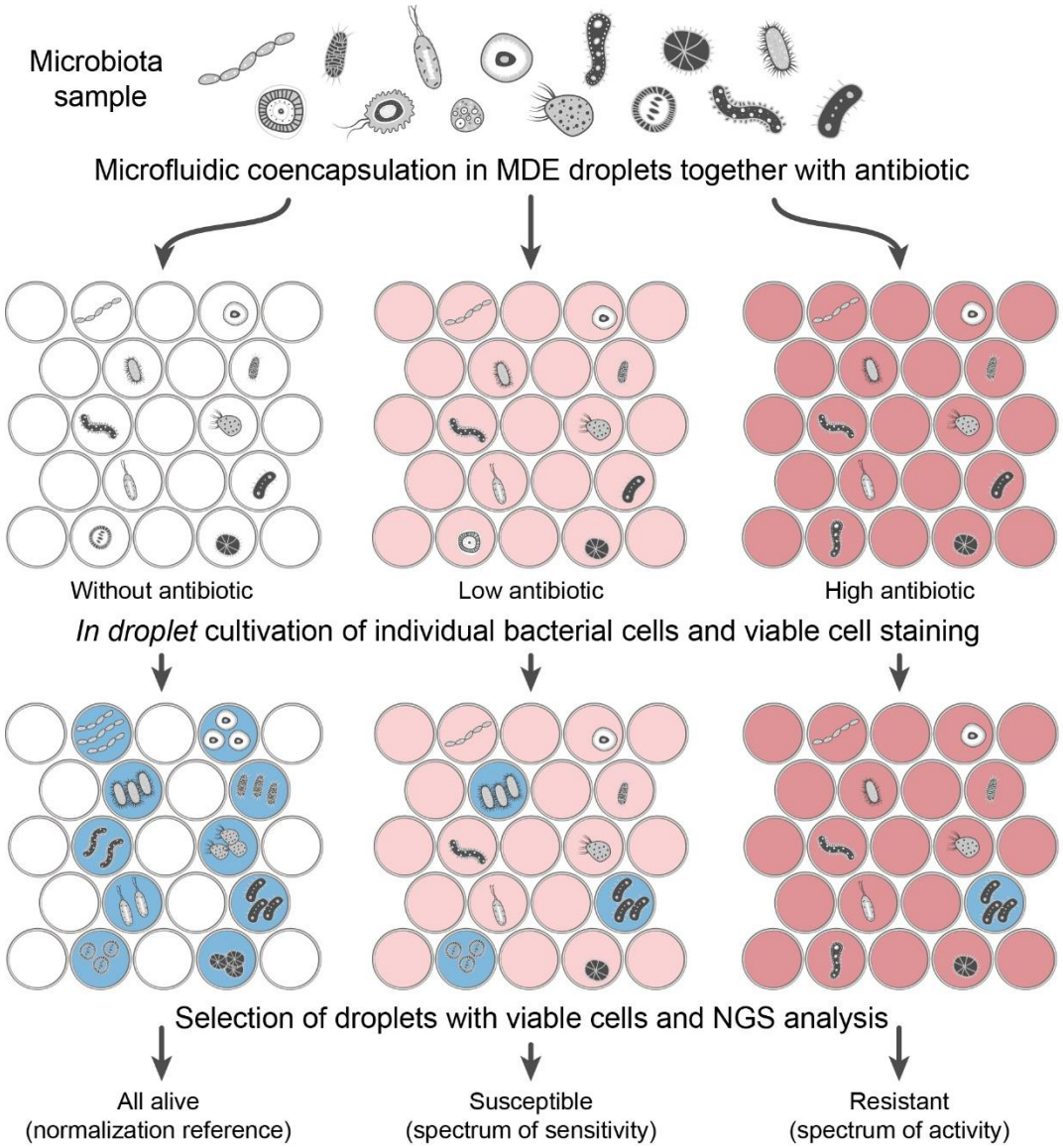

MIC prediction

Verification by MIC test *in vitro*

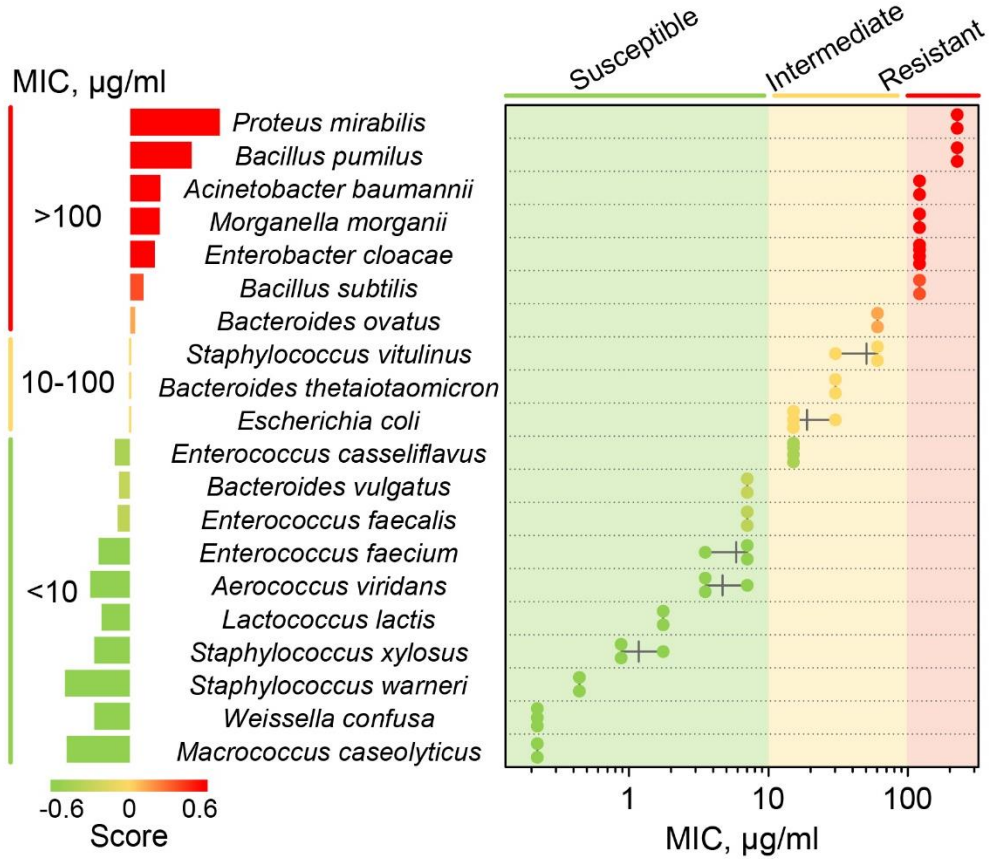

Optimization of ePCR for amplification of combinatorial libraries

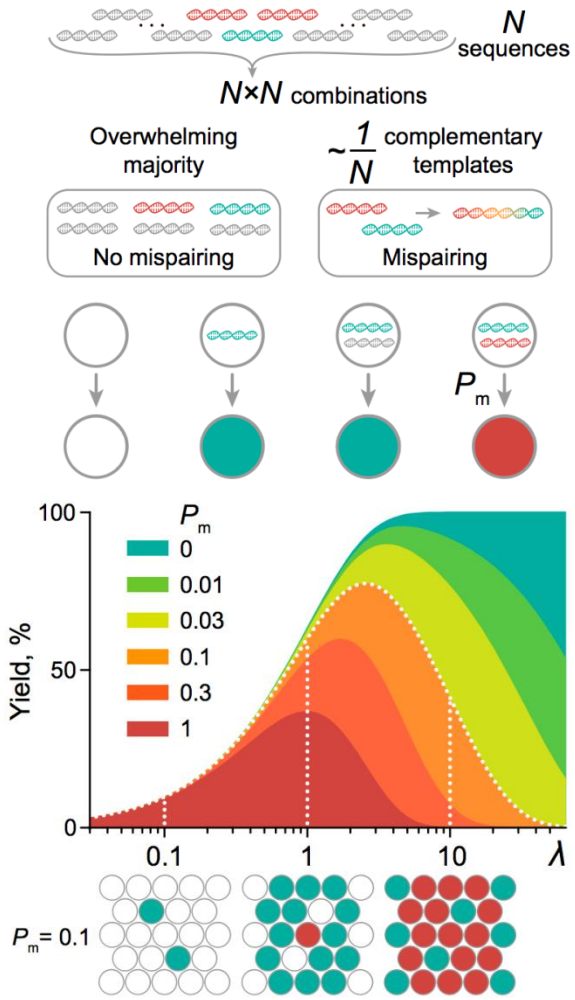

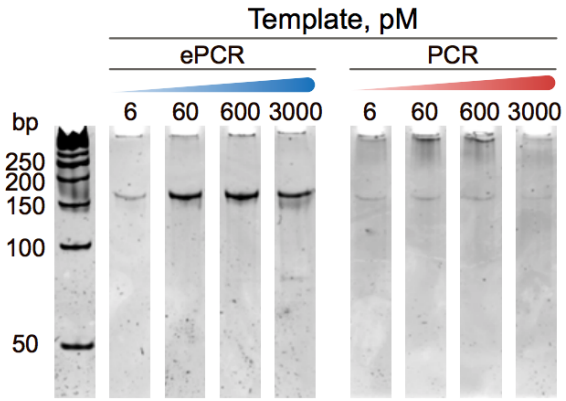

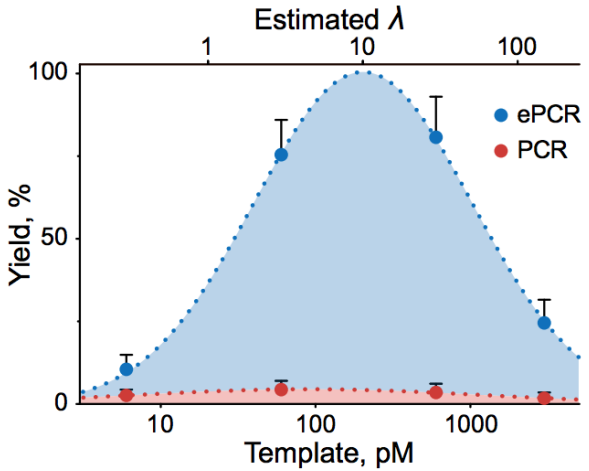

Terekhov et al. PNAS. 2020

ePCR Improves the Uniformity of Amplification over Conventional PCR.

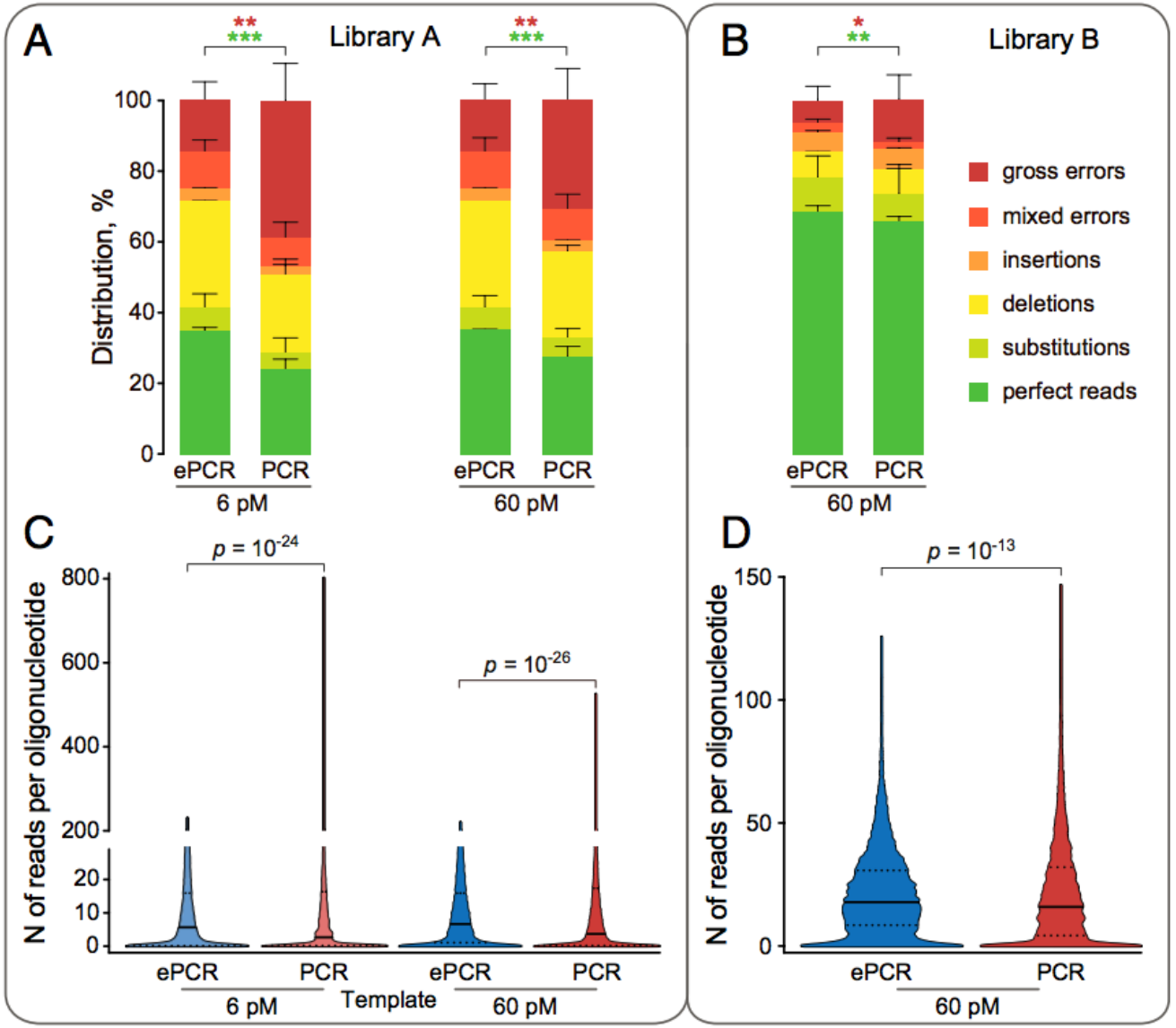

Terekhov et al. PNAS. 2020

SARS-COVID-19
cytokine Storm and Innate Immunity

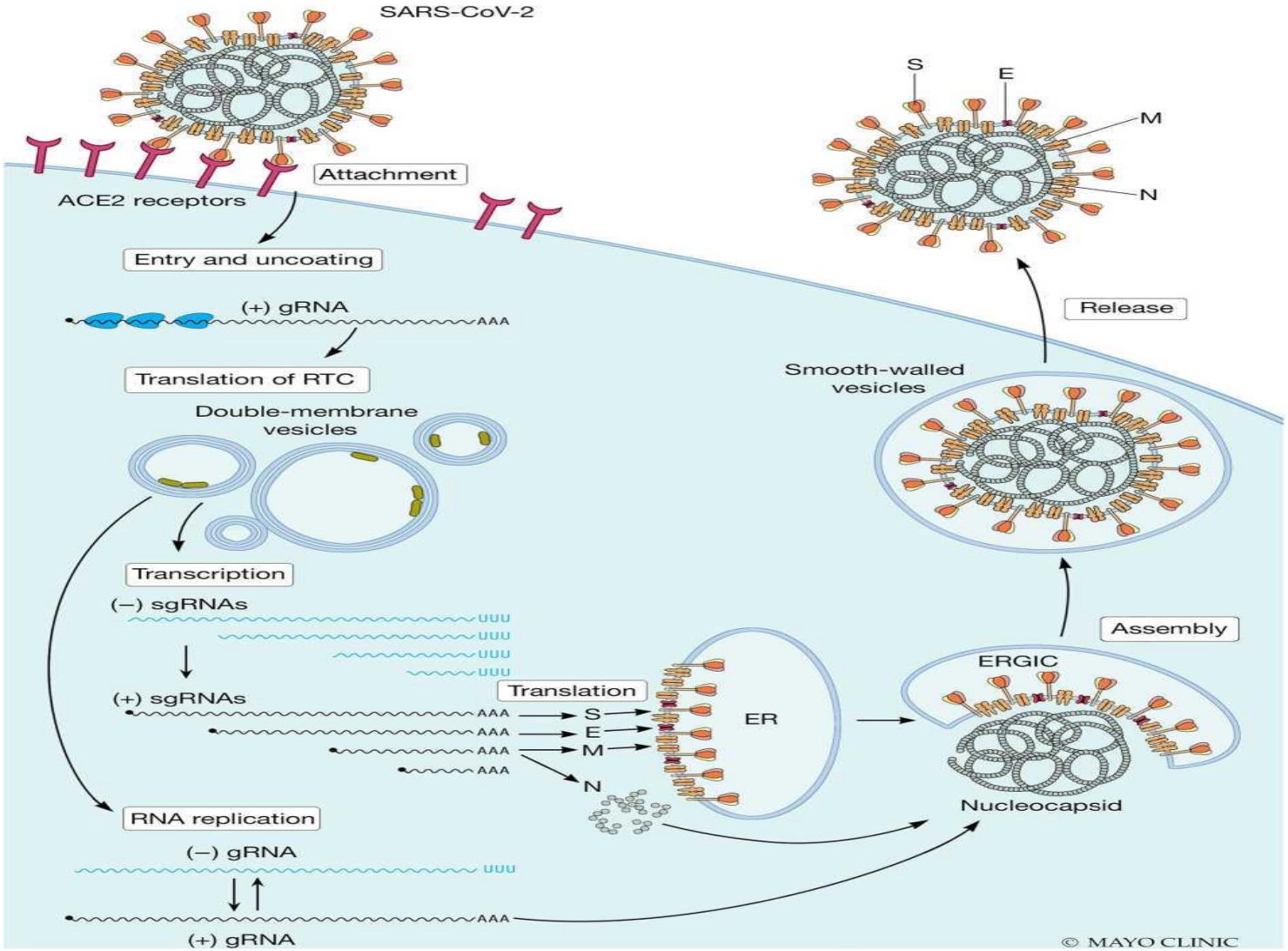

Viral replication pathway of Covid-19. The virus first attaches to the ACE2 receptor and internalizes into the respiratory epithelial cell and causes the release of its genome. The S protein (spikes on the viral surface responsible for attachment to host cell receptors), M protein (shapes the virion, promotes membrane curvature and binds to the nucleocapsid), E protein (helps with viral assembly and release)

APJAI Asian Pac J Allergy Immunol 2020;38:10-18 DOI 10.12932/AP-200220-0773

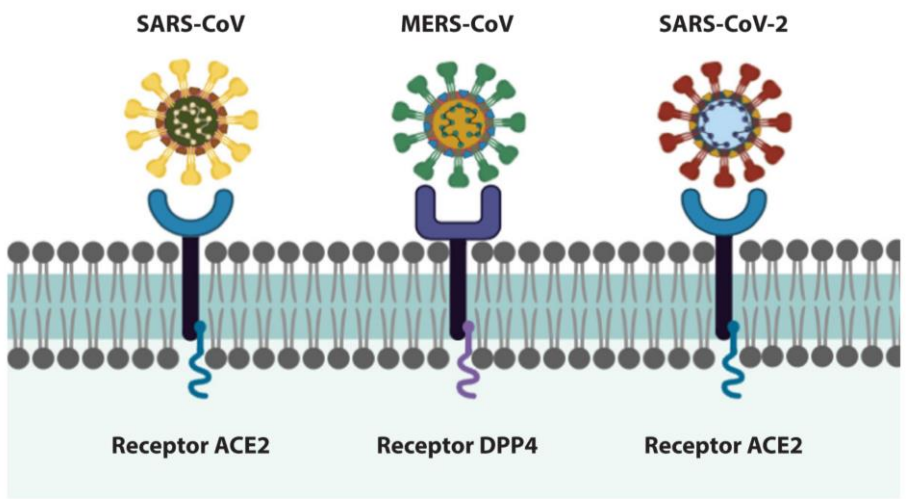

Figure 1. Graphical representation of SARS-CoV, MERS-CoV, SARS-CoV-2 and its cellular receptor.
The schematic representation shows the envelope spike proteins of SARS-CoV and MERS-CoV that binds to host receptor angiotensin-converting enzyme 2 (ACE2) and dipeptidyl peptidase 4 (DPP4), respectively. Similar like SARS-CoV, novel coronavirus SARS-CoV-2 uses ACE2 as its receptor for host entry. Binding between receptor binding domain in spike protein and the cellular receptor mediates membrane fusion and initiate the virus life cycle.

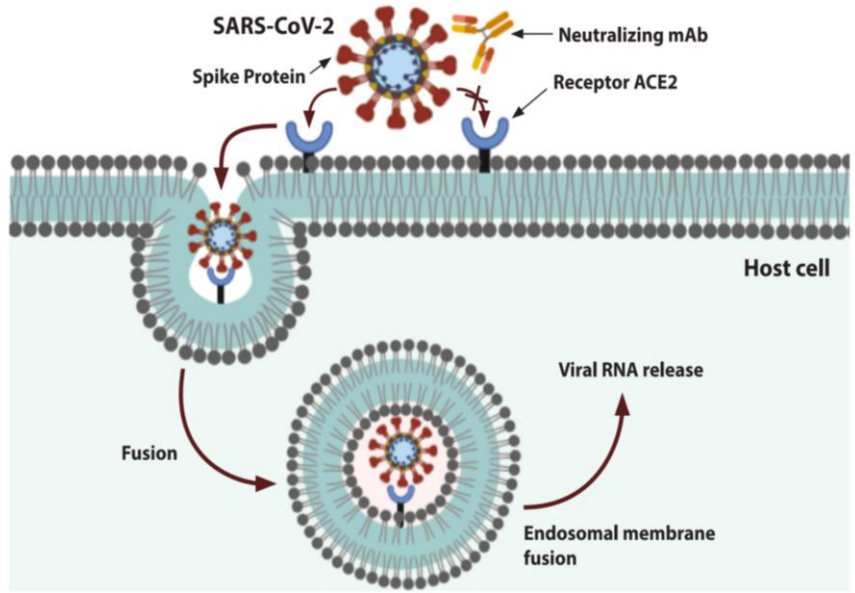

Figure 2. Schematic representation of SARS-CoV-2 neutralization mechanism.
Interaction of spike protein and the cellular receptor is required for membrane fusion and entry into the target cell. The monoclonal antibodies targeting spike protein of SARS-CoV-2 could potentially inhibit the virus binding to its cellular receptor thereby preventing its entry into the cell.

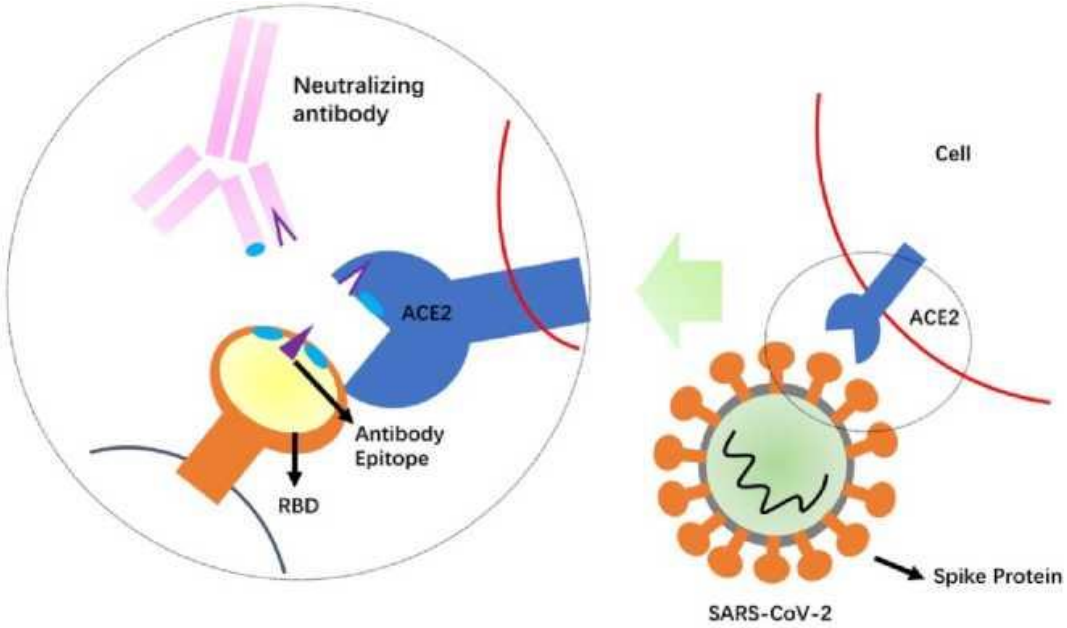

Figure 2. Schematic mechanism of the neutralizing antibodies. Competition of the neutralizing antibody with the receptor (ACE2) for binding to the receptor-binding domain (RBD) of the SARS-CoV-2 Spike protein is shown. The protruding portion (violet) of RBD is both the ACE2 receptor-binding site and the antibody epitope.

FDA gives emergency OK to Lilly's antibody treatment for Covid-19

The NEW ENGLAND JOURNAL of MEDICINE

ORIGINAL ARTICLE

SARS-CoV-2 Neutralizing Antibody LY-CoV555 in Outpatients with Covid-19

Peter Chen, M.D., Ajay Nirula, M.D., Ph.D., Barry Heller, M.D., Robert L. Gottlieb, M.D., Ph.D., Joseph Boscia, M.D., Jason Morris, M.D., Gregory Huhn, M.D., M.P.H.T.M., Jose Cardona, M.D., Bharat Mocherla, M.D., Valentina Stosor, M.D., Imad Shawa, M.D., Andrew C. Adams, Ph.D., Jacob Van Naarden, B.S., Kenneth L. Custer, Ph.D., Lei Shen, Ph.D., Michael Durante, M.S., Gerard Oakley, M.D., Andrew E. Schade, M.D., Ph.D., Janelle Sabo, Pharm.D., Dipak R. Patel, M.D., Ph.D., Paul Klekotka, M.D., Ph.D., and Daniel M. Skovronsky, M.D., Ph.D., for the BLAZE-1 Investigators*

ABSTRACT

BACKGROUND

Severe acute respiratory syndrome coronavirus 2 (SARS-CoV-2) causes coronavirus disease 2019 (Covid-19), which is most frequently mild yet can be severe and life-threatening. Virus-neutralizing monoclonal antibodies are predicted to reduce viral load, ameliorate symptoms, and prevent hospitalization.

METHODS

In this ongoing phase 2 trial involving outpatients with recently diagnosed mild or moderate Covid-19, we randomly assigned 452 patients to receive a single intravenous infusion of neutralizing antibody LY-CoV555 in one of three doses (700 mg, 2800 mg, or 7000 mg) or placebo and evaluated the quantitative virologic end

From the Department of Medicine, Women's Guild Lung Institute, Cedars–Sinai Medical Center, Los Angeles (P.C.), and Long Beach Clinical Trials, Long Beach (B.H.) — both in California; Eli Lilly, Indianapolis (A.N., A.C.A., J.V.N., K.L.C., L.S., M.D., G.O., A.E.S., J.S., D.R.P., P.K., D.M.S.), and Franciscan Health, Greenwood (I.S.) — both in Indiana; Baylor University Medical Center and Baylor Scott and White Research Institute, Dallas (R.L.G.); Vitalink Research, Union, SC (J.B.); Imperial Health, Lake

Figure 1

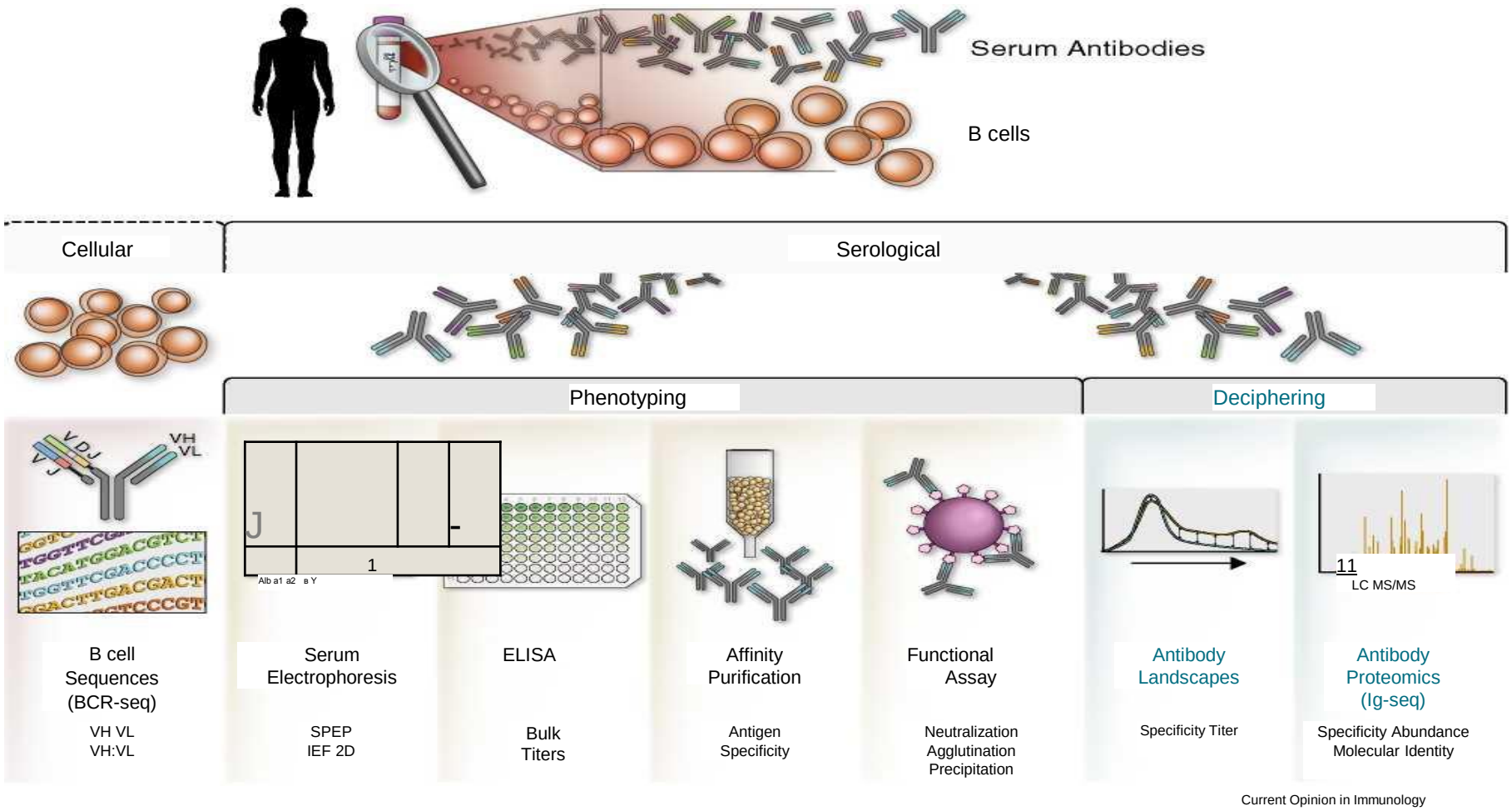

Approaches for the analysis of human antibody repertoires. Isolated B cells are sorted into several subsets based on expressed cell markers that correspond to the developmental stage of the B cell. These populations can be further processed for high-throughput sequencing to generate the antibody repertoire encoded by B cells (cellular repertoire, left side of the figure). The corresponding serum immunoglobulins are isolated from the samples and can be analyzed by various methods including well established technologies such as 2D gels or by recently established methodologies such as high resolution shotgun proteomics (serological repertoire, left side of the figure). The methodologies for serological immunoglobulin analysis can be broadly based upon the phenotype of an antibody subpopulation (e.g., ELISA titer of antigen-specific fraction) or upon decipherment of the molecular identity and sequence determination of an antibody subpopulation (e.g., LC-MS/MS immunoglobulin sequencing, Ig-seq).

Potent Neutralizing Antibodies against SARS-CoV-2 Identified by High-Throughput Single-Cell Sequencing of Convalescent Patients' B Cells

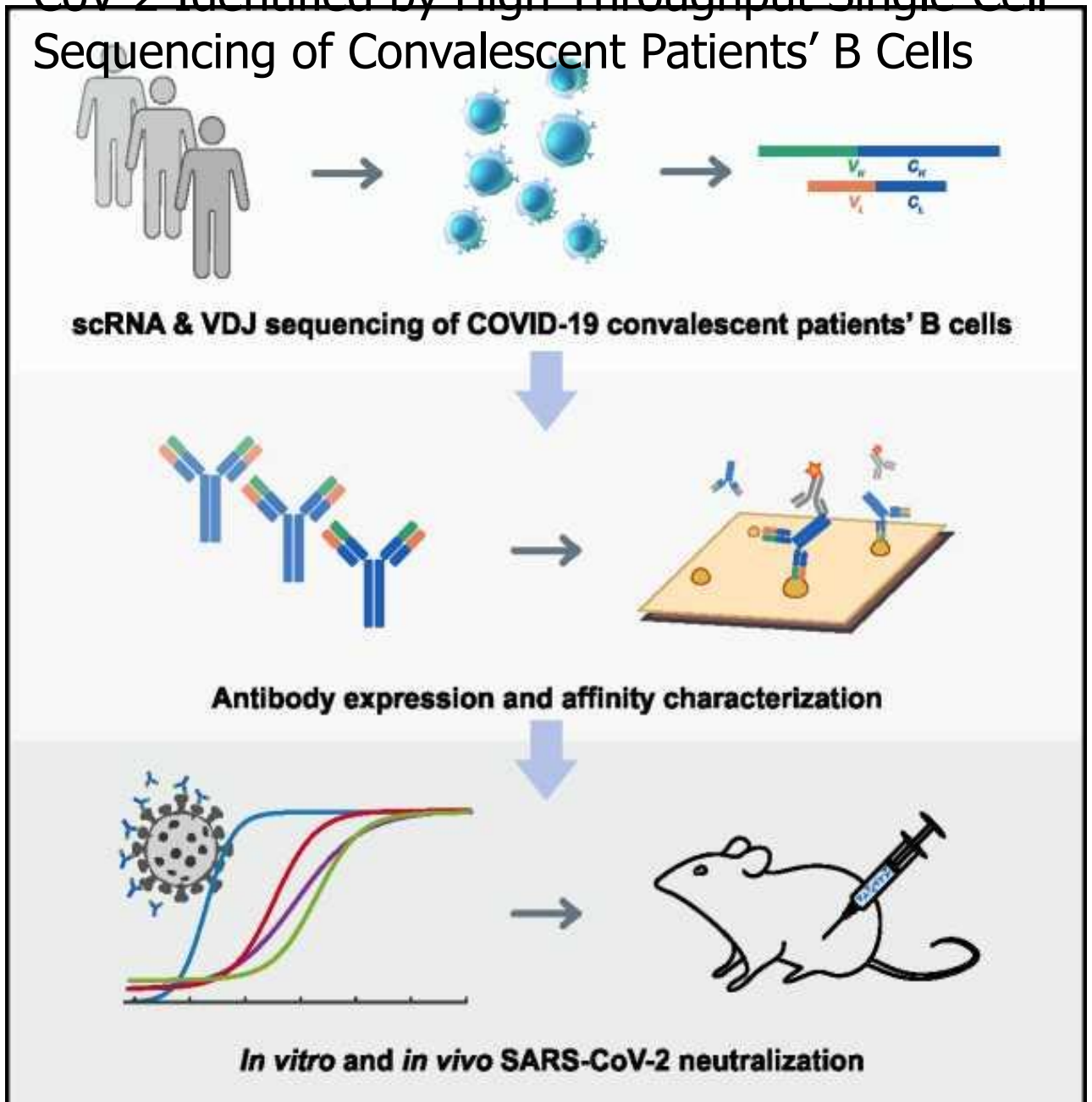

G-MAB SARS-CoV-2 Antibody Discovery Workflow. The G-MAB phage display library was panned for SARS-CoV-2 Spike S1 subunit-binding scFv fragments. Following confirmation of binding activity and blocking of S1:ACE2 interactions by candidate scFvs, the most potent of these candidates were converted to IgG1 antibodies bearing the LALA Fc modification. Candidate nAbs were characterized for binding of Spike S1 subunit and neutralization of related clinical SARS-CoV-2 isolates. Affinity maturation of potent nAbs was carried out in parallel to biophysical profiling, cell line development, and evaluation of protective efficacy for the parental nAb, STI-1499.

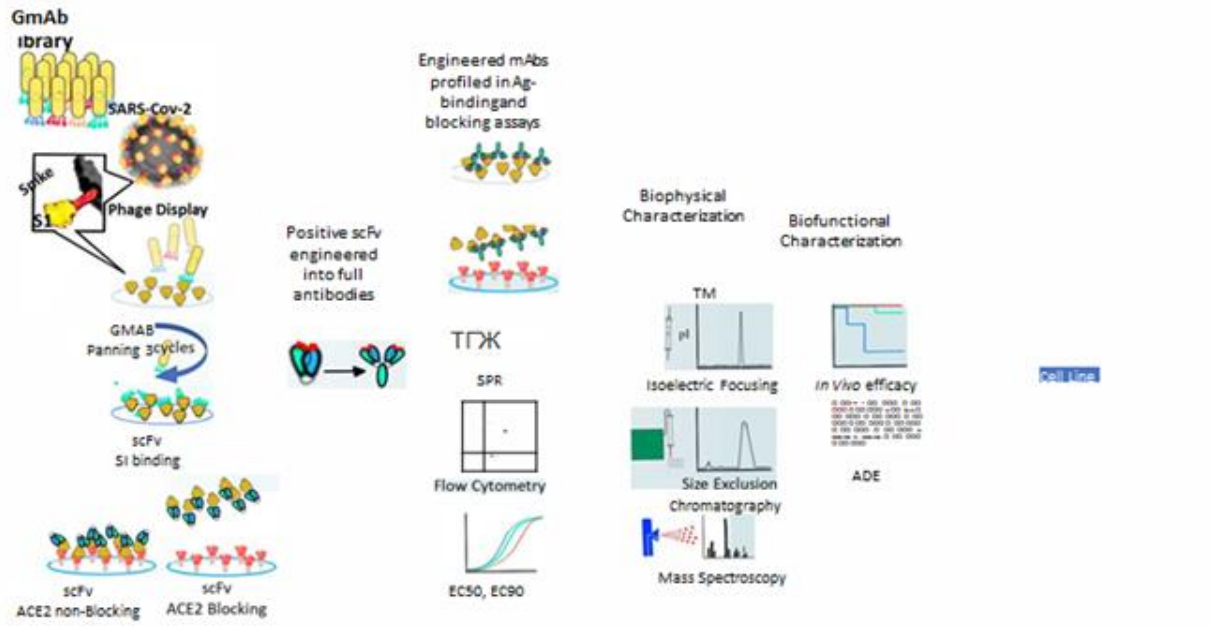

FIGURE 1

Development of neutralizing antibodies for treating COVID-19

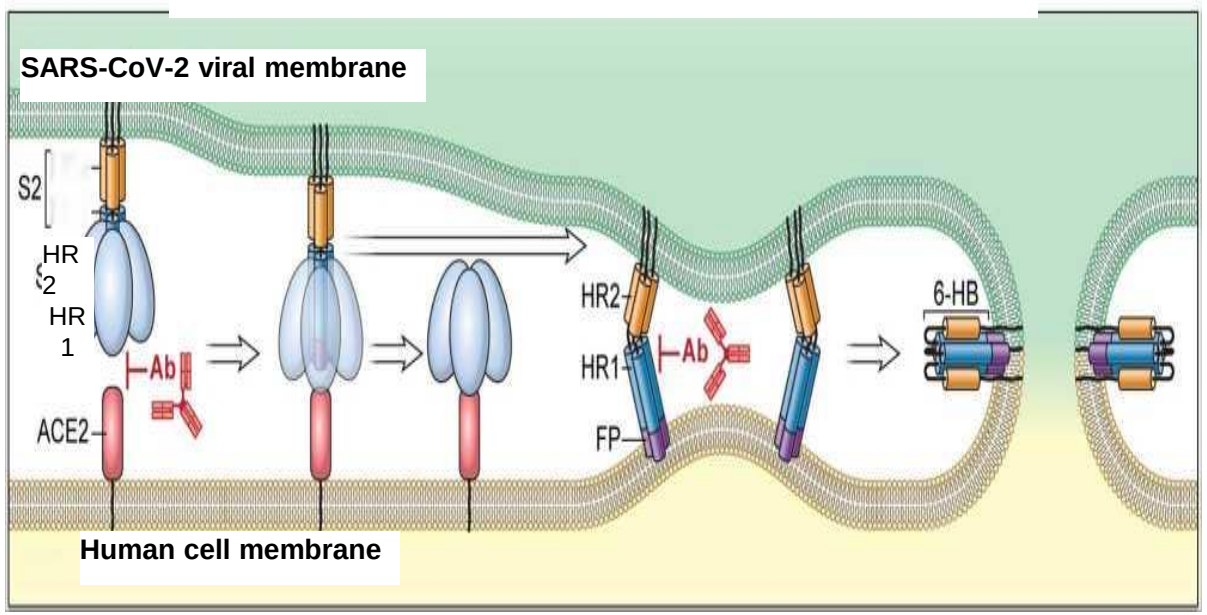

Figure 1. Development of neutralizing antibodies for treating COVID-19. In the receptor binding stage, the S1 subunit of SARS-CoV-2 binds human ACE2 on the host cell surface. Antibodies that bind the RBD domain on the S1 subunit might block the interaction of the RBD and the ACE2. Crossreactive antibodies (e.g., 47D11, S309, and VHH-72) that bind highly conserved epitopes on the RBDs of SARS-CoV and SARS-CoV-2 could have broad neutralization activities against viral infection. In the viral fusion stage, after the cleavage of S1 subunit, the viral fusion peptide (FP) on the S2 subunit inserts into the host cell membrane, inducing the conformational change of the S2 subunit, which forms a six-helix bundle (6-HB) with the HR1 and HR2 trimers. Antibodies (e.g., 1A9 against SARS-CoV) that target the HR domains might block viral fusion. Ab, antibody.

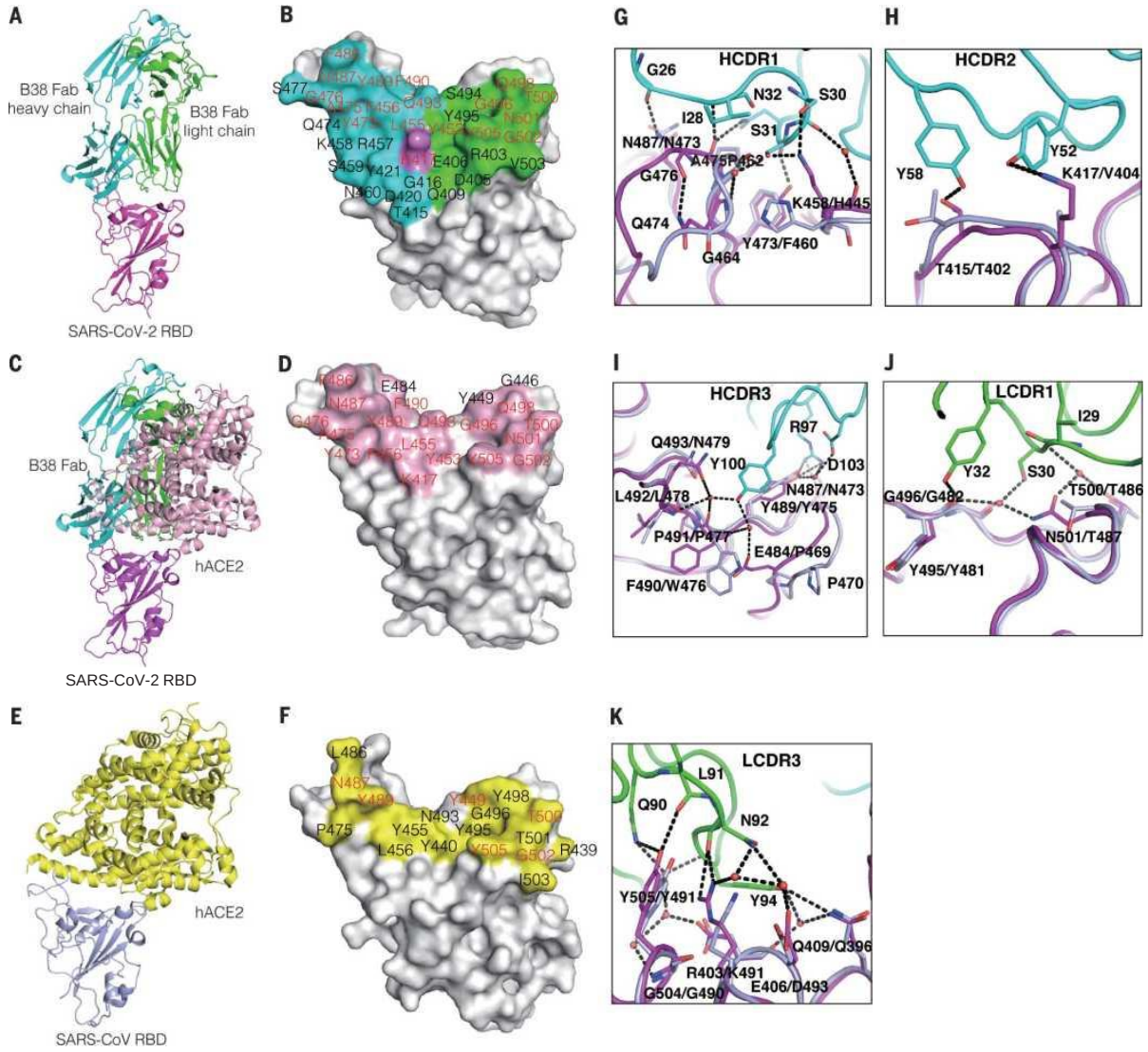

Fig. 4. Structural analysis of B38 and COVID-19 virus RBD complex and the epitope comparison between B38 and hACE2. (**A**) The overall structure of

B38 Fab and COVID-19 virus RBD. The B38 heavy chain (cyan), light chain (green), and COVID-19 virus RBD (magenta) are shown in cartoon representation. (**B**) The epitope of B38 is shown in surface representation. The contact residues by heavy chain, light chain, or both are colored in cyan, green, and magenta, respectively.

The residues on RBD involved in both B38 and hACE2 binding are labeled in red. (**C**) Superimposition of RBD-B38 and RBD-hACE2 [Protein Data Bank (PDB) ID 6LZG]. All molecules are shown in cartoon representation, with the same colors as binding are labeled in red. (**E**) The complex structure of SARS-CoV RBD (light blue) and hACE2 (yellow) (PDB ID 2AJF). (**F**) The residues in contact with hACE2 are colored in yellow. The residues are numbered according to SARS-CoV RBD. The residues involved in hACE2 binding of two RBDs are labeled in red. (**G** to **I**) The detailed interactions between COVID-19 virus RBD and CDR loops of the heavy chain. (**J** and **K**) The detailed interactions between COVID-19 virus RBD and CDR loops of the light chain. The residues are shown in stick representation, with the same colors as in (C). The water molecules are shown as red spheres. Singleletter abbreviations for the amino acid residues are as follows: A, Ala; D, Asp;

E, Glu; F, Phe; G, Gly; I, Ile; K, Lys; L, Leu; N, Asn; P, Pro; Q, Gln; R, Arg; S, Ser;

HFB30132A is Uniquely Positioned Among Most Competitors

- **HFB30132A, Superior Antibody Property:** Engineered IgG4 with minimal ADE, better distribution and extended half-life
- HFB30132A is **uniquely positioned to help high risk patients who have asymptomatic or mild to moderate COVID-19**

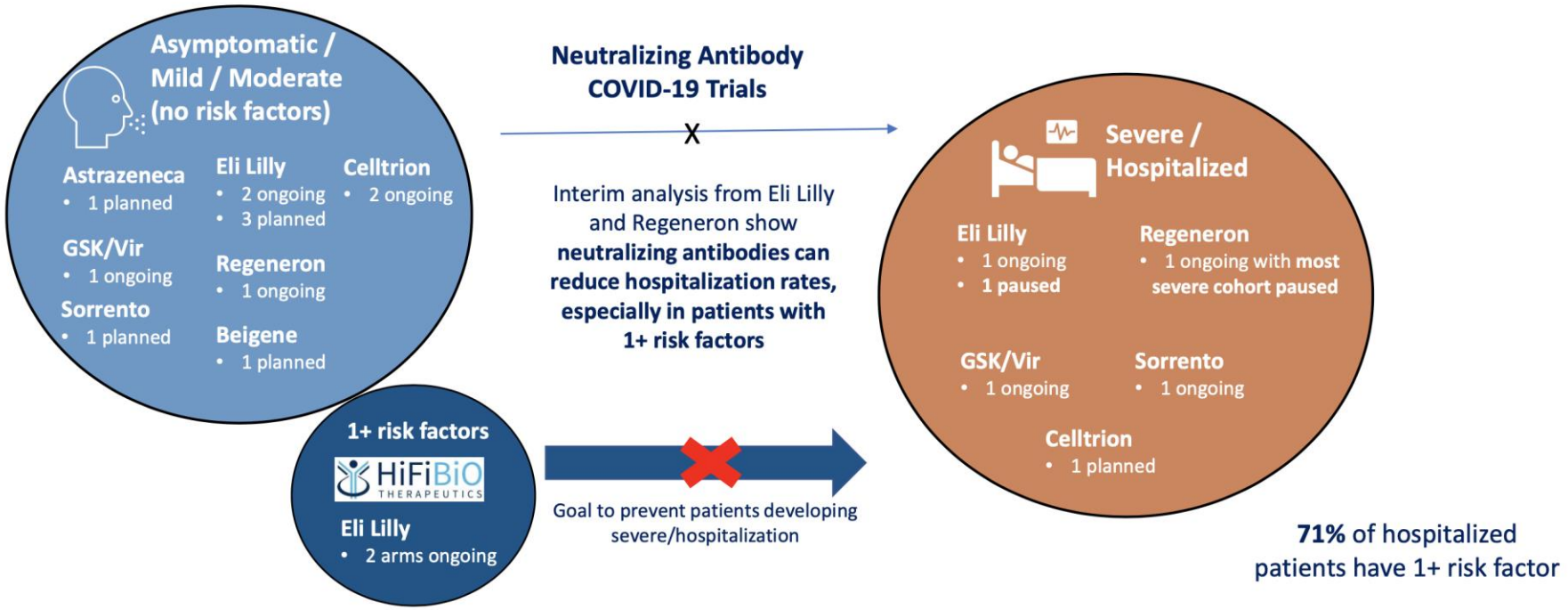

71% of hospitalized patients have 1+ risk factor

Antibody HFB30132A

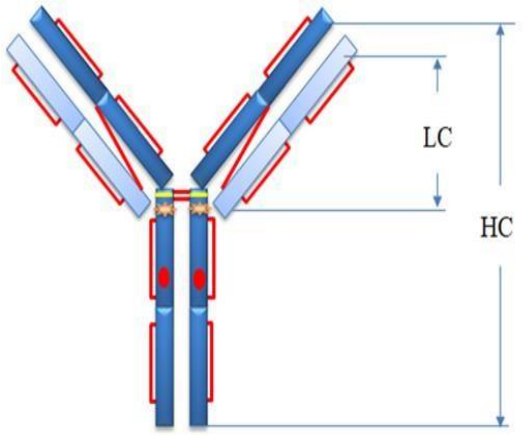

Disulfide bridges within one chain and between chains
S228P mutation
M252Y / S254T / T256E mutations
N297-linked glycan

HBF30132A is a fully human monoclonal antibody of the IgG4 isotype directed against the receptor binding domain (RBD) of the Severe Acute Respiratory Syndrome Coronavirus 2 (SARS-CoV-2) spike (S) protein. HFB30132A has modifications in its Fc fragment, with amino acid substitutions S228P and M252Y / S254T / T256E (YTE), made in order to avoid the exchange of Fab fragments and, accordingly, to increase the half-life of antibodies. The IgG4 isotype was chosen to reduce the risk of antibody-dependent enhancement (ADE) infection that can occur with coronavirus infection and, together with the YTE mutation, this choice potentially increases the penetration of the injected antibody into the mucous membrane of the respiratory tract.

Microfluidic droplet platform for ultrahigh-throughput single-cell screening of biodiversity

Stanislav S. Terekhov[a,b,1], Ivan V. Smirnov[a,c,1], Anastasiya V. Stepanova[a], Tatyana V. Bobik[a,c], Yuliana A. Mokrushina[a], Natalia A. Ponomarenko[a,2], Alexey A. Belogurov Jr.[a,c], Maria P. Rubtsova[b,d], Olga V. Kartseva[c], Marina O. Gomzikova[c], Alexey A. Moskovtsev[e], Anton S. Bukatin[f], Michael V. Dubina[f], Elena S. Kostryukova[g,h], Vladislav V. Babenko[g], Maria T. Vakhitova[h], Alexander I. Manolov[g], Maja V. Malakhova[g], Maria A. Kornienko[g], Alexander V. Tyakht[g,h], Anna A. Vanyushkina[g], Elena N. Ilina[g], Patrick Masson[c,i], Alexander G. Gabibov[a,b,c,3], and Sidney Altman[j,3]

[a]Shemyakin-Ovchinnikov Institute of Bioorganic Chemistry, Russian Academy of Sciences, 117997 Moscow, Russian Federation; [b]Department of Chemistry, Lomonosov Moscow State University, 119991 Moscow, Russian Federation; [c]Kazan Federal University, 420008 Kazan, Russian Federation; [d]Skolkovo Institute of Science and Technology, 143026 Skolkovo, Russian Federation; [e]Institute of General Pathology and Pathophysiology, 125315 Moscow, Russian Federation; [f]St. Petersburg Academic University, 194021 St. Petersburg, Russian Federation; [g]Research and Clinical Centre of Physical-Chemical Medicine, 119435 Moscow, Russian Federation; [h]Moscow Institute of Physics and Technology, 141701 Dolgoprudny, Russian Federation; [i]French Academy of Pharmacy, 75270 Paris, France; and [j]Department of Molecular, Cellular and Developmental Biology, Yale University, New Haven, CT 06520

nature COMMUNICATIONS

A SARS-CoV-2 neutralizing antibody with exceptional spike binding coverage and optimized therapeutic potentials

Authors: Yu Guo[1,7,12,*,†], Lisu Huang[2,†], Guangshun Zhang[1,4,†], Yanfeng Yao[5,†], He Zhou[3,†], Shu Shen[7,†], Bingqing Shen[3], Bo Li[1,4], Xin Li[1,4], Mingjie Chen[3], Da Chen[1,4], Jia Wu[3], Dan Fu[1], Xinxin Zeng[2], Mingfang Feng[3], Chunjiang Pi[3], Yuan Wang[1,4], Xingdong Zhou[1,4], Minmin Lu[3], Yaohui Fang[7], Yun-Yueh Lu[3], Xue Hu[7], Shanshan Wang[3], Wanju Zhang[2], Qian Zhang[3], Ge Gao[5], Francisco Adrian[3], Qisheng Wang[10], Feng Yu[10], Yun Peng[5], Alexander G. Gabibov[11], Juan Min[5], Yuhui Wang[1,4], Heyu Huang[2], Alexey Stepanov[11], Wei Zhang[1,4], Yan Cai[6], Junwei Liu[6], Zhiming Yuan[5], Zhiyong Lou[8,*], Fei Deng[7,*], Hongkai Zhang[1,4,9,12*], Chao Shan[7,*], Liang Schweizer[3,*], Kun Sun[2,*], Zihe Rao[1,4,*]

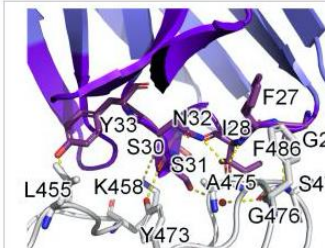

Structure of the complex of the Fab fragment HBF30132A with the receptor-binding domain of the SARS-CoV-2 spike protein

Autocrine-based selection of malignant Follicular Lymphoma B cell receptors ligands

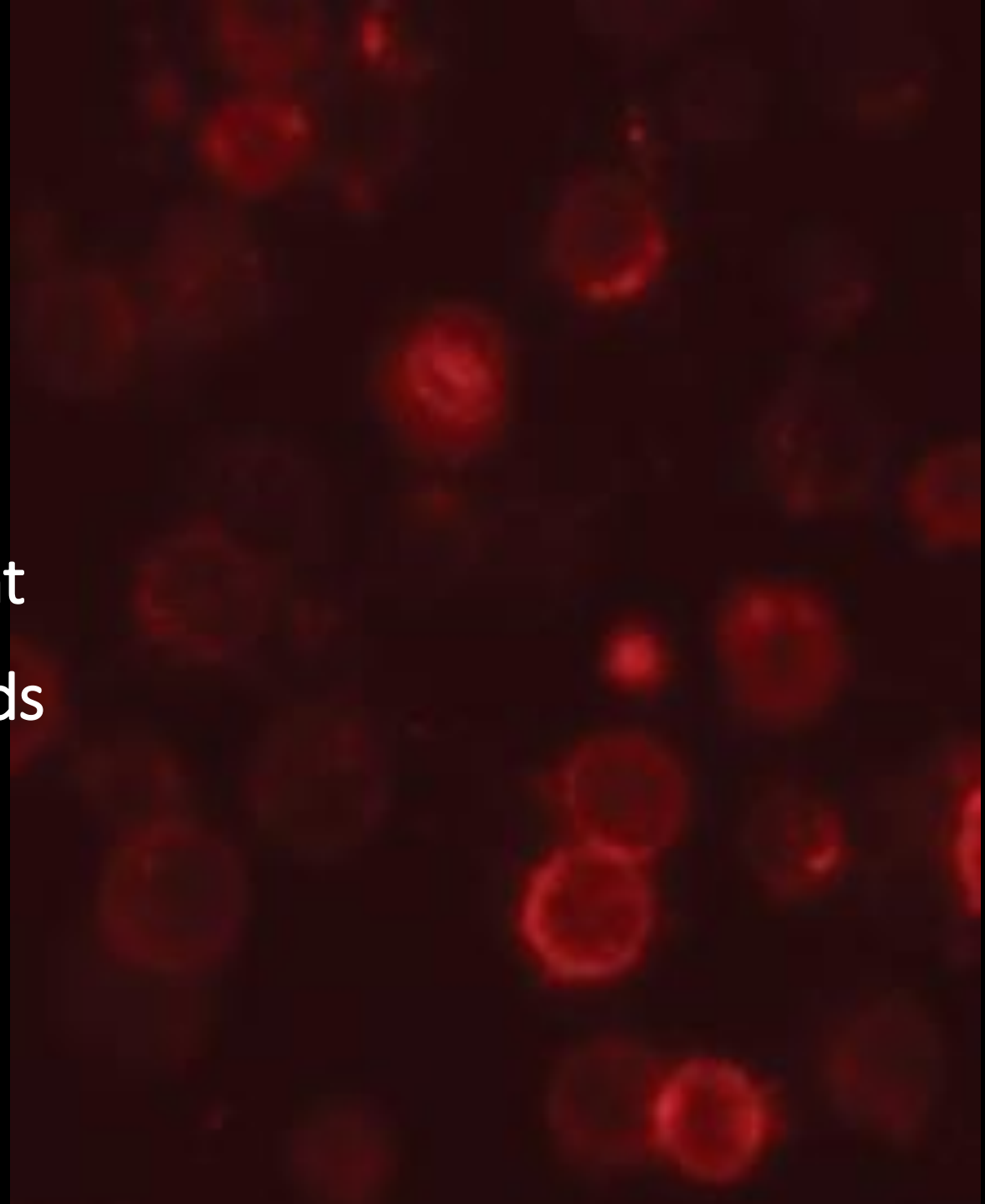

MESSAGE

Reengineering T cells using combinatorial approaches

В норме, Т клетки человека распознают опухолевые клетки с помощью главного комплекса гистосовместимости и рецептора Т клеток и уничтожают их.

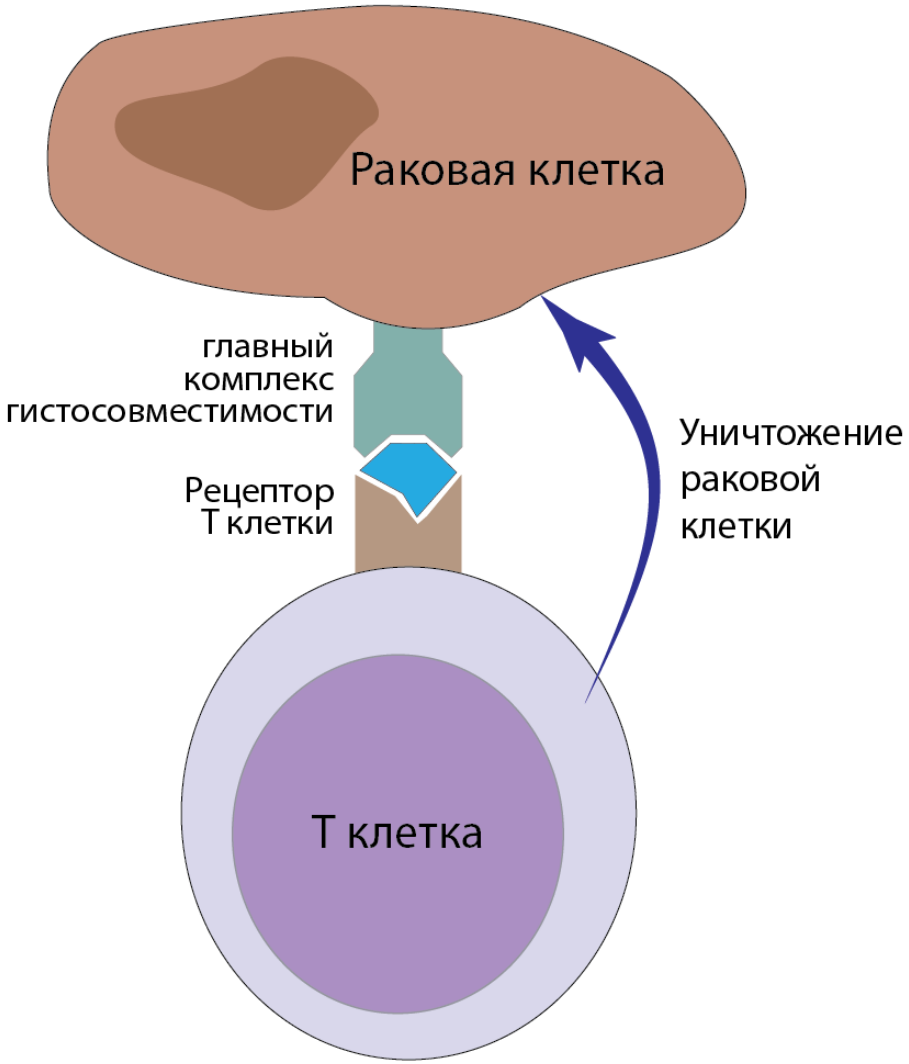

При нарушении данного механизма защиты раковые клетки неограниченно делятся , что приводит к онкологическому заболеванию.

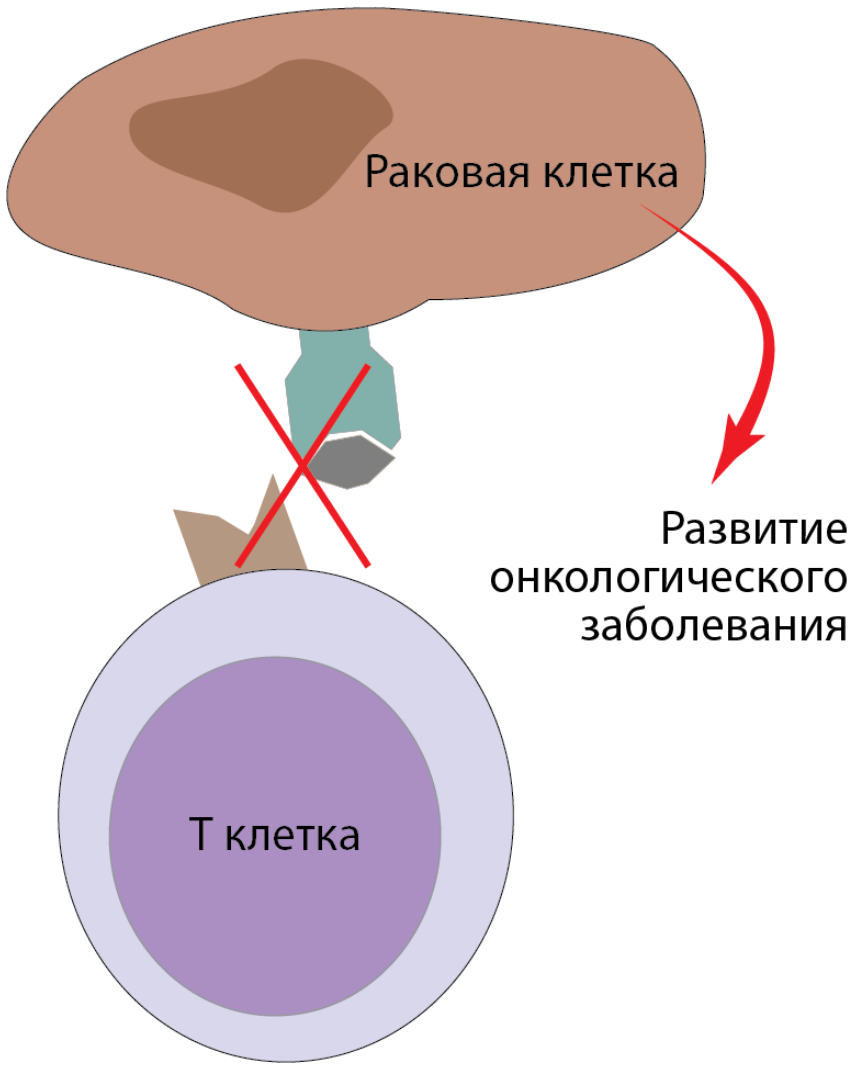

Для того, чтобы вернуть Т-клеткам способность «видеть» раковые клетки были разработаны химерные антигенные рецепторы (chimeric antigen receptor, CAR).
CAR распознают опухолевые клетки напрямую и не зависят от главного комплекса гистосовместимости.

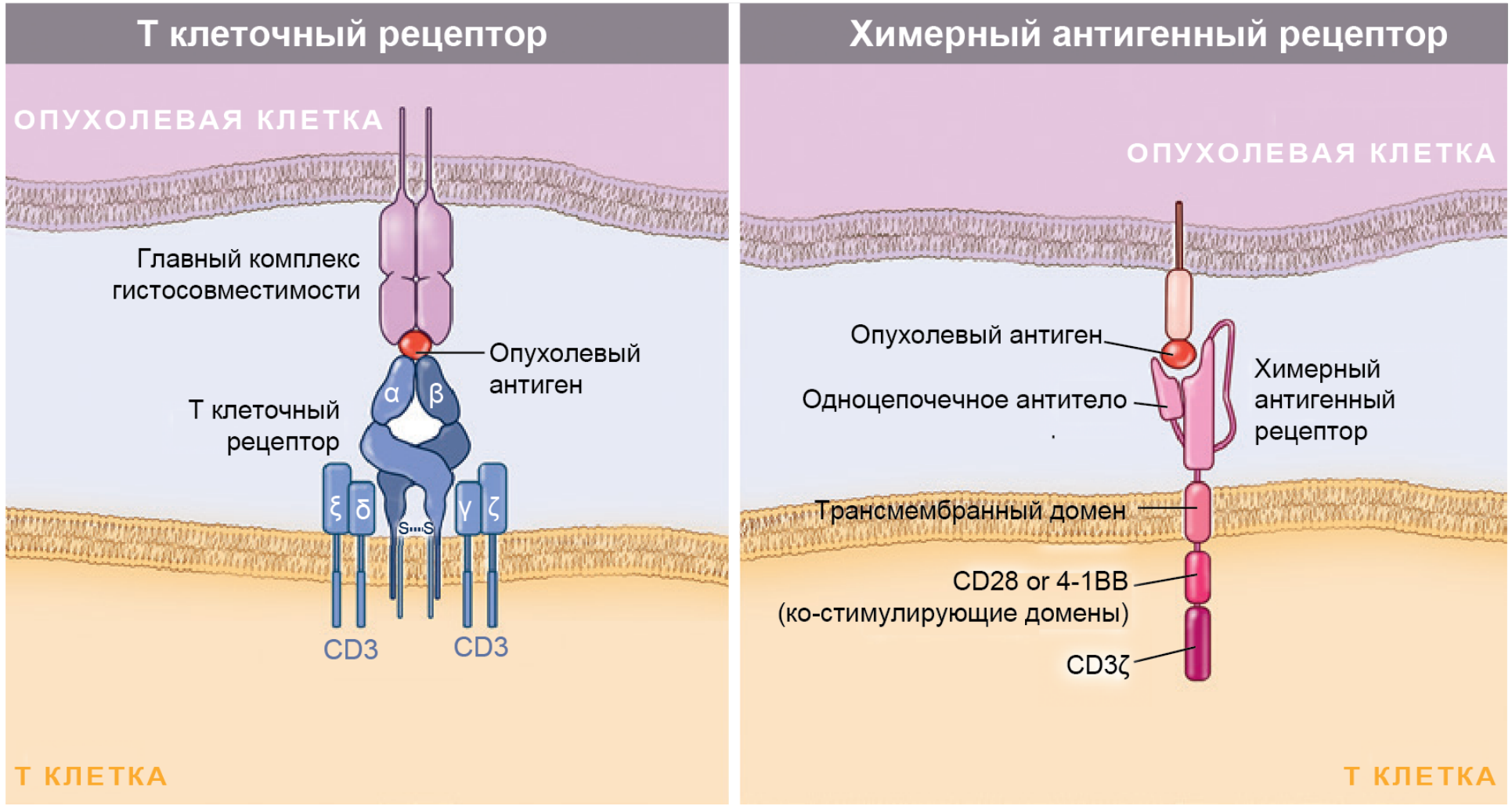

Адаптивная клеточная терапия с помощью химерного антигенного рецептора (CAR) показала свою эффективность и была одобрена FDA для терапии острого лимфобластного лейкоза

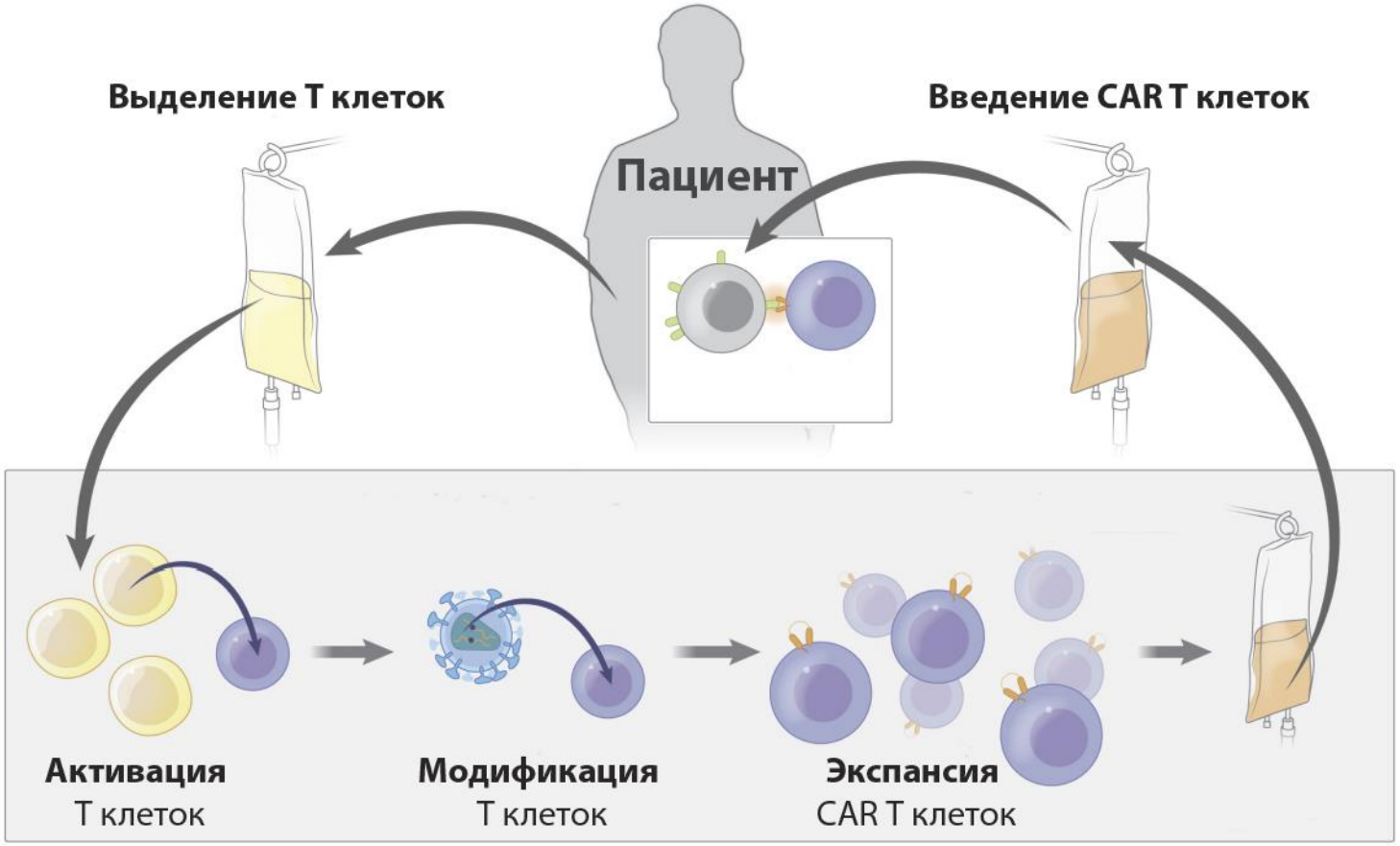

Основными недостатками существующих химерных антигенных рецепторов является **неспецифическая** цитотоксичность по отношению к здоровым клеткам

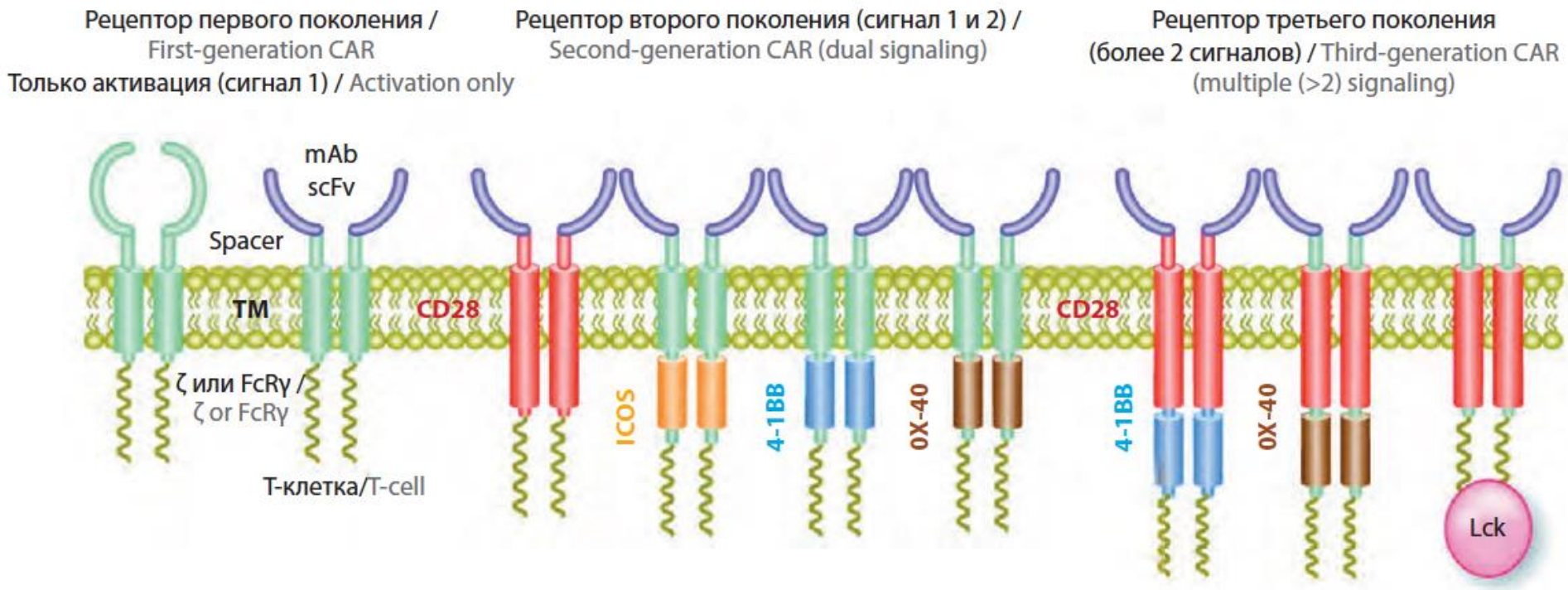
Рецептор первого поколения / First-generation CAR
Только активация (сигнал 1) / Activation only
Рецептор второго поколения (сигнал 1 и 2) / Second-generation CAR (dual signaling)
Рецептор третьего поколения (более 2 сигналов) / Third-generation CAR (multiple (>2) signaling)
mAb
scFv
Spacer
TM
CD28
ζ или FcRγ / ζ or FcRγ
Т-клетка/T-cell
ICOS
4-1BB
OX-40
CD28
4-1BB
OX-40
Lck


раковая клетка
антиген
CAR
распознаю-
щий элемент
"спейсер"
сигнальный
домен
Т-клетка
CAR I поколения
дополни-
тельный
сигнальный
домен
CAR II поколения
доп.
рецептор
дополни-
тельные
сигнальные
домены
CAR III поколения
Эволюция ›

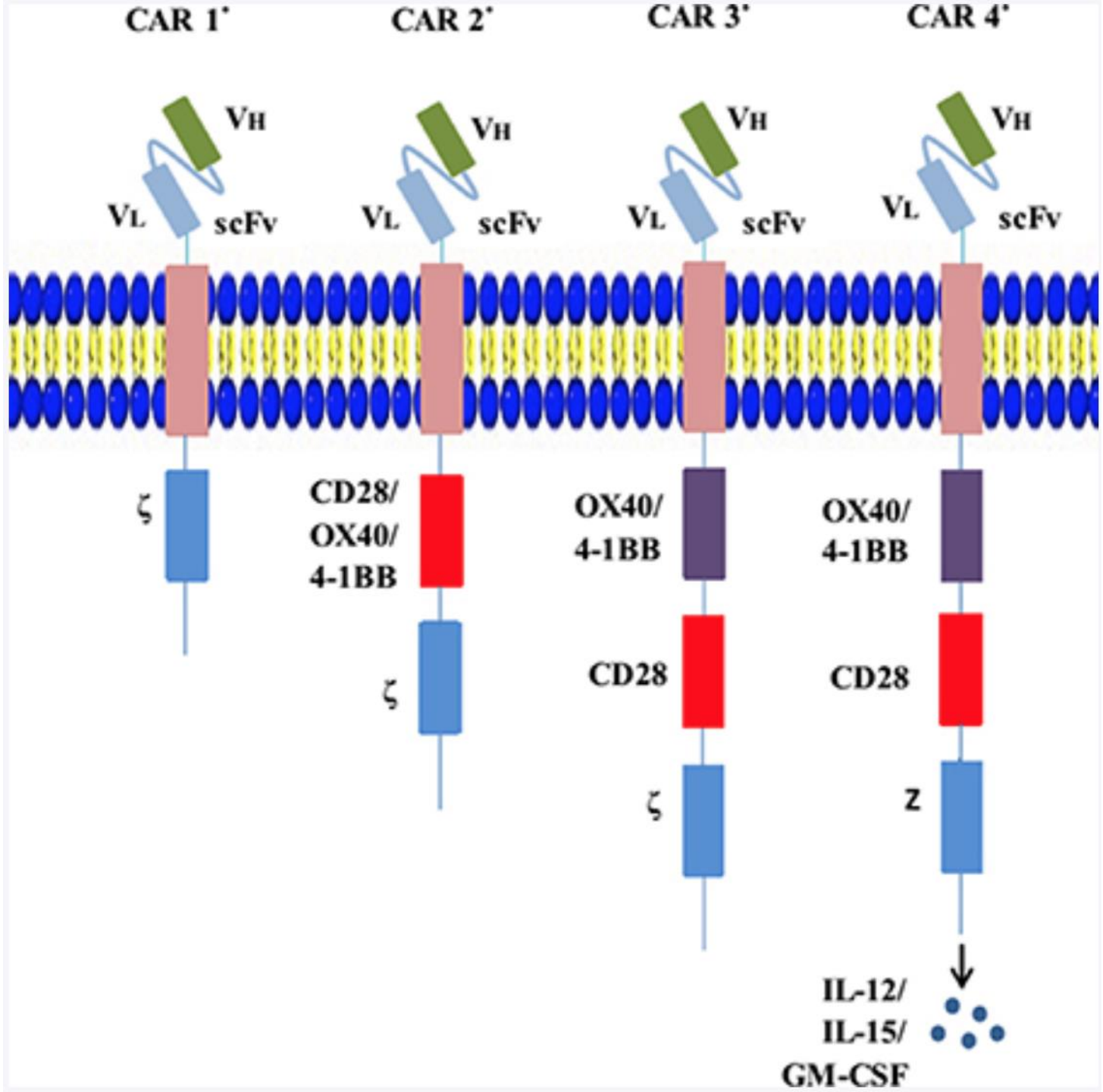
CAR 1'
CAR 2'
CAR 3'
CAR 4'
VH
VL
scFv
ζ
CD28/
OX40/
4-1BB
OX40/
4-1BB
CD28
Z
IL-12/
IL-15/
GM-CSF

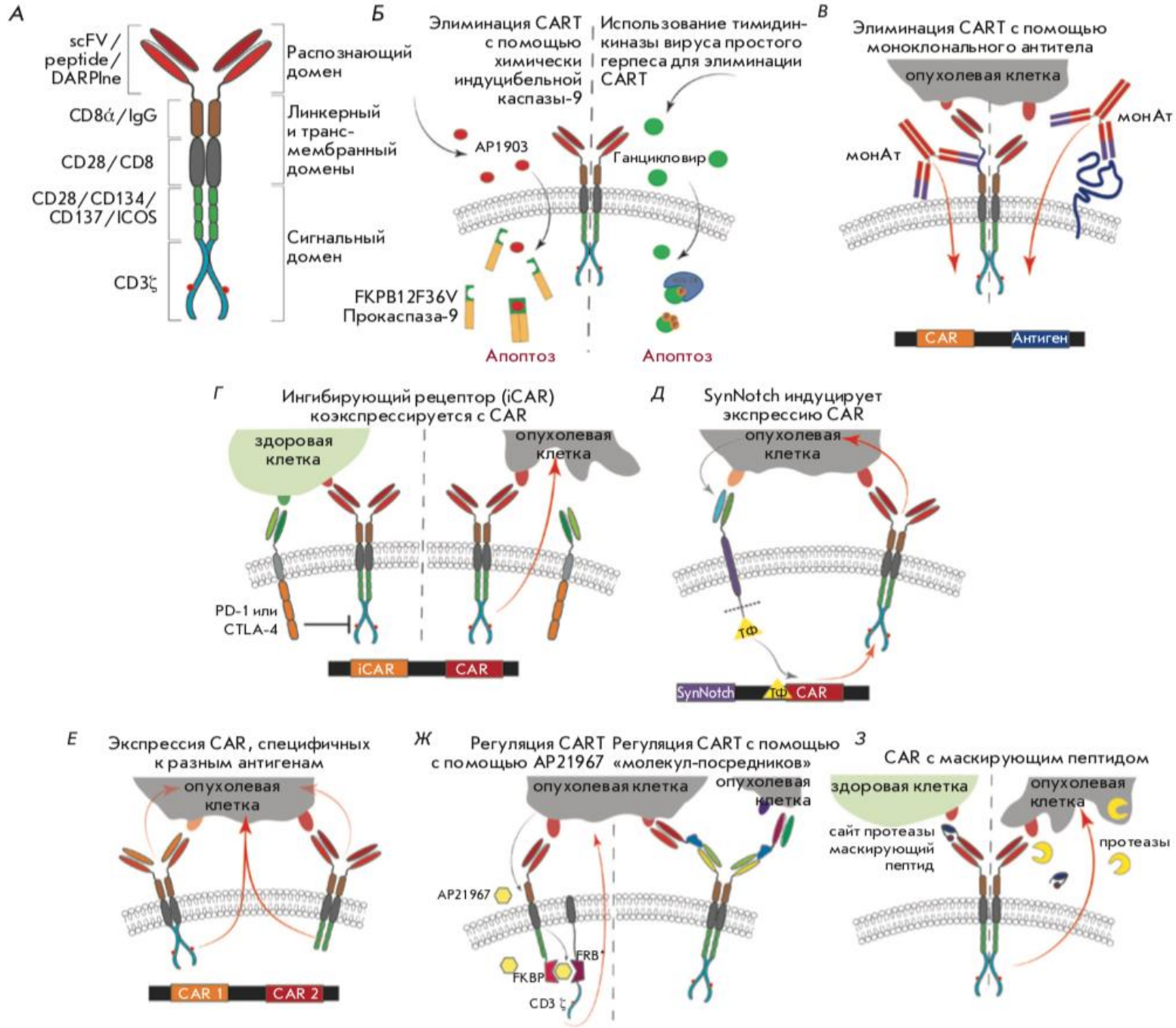
А
scFV / peptide / DARPIne
CD8α / IgG
CD28 / CD8
CD28 / CD134 / CD137 / ICOS
CD3ζ
Распознающий домен
Линкерный и трансмембранный домены
Сигнальный домен
Б
Элиминация CART с помощью химически индуцибельной каспазы-9
Использование тимидинкиназы вируса простого герпеса для элиминации CART
AP1903
Ганцикловир
FKPB12F36V
Прокаспаза-9
Апоптоз
Апоптоз
В
Элиминация CART с помощью моноклонального антитела
опухолевая клетка
монАт
монАт
CAR
Антиген
Г
Ингибирующий рецептор (iCAR) коэкспрессируется с CAR
здоровая клетка
опухолевая клетка
PD-1 или CTLA-4
iCAR
CAR
Д
SynNotch индуцирует экспрессию CAR
опухолевая клетка
ТФ
SynNotch
ТФ
CAR
Е
Экспрессия CAR, специфичных к разным антигенам
опухолевая клетка
CAR 1
CAR 2
Ж
Регуляция CART с помощью AP21967
Регуляция CART с помощью «молекул-посредников»
опухолевая клетка
опухолевая клетка
AP21967
FRB
FKBP
CD3 ζ
З
CAR с маскирующим пептидом
здоровая клетка
опухолевая клетка
сайт протеазы маскирующий пептид
протеазы

Autocrine-based selection of malignant FL-BCR ligands

Principal scheme of reporter system

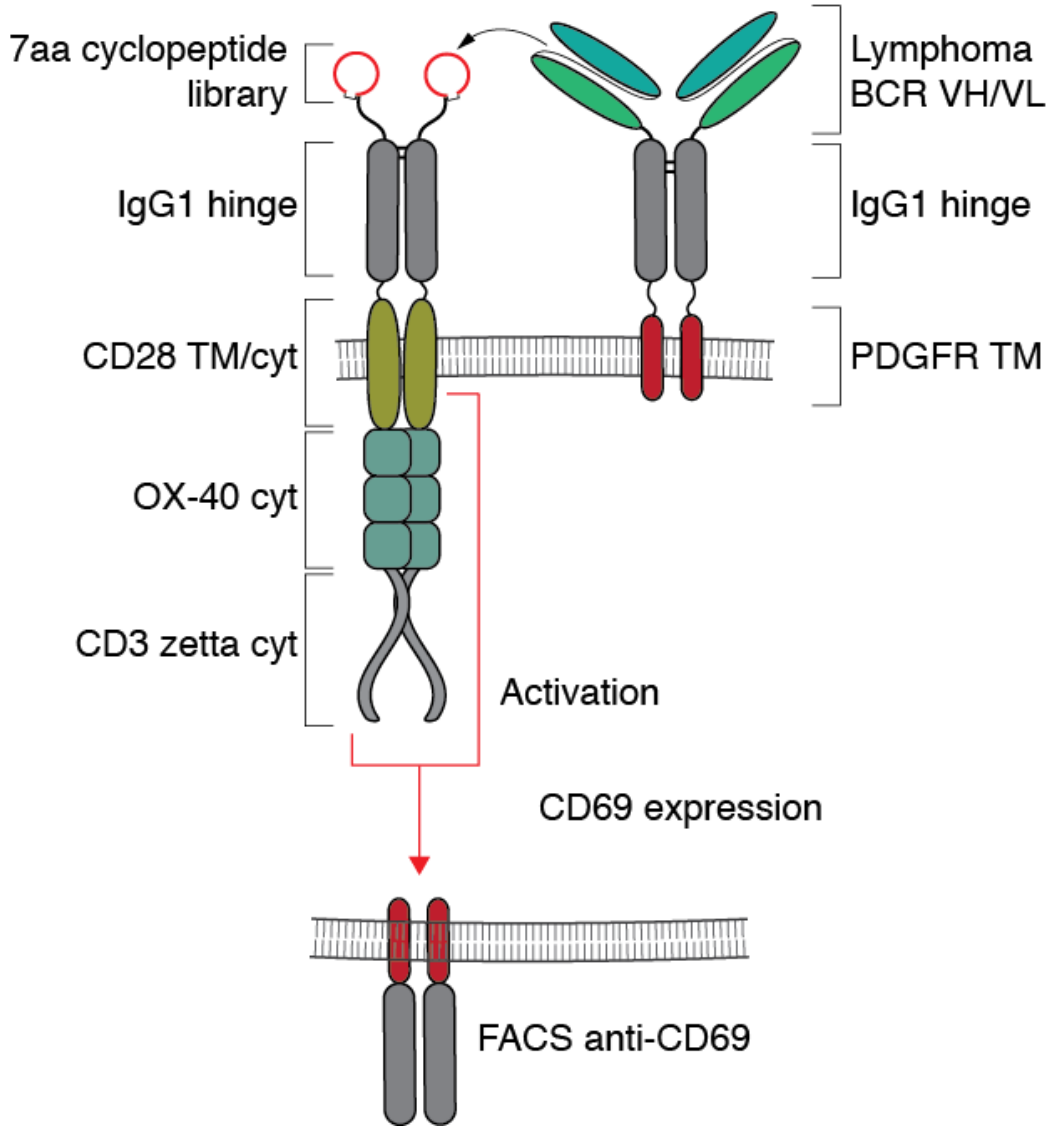

MESSAGE

Combinatorial selection of peptides to develop novel CAR-mediated technology.

Stepanov et al. Science Adv., 2018

Jinqi Huang, Stepanov Alexey et al. Leukemia, 2019

Autocrine-based selection of ligands that target lymphoma cells utilizing redirected CTLs

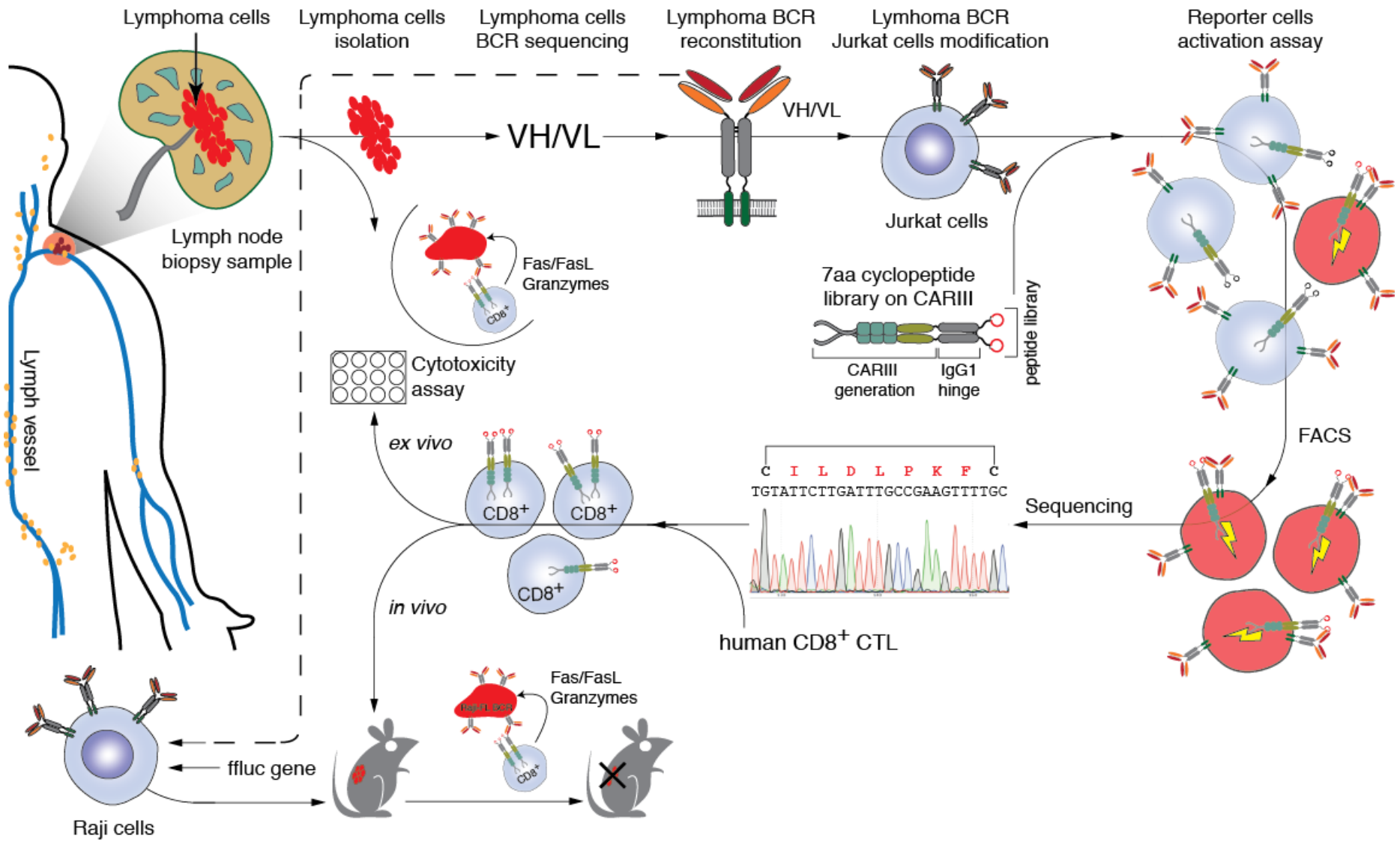

Workflow for selection of ligands for the personalized CDR3-selective lymphoma and leukemia CAR-T therapy

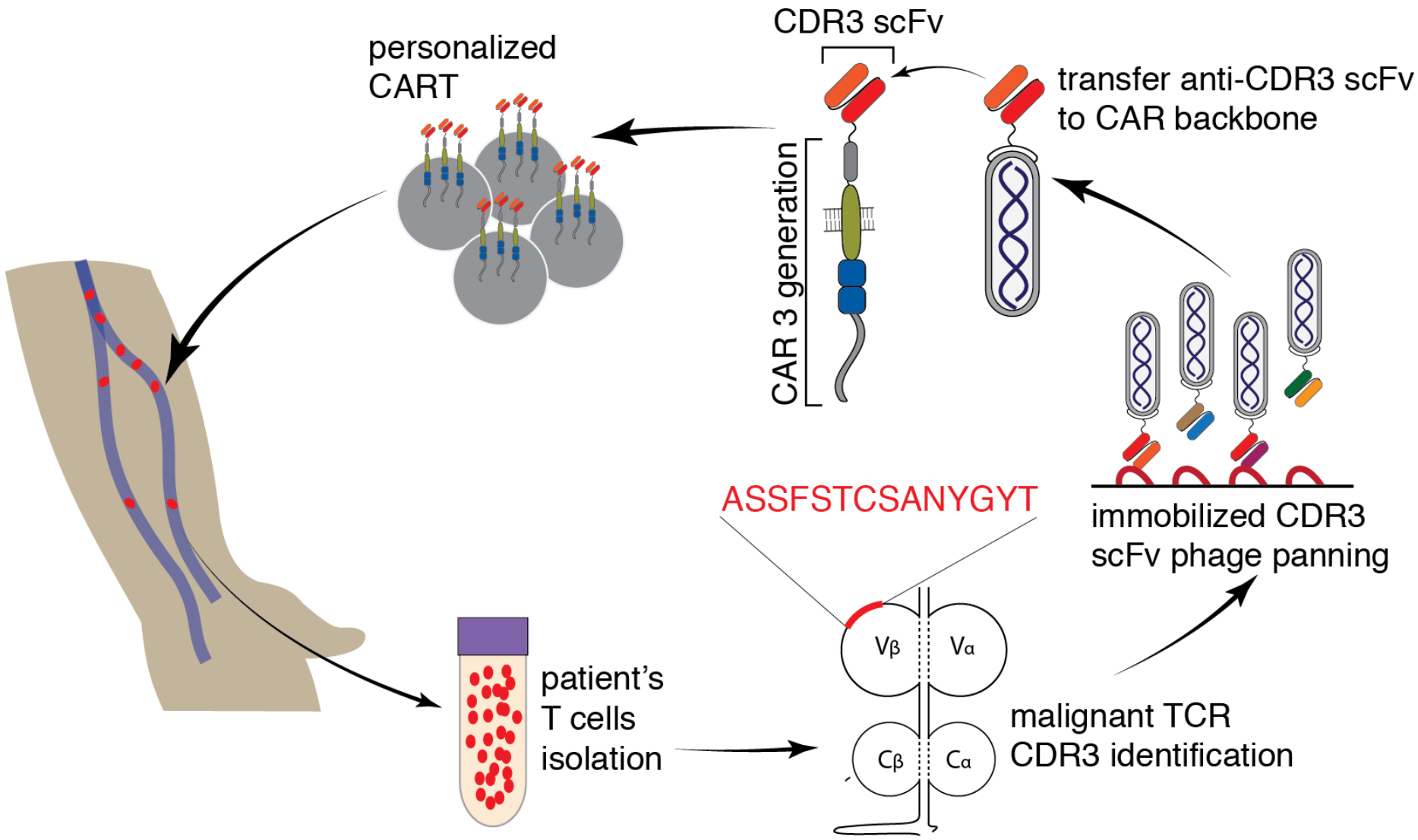

A biopsy sample from a patient with lymphoma or leukemia is isolated, and the collected tumor cells are utilized for identification of the malignant TCR CDR3 genes. The identified CDR3 sequences chemically synthesized and used for scFv phage panning. Selected scFv clones sequenced and transferred to the chimeric antigen receptor backbone. Modification of autological T cells by personalized patient CDR3-selective CAR.

CDR3-selective CARTs selectively eliminate malignant clone *ex vivo*

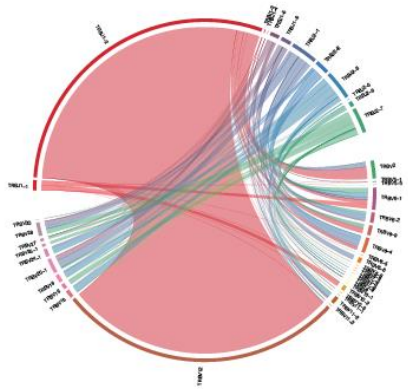

Jurkat + Mock T

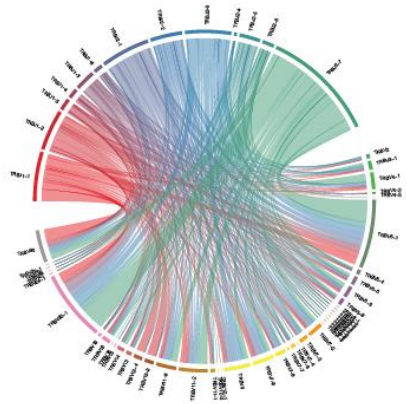

Jurkat + J-CART

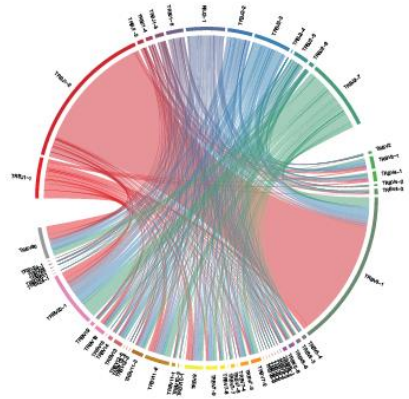

P#1 biopsy + Mock T

P#1 biopsy + P#1-CART

Injection of CDR3-selective J-CART suppress the tumor burden and improve animals survival

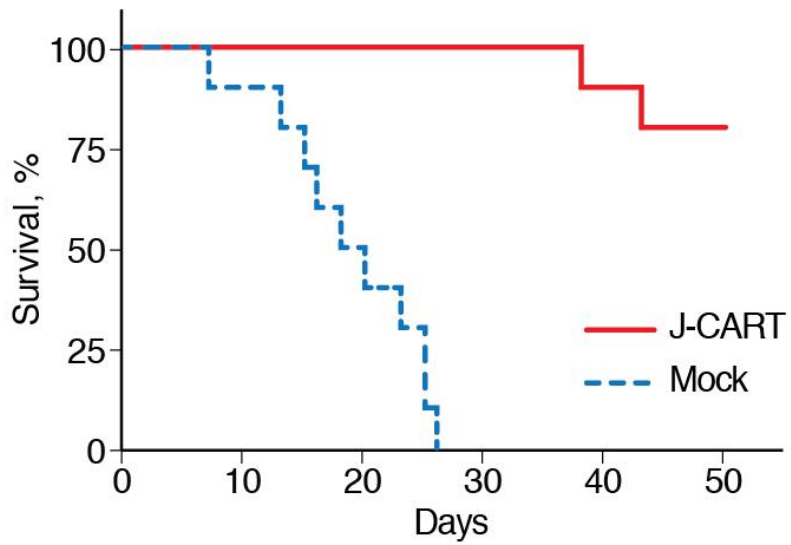

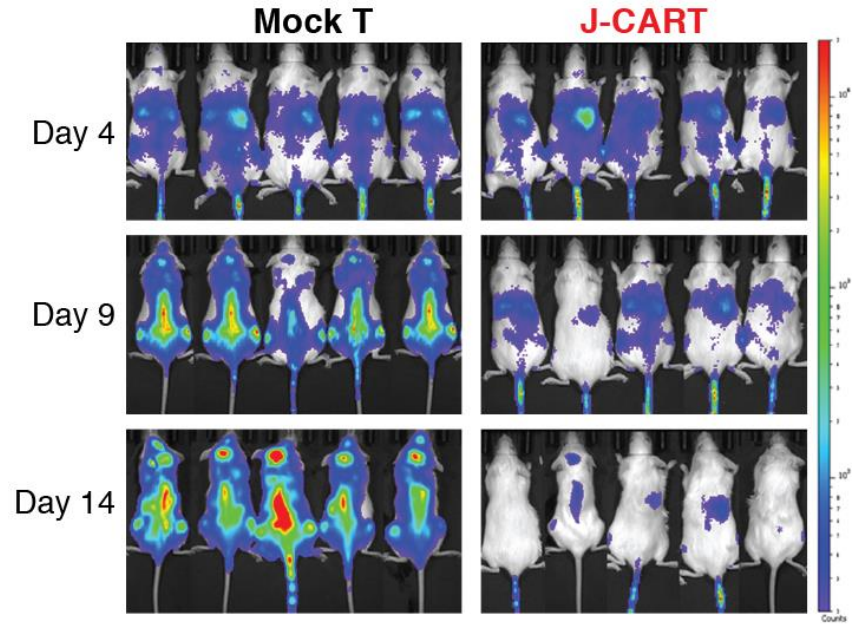

Catalytic Chimeric Antigen Receptor for the Remote Control Over Therapeutic T Cells

OFF

ON

60% efficiency

tunable

Covalent binding

Prepared folic acid-diketone

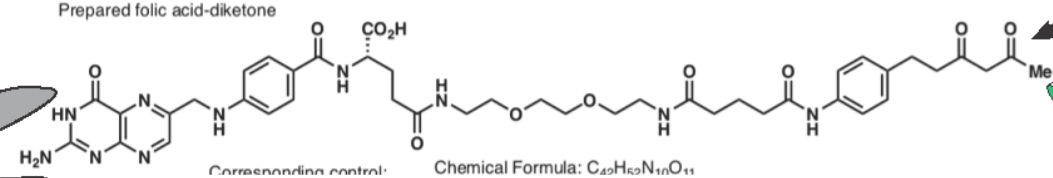

Chemical Formula: $C_{42}H_{52}N_{10}O_{11}$

folic acid-1,3-diketone

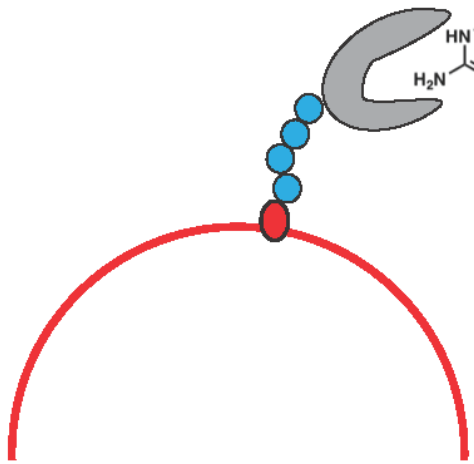

Cancer cell with Folate Receptor

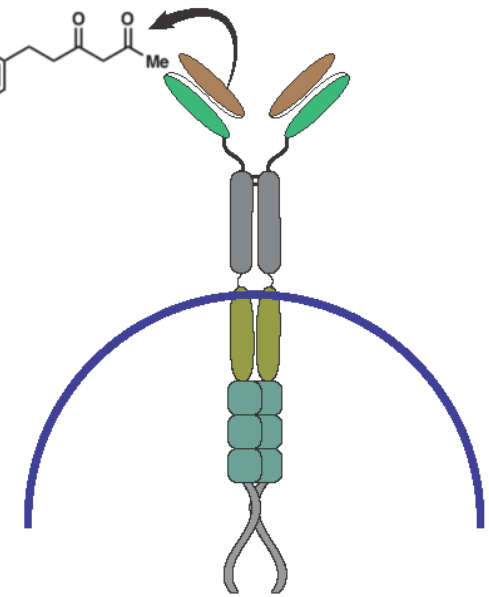

38C2 catalytic antibody CART cell

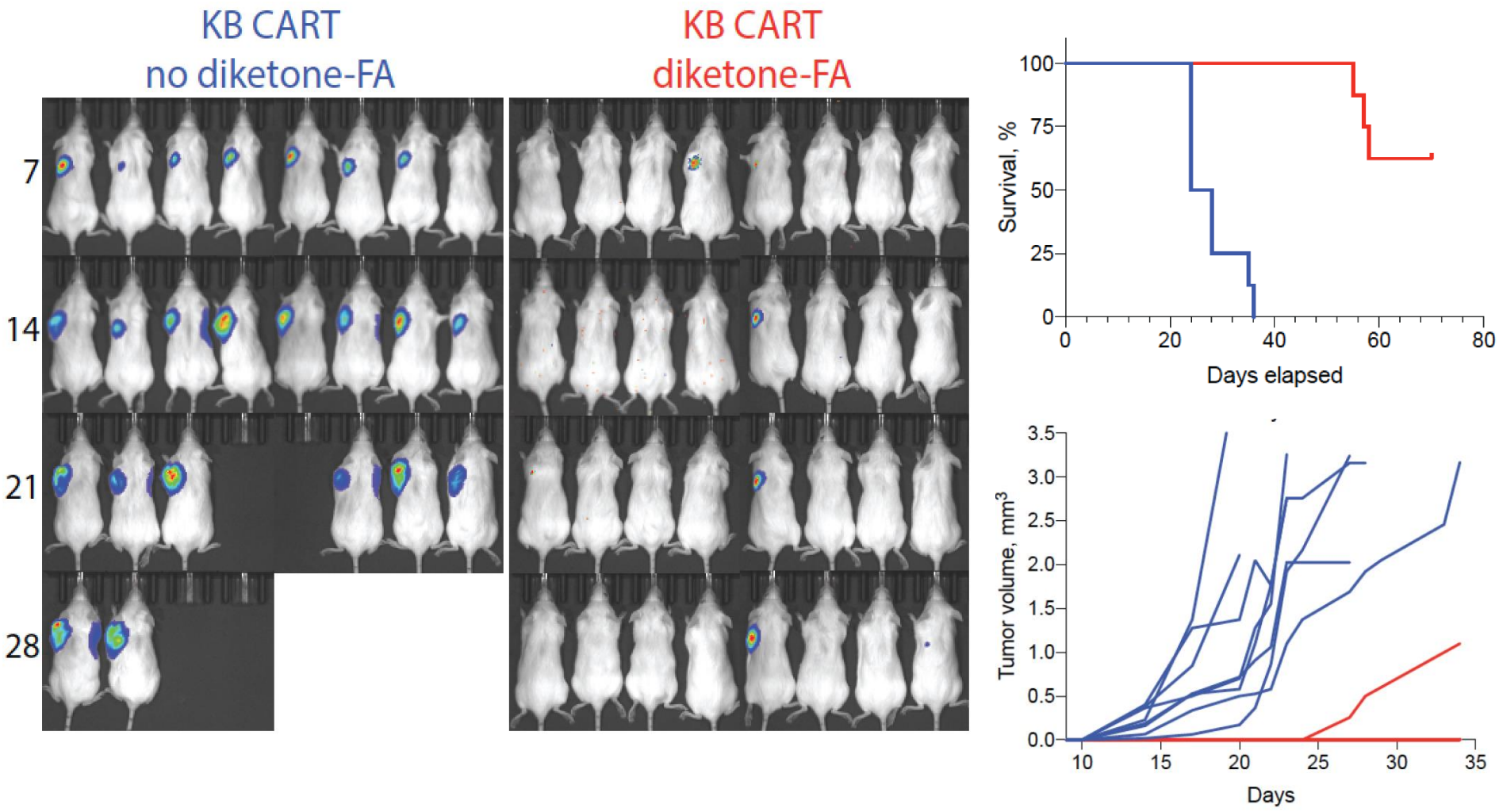
KB CART
no diketone-FA
KB CART
diketone-FA
7
14
21
28
Survival, %
100
75
50
25
0
0
20
40
60
80
Days elapsed
Tumor volume, mm3
3.5
3.0
2.5
2.0
1.5
1.0
0.5
0.0
10
15
20
25
30
35
Days

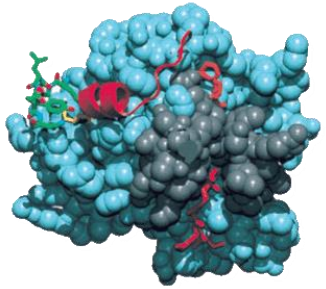

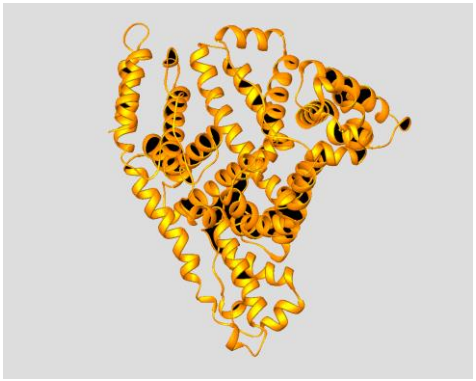

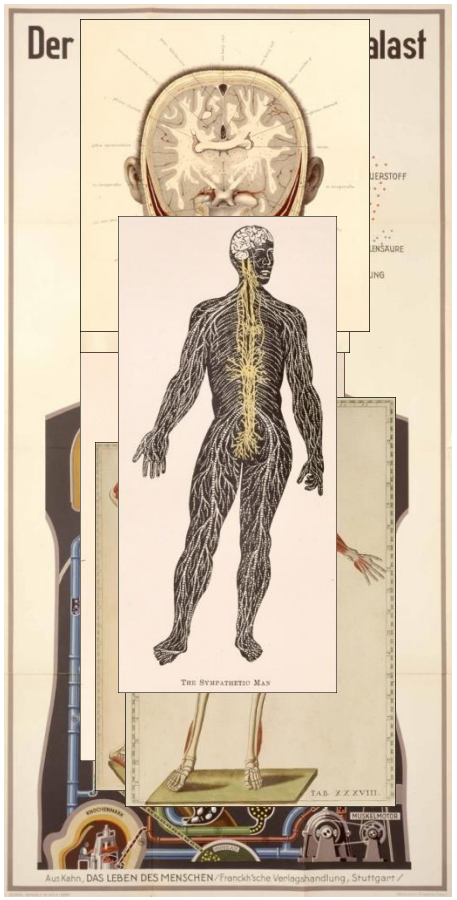

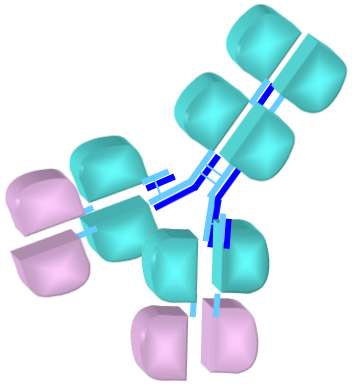

Der Mensch als Industriepalast (Man as Industrial Palace) Stuttgart, 1926. Chromolithograph. National Library of Medicine. Fritz Kahn (1888-1968) Kahn's modernist visualization of the digestive and respiratory system as "industrial palace," really a chemical plant

M.M. Shemyakin & Yu.A. Ovchinnikov
Institute of Bioorganic Chemistry,
Russian Academy of Sciences

Authors:
Alexey A. Belogurov Jr., Ivan V. Smirnov, Alexey Stepanov, Jacob Lomakin, Natalie A. Ponomarenko, Anastasia Stepanova, Stanislav Terekhov, Maria Zakharova, Yuliana Mokrushina, Inna Kurkova, Andrey Golovin, Azad Mamedov

RUSSIA

Vadim Govorun**,** *Inst. of Physico-chemical medicine*

Elena Ilina, Elena Kostryukova,Andrey Golovin,Artur Zalevsky

Evgeny Nikolaeyev, Maria Rubtsova, SkolTech

Alexey Boyko, Olga Favorova, Pirogov Medical University,Moscow

Dmitry Knorre, Valetin Vlasov, Olga Fedorova,

Marina Zenkova, Nikita Kuznetsov

Siberian division, RAS

Dmitry Genkin, Dobroslav Melamed

Pharmsyntez, S-P

ENGLAND

Michael Blackburn**,** *University of Sheffield*

USA

Sidney Altman

Richard Lerner

Scripps Research Insitute,CA

Al Tramontano, *UC Davis, Medical school*

ISRAEL

Aaron Ciechanover**,** *Technion, Haifa Germany*

GERMANY

Wilmanns Matthias, Chatziefthimiou Spyros, Viktor Lamzin

FRANCE

Daniel Thomas, Alain Friboulet, Berangere Avalle.

The University of Technology, Compiegne

Patrick Masson, Eugénie Carletti, Florian Nachon

Département de Toxicologie – CRSSA Institut de Recherche Biomédicale des Armées